SIMULTANEOUS BIOCHEMICAL REACTION AND SEPARATION IN A CONTINUOUS ROTATING ANNULAR CHROMATOGRAPH

MOHAMAD ROJI SARMIDI

Doctor of Philosophy

THE UNIVERSITY OF ASTON IN BIRMINGHAM

March 1993

THE UNIVERSITY OF ASTON IN BIRMINGHAM

Simultaneous Biochemical Reaction and Separation in a Continuous Rotating Annular Chromatograph

Mohamad Roji Sarmidi PhD 1993

SUMMARY

The aim of this work has been to investigate the behaviour of a continuous rotating annular chromatograph (CRAC) under a combined biochemical reaction and separation duty. Two biochemical reactions have been employed, namely the inversion of sucrose to glucose and fructose in the presence of the enzyme invertase and the saccharification of liquefied starch to maltose and dextrin using the enzyme maltogenase.

Simultaneous biochemical reaction and separation has been successfully carried out for the first time in a CRAC by inverting sucrose to fructose and glucose using the enzyme invertase and collecting continuously pure fractions of glucose and fructose from the base of the column. The CRAC was made of two concentric cylinders which form an annulus 140 cm long by 1.2 cm wide, giving an annular space of 14.5 dm^3. The ion exchange resin used was an industrial grade calcium form Dowex 50W-X4 with a mean diameter of 150 microns. The mobile phase used was deionised and dearated water and contained the appropriate enzyme. The annular column was slowly rotated at speeds of up to 240^o h^{-1} while the sucrose substrate was fed continuously through a stationary feed pipe to the top of the resin bed.

A systematic investigation of the factors affecting the performance of the CRAC under simultaneous biochemical reaction and separation conditions was carried out by employing a factorial experimental procedure. The main factors affecting the performance of the system were found to be the feed rate, feed concentrations and eluent rate. Results from the experiments indicated that complete conversion could be achieved for feed concentrations of up to 50% w/v sucrose and at feed throughputs of up to 17.2 kg sucrose per m^3 resin/h.

The second enzymic reaction, namely the saccharification of liquefied starch to maltose employing the enzyme maltogenase has also been successfully carried out on a CRAC. Results from the experiments using soluble potato starch showed that conversions of up to 79% were obtained for a feed concentration of 15.5% w/v at a feed flowrate of 400 cm^3/h. The product maltose obtained was over 95% pure.

Mathematical modelling and computer simulation of the sucrose inversion system has been carried out. A finite difference method was used to solve the partial differential equations and the simulation results showed good agreement with the experimental results obtained.

Key Words:

Annular chromatograph, Biochemical reactor, Chromatographic reactor, Invertase, Maltogenase

Dedicated to my family

ACKNOWLEDGEMENTS

The author wishes to thank the following:

Professor B Tighe, Dr E L Smith and the Department of the Chemical Engineering and Applied Chemistry for for making the research facilities available.

Professor P E Barker, my research supervisor for his advice and guidance throughout this work.

Mr M Lea, Mr M Santoro, Mr I R Murkett, Mr D Bleby, Mrs Lyn Wright and all the staff in the staff in the department for all their time and effort.

Dr B Martin of the Mathematics and Computer Science department and Dr Ann Spooner of Business School, Aston University for their helpful advice and suggestions towards the development of the mathematical modeling and statistical analysis of the process.

Dr John Ajongwen, Mr Steven J Setford and my fellow research students in the separation and purification group for their practical help and useful discussions.

Finally I would like to thank the Public Service Department of Malaysia for their financial support throughout this work.

LIST OF CONTENTS

LIST OF TABLES

LIST OF FIGURES

CHAPTER ONE

INTRODUCTION

1.1 Integrated Biochemical Reaction and Separation

Bioprocessing as a means of producing specialised and high-value products is becoming more significant in terms of volume and sales within the chemical process industry. The most important components of bioprocess activities are the bioreaction step and the downstream processing step [1]. Both of these aspects are technically challenging and are a high cost activity. This is due to the nature of bioprocess streams which are often complex and sensitive to processing parameters such as temperature, pH, the type of solvent and shear force [2]. Moreover in many cases, aseptic conditions are required for some of the process steps. The components in the process streams often include macromolecules, salts, microbial, animal or plant cells. In addition, the desired products are often present in low concentration, due to the inherent product or substrate inhibition effect, common to most biological reaction systems.

In comparison to chemical reaction engineering, bioreaction engineering is relatively not well developed. This is also true for downstream processing in bioprocesses. Despite of major developments in biomolecular separation techniques, the downstream process still accounts for 50-80% of the production cost [3].

The key to reducing the processing cost is to limit the number of steps in the overall process. If there are more than three processing steps, each with 80% efficiency, the total efficiency falls to about 50% [1]. Therefore, demand to improve the performance of bioprocesses within the industry is increasing.

One of the approaches being used to improve the performance is to intensify the process by integrating the reaction and product recovery into a single step. The main feature of this approach is for bioreaction and products separation to take place simultaneously in the

same unit operation. This feature is especially of advantage in bioreaction systems where substrate or product inhibition to the reaction is present.

In the case of product inhibition, removal of products or reaction intermediates from the reaction zone as soon as they are formed will enhance the rate of the reaction and the yield [7]. This principle was successfully applied to the production of ethanol using *Saccharomyces cerevisiae* by a vacuum fermentation technique [4,5]. In traditional batch or continuous fermentations, the accumulation of the product ethanol reduces the specific cell growth and product formation. To minimise the product inhibition effect a dilute substrate was used so that the product concentration will always be below the inhibitory level. However this practice requires a large volume of water to be processed thus reducing the volumetric productivity of the process.

In a vacuum fermentation technique, simultaneous removal of the product ethanol from the fermentation broth was found to minimise this inhibitory effect [4,5]. This permited a higher substrate concentration to be used and as a result the cell density and the volumetric productivity of the fermentation were increased. Ramalingham and Finn [4] demonstrated that in a continuous vacuum fermentation operated at 30°C and 32 mm of mercury, 98% glucose conversion was achieved for substrate concentrations of up to 50% w/v.

To harness the attractive potential of integrated bioreaction and separation techniques, a few systems have been proposed. The choice of the integrated bioreaction and separation system is governed by the biocompatibility of the separation method. The systems include; the hollow fibre bioreactor for the production of monoclonal antibodies [6], centrifugal-biochemical reactor separators for the biosynthesis of the polyglucose dextran [8,9] and chromatographic biochemical reactors for several applications [10-13].

Hollow fibre bioreactors have been successfully used in the production of monoclonal antibodies [6]. Altshuler *et al.* [6] grew murine hybridoma cell line on the shell side of a hollow fibre bioreactor with a one hundred thousand dalton cut-off size producing a maximum monoclonal antibodies concentration of 740 $\mu g/cm^3$. This value compares to

conventional spinner flask and tissue culture flask results which are about 3.0 $\mu g/cm^3$ and 1.0 $\mu g/cm^3$ respectively. In terms of monoclonal antibody productivity expressed as $\mu g/cm^3$ per day, the values were found to be 65, 1.0 and 0.25 for hollow fibre bioreactor, spinner flask and tissue culture flask methods respectively.

Setford [8,9] succesfully carried out biochemical reaction and separation using a rate-zonal centrifugation technique. By layering thin zones of dextransucrase enzyme onto sucrose gradients and centrifuging, very high molecular weight dextran-enzyme complexes were formed. The dextran-enzyme complex was then rapidly sedimented through the sucrose substrate gradients under the influence of the applied centrifugal field. The low molecular weight fructose by-product sedimented at reduced rates and was thus separated from the enzyme and dextran during the reaction.

The molecular weight distribution of dextran recovered from the centrifugal bioreactor was compared with that from a conventional batch biochemical reactor. The results indicated that the centrifugal biochemical reactor-separator produced up to 100% more clinical dextran with molecular weights between 12,000 and 98,000 at 20% w/w sucrose concentration than conventional biochemical reactors. This was due to the removal of acceptor fructose molecules from the sendimenting reaction zone by the action of centrifugal forces.

Therefore, simultaneous biochemical reaction and separation offer several significant advantages in process integration and also in process intensification.

The object of the work recorded in this thesis was to investigate for the first time the possibility of carrying out simultaneous biochemical reaction and separation in a continuous chromatograph using a rotating annular chromatograph (CRAC). Two biochemical reactions were chosen for study, namely the inversion of sucrose to glucose and fructose in the presence of the enzyme invertase and the saccharification of liquefied starch to maltose using the enzyme maltogenase. Maltogenase is a heat stable, high maltose producing, exo-acting alpha-amylase. Besides studying the feasibility of such

processing the other objectives were to elucidate the main factors effecting a biochemical reaction and separation on a CRAC and also to model and simulate the system.

1.2 Thesis Outline

The thesis is organised as follows. Chapter 2 reviews previous work in liquid chromatographic reactors. Various types have been examined with a greater emphasis on continuous and semi-continuous systems. The potential of continuous chromatographic-reactor separators to carry out simultaneous biochemical reaction and separation has been discussed and highlighted and several applications described.

Chapter 3 deals with the construction and design of CRAC equipment and its operating procedure. The analytical methods used in the research and the enzyme assays techniques have been described.

Chapter 4 describes the separation and reaction systems used in the CRAC.

Chapter 5 describes the preliminary biochemical reaction and separation experiments involving the inversion of sucrose using the enzyme invertase. Further work involving two level and four factor factorial experiments were undertaken. The main factors affecting the performance of the CRAC under simultaneous reaction and separation conditions were highlighted.

Chapter 6 examined further the performance of the CRAC under simultaneous biochemical reaction and separation conditions. Saccharification of modified starch to maltose using the enzyme maltogenase was considered. Initial experiments were carried out in a 1.98 cm internal diameter and 150 cm length batch chromatographic column. The experimental conditions were then used as the basis for the experiments on a CRAC. Simple optimization procedures involving both volume and concentration overload were used.

Chapter 7 describes the mathematical modelling and computer simulation work of a CRAC as a combined bichemical reactor-separator. A differential model was employed and the

resulting second order nonlinear mixed type partial differential equations were solved using finite different methods implemented on a Vax 8650 computer. Data for the inversion of sucrose to glucose and fructose was used in the modelling study.

Finally in Chapter 8, the research is concluded by concisely highlighting the performance of a CRAC as a combined biochemical reactor-separator. Details of further recommended work is also given.

CHAPTER TWO

LIQUID CHROMATOGRAPHIC REACTORS

2.1 Introduction

During the past two decades, liquid chromatography has emerged as one of the most powerful techniques for the separation and identification of chemicals and biochemicals [15]. This is due to its speed, accuracy, versatility and freedom from the volatility requirements of gas chromatography.

The application of modern liquid chromatography range from simple organic compounds to complex macromolecules such as polysaccharides, polypeptides and glycoproteins. It is predicted that the use of liquid chromatograpy will grow by 14-20% annually for the first half of the 1990s [16].

Liquid chromatographic columns have also been used to study physico-chemical phenomena such as intraparticle diffusion [17] and sorption kinetics [18-20]. Another application of liquid chromatography is as chemical reactor-separators, both for chemical kinetic studies [15,21-27] as well as for preparative purposes. However, the use of chromatographic reactors for preparative purposes has been very limited [28-31]. The increasing use of commercial production-scale liquid chromatography [16,32] could contribute to a wider research interest in the application of liquid chromatography as chromatographic reactor-separators.

A chromatographic reactor-separator is defined as column or a system in which one or more components are converted partially or totally to different chemical species and the products formed are separated simultaneously by the chromatographic principle. The chemical or reaction can take place either on the stationary phase or in the mobile phase or both [36].

This chapter reviews the application of liquid chromatography as combined reactor-separators. Specifically, the review focussed on the development of continuous reaction chromatography applied to biochemical field. However, a brief account of the earlier work in the batch gas chromatographic reactor and batch liquid chromatographic reactor fields will be discussed.

2.2 Batch Chromatographic Reactor

2.2.1 Introduction

Attempts to adapt chromatographic columns as combined chemical reactor and separation devices have been made since the late 1950s [33-39]. Almost all of the earlier work on chromatographic reactors was carried out in gas chromatographic columns, operated under the batch elution mode. The general approach involved the injection of a reactant or reaction mixture as a pulse into a continuous stream of mobile phase. In some cases the mobile phase itself could serve as one of the reactants. As mobile phase swept the reactants and the products through the column simultaneous reaction and separation occurred. The migration velocities of the reactants and the products are determined by their affinity for the stationary phase.

The advantages [15] of carrying out a chemical reaction in chromatographic reactor are ; (a) the presence of integrated chemical reaction and separation in a single unit operation; (b) the enhancement of forward reaction rate and the possibility of exceeding equilibrium conversions in equilibrium limited reactions as well as selective production of reaction intermediates in series reactions; (c) the relative ease in measuring the rate of reaction especially in catalytic reactions; (d) the ease of manipulation and control of chromatographic apparatus and associated detectors.

2.2.2 Batch Gas Chromatographic Reactor

The advantages of carrying out chemical reaction in a chromatographic column attracted considerable research interest in the 1960s [33-40]. A few industrially important gas phase reactions were studied experimentally. These include the dehydrogenation of cyclohexane to benzene [33], the conversion of butene to butadiene [34] and the Haber ammonia synthesis process [35]. In the dehydrogenation of cyclohexane into benzene, Matsen *et al.* [33] demonstrated that yields of up to 30% beyond those predicted by equilibrium were obtainable. In the conversion of butene into butadiene Roginski *et al.* [34] reported 20-30% yield improvements compared to other continuous flow reactors. When studying the Haber ammonia synthesis process, similar trends in yield improvement were obtained by Unger [35]. In addition, the ammonia synthesis can be carried out at pressures below 100 atmosphere which is not possible with the conventional process.

2.2.3 Batch Liquid Chromatographic Reactor

The use of liquid chromatography as chemical reactors did not occur until the middle of the 1970s. Most of the earlier applications reported were for reaction kinetic studies[15,21-27].

Theory advancement and experiments with gas chromatographic reactors have facilitated in the development of liquid chromatographic reactors. Many of the principles derived from gas chromatographic reactors could be applied to liquid chromatographic reactors.

2.2.3.1 Preparative Applications

The earliest reported work on liquid chromatographic reactors was that of Wetherold *et al.* [28]. They carried out a liquid phase hydrolysis of methyl formate to methanol and formic acid (equation 2.1) in a batch chromatographic column using activated charcoal as the adsorbent material.

$$HCOOCH_3 + H_2O \overset{H^+}{\rightleftharpoons} CH_3OH + HCOOH \qquad 2.1$$

It was demonstrated that simultaneous reaction separation drove the conversion beyond the equilibrium value.

A similar reaction was used by Cho *et al.* [29] in the study of a continuous rotating annular chromatograph as a chemical reactor-separator and will be described in section 2.3.2 of this chapter.

Sardin and Villermaux [30,31] investigated three types of reaction with batch chromatographic reactors.

1. Esterification of acetic acid to ethyl acetate using ethanol (equation 2.2)
2. Transesterification of menthyl acetate (equation 2.3).
3. Hydrolysis of glycol diacetate to glycol and sodium acetate (equation 2.4).

The first reaction was of the type $A + B \rightleftharpoons C + D$ and was carried out in a batch chromatographic column using a mixture of cation-exchange resin and alumina as the packing and adsorbent materials

$$CH_3COOH + C_2H_5OH \rightleftharpoons CH_3COOC_2H_5 + H_2O \qquad 2.2$$

A conversion of 90% was obtained in the chromatographic reactor as compared to 67% equilibrium conversion using a conventional reactor.

The second reaction is also of the type $A + B \rightleftharpoons C + D$ as shown in equation 2.3. It was carried out in a batch chromatographic column packed with acidic cation-exchange resin.

$$\text{Menthol} + \text{Ethyl acetate} \rightleftharpoons \text{Menthyl acetate} + \text{Ethanol} \qquad 2.3$$

In equation 2.3, the reactant ethyl acetate also served as the mobile phase. A complete menthol conversion was obtained. However excessive mobile phase was required to elute the strongly adsorbed ethanol, this caused the process to be economically unatractive.

The third reaction was a consecutive irreversible reaction of

type $A + B \longrightarrow R$, $R + B \longrightarrow S$. The reaction are as follow;

$$\underset{A}{\text{Glyco diacetate}} + \underset{B}{\text{NaOH}} \longrightarrow \underset{R}{\text{Glycol mono acetate}} + \underset{E}{\text{Sodium acetate}}$$

$$\underset{R}{\text{Gycol monoacetate}} + \underset{B}{\text{NaOH}} \longrightarrow \underset{S}{\text{Glycol}} + \underset{E}{\text{Sodium acetate.}} \qquad 2.4$$

The mobile phase and the stationary phase consisted of 2.5% ethanol in water and activated charcoal respectively. The result of the experiment confirmed that in a consecutive irreversible reaction no improvement in the yield could be obtained by carrying out the reactions in a chromatographic reactor.

2.2.3.2 Chemical Kinetic Applications

Apart from the above work which focuses on reactor performance, most of the work in liquid chromatographic reactors was directed towards obtaining kinetics data [15,21-27]. Melton *et al.* [23] carried out the study of immobilised enzyme lactase activity on porous glass beads by carrying out the hydrolysis of α-nitrophenyl-β-D-galactopyranoside in a chromatographic column.

Other work using the liquid chromatographic reactor for kinetic data determination was the oxidation of hydroquinone to benzoquinone (equation 2.5) in a chromatographic column packed with iron(III)-modified silica [24]. In this work, the method of stastistical moments was used to estimate the rate of reaction from the elution profiles of the reactant and the product.

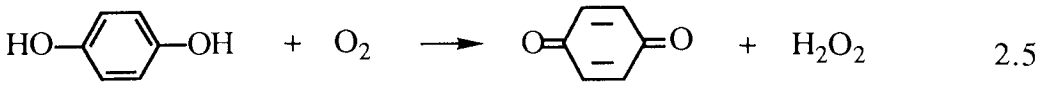

2.5

The same reaction (equation 2.5) was also used in experimental work performed by Jeng and Langer [25] as a probe to study the contamination of transition metal ions from the stainless steel component of HPLC hardware.

Chu and Langer carried out [26,27] solvolysis reactions of tetrachloroterepthaloyl chloride with methanol in a C_{18} bonded-phase liquid chromatograph. The use of bonded-phase liquid chromatography as a chemical reactor was to obtain the kinetic parameters [26], the nature of the the stationary phase structure [27] and its retention mechanisms [26].

2.2.3.3 Biochemical Reactor Applications

The application of batch liquid chromatography as an enzymic reactor-separator did not occur until in the 1980s. Zafar [41] reported that there are three possible methods of contacting enzymes with substrates in an enzymic chromatographic reactor-separator;

1. The enzyme is mixed with the eluent and the reaction takes place in the mobile phase. The stationary phase acts only as an adsorbent.

2. The reaction occurs in the mobile phase as in the first method, however the enzyme is mixed with the substrate just before being introduced into the chromatograph.

3. The use of an immobilised enzyme, immobilised directly on to the stationary phase or immobilised on another solid support

The first method is appropriate when the enzyme and the substrate have different distribution coefficient (K_d) values. The presence of the enzyme throughout the column ensures intimate contact between the enzyme and the substrate.

The second method is suitable for an enzyme which has a similar K_d value as the substrate. An enzymatic reaction will take place since there is no separation between the enzyme and

the substrate as they are eluted through the chromatograph. The advantage of this method is that less enzyme is required compared to the first method.

Barker *et al.* [10] were the first to demonstrate the used of a batch chromatographic column as an enzymic reactor-separator. They carried out the biosynthesis of polyglucose dextran from sucrose using the enzyme dextransucrase as the catalyst.

$$n C_{12}H_{22}O_{11} \xrightarrow{\text{Dextransucrase}} (C_6H_{10}O_5)_n + n C_6H_{12}O_6 \qquad 2.6$$

The work was carried out in batch chromatographic reactor-separators of 0.97 cm to 5.4 cm internal diameter and 30 cm to 200 cm column length. It was reported that under chromatographic conditions, almost twice the amount of high molecular weight dextran (molecular weight above 160,000 daltons) was obtained compared to a conventional batch reactor. This was due to the instantaneous removal from the reaction zone of the by product fructose which acts as an acceptor molecule and terminates the growth of the dextran chain.

The potential of batch liquid chromatography as a combined biochemical reactor-separator is still not fully realised. The main advantage of batch liquid chromatographic reactor-separators over other chromatographic systems is in the simplicity of the former. Techniques such as the stop-flow method [19] have not yet been tried for biochemical reaction in batch liquid chromatography. The stop flow-method is a technique to prolong the contact time between the enzyme and the substrate in the column. This technique could be used for a wider range of reaction kinetics and allow the use of a shorter chromatographic column.

The prospects for further developments in this area are favourable.

2.2.4 Analysis of Batch Liquid Chromatographic Reactors

There are two approaches in modelling the dynamics of a batch chromatographic reactor; the mixing cells model and the differential model [15].

2.2.4.1 Mixing Cell Model

The mixing cell model is generally simple and has been widely used for physical separation studies [42-44].

Schweich and Villermaux [30] were the first to report on the use of a mixing cell model to analyse the behaviour of a batch liquid chromatographic reactor. The column is regarded as being divided into J mixing cells of identical volume V/J (figure 2.1). The model was developed for its simplicity as it gives rise to a set of ordinary differential equations instead of partial differential equations as with a continuous model.

The mass balance for component A in cell number k for reaction of the type $A \rightleftharpoons B + C$ is as follows [45];

$$Qc_{A,\,k-1} - \frac{RV}{J} = Qc_{A,\,k} + (1 + \alpha_A)\frac{V}{J}\frac{dc_{A,\,k}}{dt} \qquad 2.7$$

where α_A = Capacity factor of the column

Q = Volumetric flowrate

R = Rate of reaction

V = Volume of the stationary phase or mobile phase

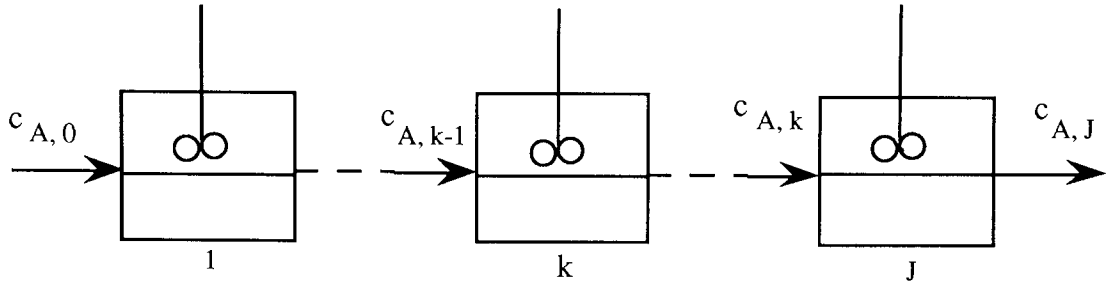

Figure 2.1 Mixing cell in a series model

The plate-height values used in the model tend to lose physical significance and become difficult to determine experimentally when chemical reactions confound other dynamic chromatographic processes [15]. Thus the model was limited to applications where the condition of an ideal chromatographic reactor was approached.

2.2.4.2 Differential Model

A more general approach to modelling the dynamics of liquid chromatographic reactors is by using the differential model [15]. A differential balance (figure 2.2) for an isothermal and homogeneous chromatographic reactor column over a differential section of the column at position z and time t is;

$$\frac{\partial c}{\partial t} + \left(\frac{1-\varepsilon}{\varepsilon}\right)\frac{\partial q}{\partial t} + \frac{\partial}{\partial z}(vc) = D_Z\frac{\partial^2 c}{\partial z^2} - R. \qquad 2.8$$

$$(1-\varepsilon)\frac{\partial q}{\partial t} = k_o a\, F(q, c) \qquad 2.9$$

where

c = concentration of reactant in the mobile phase

q = concentration of reactant in the stationary phase

D_z = axial dispersion coefficient

v = interstitial velocity of fluid through the bed

R = rate of reaction

F = relationship between concentration of solute in mobile phase and stationary phase

k_o = mass transfer cofficient

ε = bed voidage

t = time

z = space variable along the bed

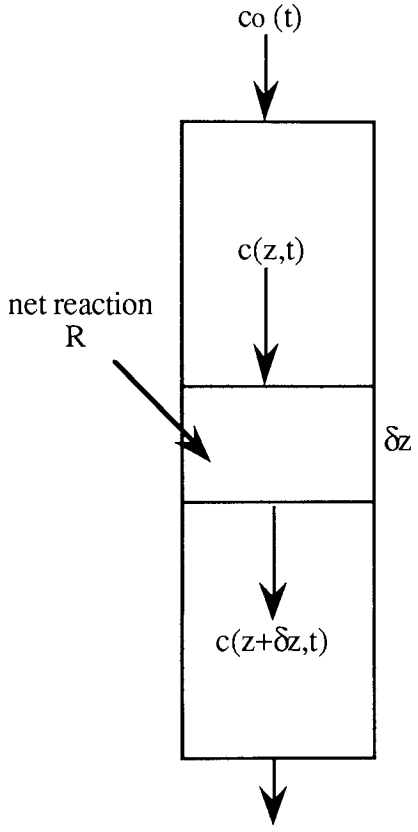

Figure 2.2 Shell balance for the differential model

Equations 2.8 and 2.9 involve no assumptions about the mechanism of sorption and the rate of reaction. The equation can be solved for different cases with several appropriate assumptions.

Under the ideal chromatographic reactor conditions [24], equation 2.8 reduces to its simplest form.

$$\frac{\partial c}{\partial t} + \left(\frac{1-\varepsilon}{\varepsilon}\right)\frac{\partial q}{\partial t} + v\frac{\partial c}{\partial z} = R. \qquad 2.10$$

An analytical solution has been obtained by Jeng and Langer [24] using Laplace transformation and a statististical moments method. The same method was applied by Chu [27] to obtain an analytical solution of equation 2.8 with the presence of axial dispersion. Under nonlinear adsortion isotherm and higher order rate of reaction conditions equation 2.8 can be solved numerically.

Zafar and Barker [12] used the differential model to simulate the behaviour of simultaneous biochemical reaction and separation of sucrose to dextran and fructose in a batch chromatographic reactor. The reaction was assumed to occur in the mobile phase and follow a Michaelis-Menten type kinetic. Under negligible axial dispersion equation 2.8 then reduced to equation 2.11. The equation was solved numerically using a finite difference method.

$$\left(1 + \frac{1-\varepsilon}{\varepsilon} k_{dS}\right) \frac{\partial c_S}{\partial t} + V \frac{\partial c_S}{\partial z} + \frac{c_S V_{max}}{c_S + K_M} = 0. \qquad 2.11$$

where V_{max} = Maximum reaction rate

K_M = Michealis-Menten constant

2.3 Continuous Chromatographic Reactor

2.3.1 Introduction

Even though the potential applications of chromatographic reactors have been successfully demonstrated, no applications can be found in the process industry. The lack of throughput with batch operation and inherently low product concentrations would seem to make it unattractive for process-scale applications. An obvious method to increase the throughput is to use automated repetitive injection as in production scale batch chromatography. However, large diameter chromatographic columns are prone to reduced

performance especially with peak resolution due to the difficulty in obtaining homogeneous packing [46].

Another approach to improve the throughput is to make the chromatographic operation continuous. A chromatographic operation may operate continuously if there is a relative motion between the adsorbent phase and the point where the feed is introduced into that phase. Under these circumstances the differences in retention times of the components are transformed into physical displacements. Each component may be withdrawn continuously at a fixed and characteristic distances from the feed point. This can be accomplished by either operating in a continuous counter-current [47-51] or a cross-current flow arrangement [52-58].

Reactions in which a single reactant is converted to more than one product such as the type $A \rightleftharpoons B + C$ or $A = B + C$ are most appropriate for the cross-flow arrangement by using a continuous rotating annular chromatograph [59]. This type of equipment is capable of carrying out multicomponent separations. Furthermore the separation of the products B and C will supress the reverse reaction. In the counter-current arrangement, only two fractions can be separated at a time. Hence reactions of the type $A \rightleftharpoons B$ or $A = B + C$ are suitable.

In the reaction of the type $A \rightleftharpoons B + C$, separation of the product B will prevent the reverse reaction thus high conversion and pure product B could be obtained. The second reaction scheme is only suitable if the reaction is fast and could be driven to completion.

2.3.2 Continuous Rotating Annular Chromatographic Reactor

The principle of operation of a continuous rotating annular chromatograph as a combined reactor-separator is described in figure 2.3. The annulus is rotated slowly about its centre. The reactant are introduced continuously at a fixed point through a feed pipe just below the top of the resin bed and is eluted through the column by the eluent. The movement of

the reactants and the products formed through the column depend on the affinity of the components for the stationary phase.

At the molecular level however, chromatographic separation is a dynamic process involving continuous reversible transfer of solute molecules between the mobile and the stationary phases. In a continuous rotating annular chromatograph, each time a molecule is complexed or adsorbed by the stationary phase, its movement is purely horizontal and each time a molecule spends in the mobile phase its movement is axial. However, since the column is rotating, a solute movement relative to the fixed feed position is effectively tangential. As a result, the movement of a molecule follows a helical path from the feed pipe to the point at which it exits from the base of the column. Each component has a characteristic helical path under a given set of operating conditions and will emerge at a characteristic angular position at the base of the column relative to the feed point (see figure 2.3).

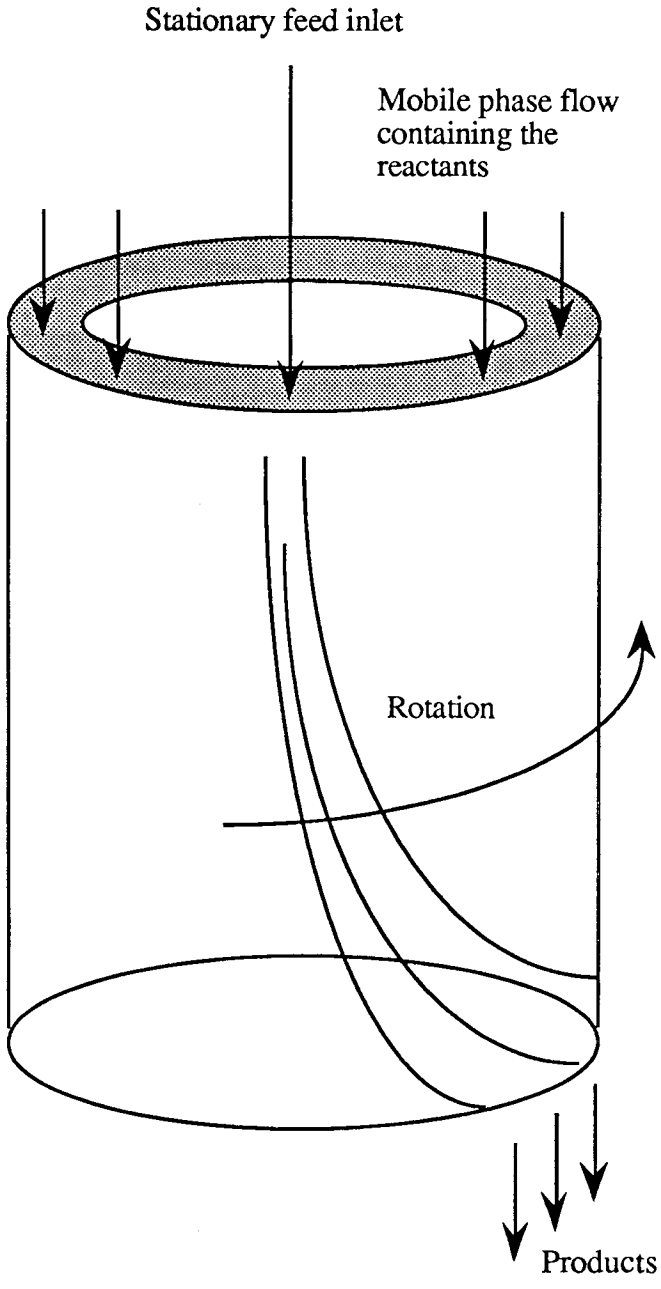

Figure 2.3 Operating principle of continuous rotating annular chromatographic reactor-separator

To date there are only two chemical reactions that have been carried out in a continuous rotating annular chromatograph [29,60]. Both were of the type $A \rightleftharpoons B + C$
The first was a liquid phase reaction, the acid catalysed hydrolysis of methyl formate into formic acid and methanol [29].

The hydrolysis was carried out by Cho [29] in a preparative scale continuous rotating annular chromatograph. The rotating annular chromatograph was made up of two concentric acrylic cylinders, the outer being 8 in. outside diameter, which formed an annulus 16 in. long and 0.25 in. wide. The annular space was packed with 60-80 mesh activated charcoal. The chromatograph was operated in such a manner that the feed pipe was rotated while keeping the annulus stationary. This arrangement however did not allow the product fractions to be collected easily as it required the product collection port to rotate at the same speed as the feed pipe.

The system showed that complete conversion could be achieved as compared to 75% equilibrium conversion with a non-separating reactor. However, one of the products formic acid was spread throughout the annulus without forming a peak. As for methanol the peak showed evidence of asymmetry with a prominent skew away from the feed point.

A mathematical model was developed for prediction of the reactor performance. The model was based on an ideal chemical chromatographic reactor with a Freundlich adsorption isotherm [29]. The reaction kinetics was first order reaction in the forward direction and second order reaction in the reverse direction. The material balance for each component of the $A \rightleftharpoons B + C$ reaction gave the following set of equations.

$$\varepsilon v \frac{\partial c_i}{\partial z} + \omega \frac{\partial}{\partial \phi} (\varepsilon c_i + \rho_B n_i) = \alpha_i [H^+] k \left(c_A - \frac{c_B c_C}{K_e} \right) \quad (i=A, B, C) \qquad 2.12$$

In this equation, the stoichiometric coefficient of the ith component α_i was -1 for species A and 1 for B and C. The model equations were solved numerically.

The second chemical reaction in a continuous rotating annular chromatograph was carried out by Wardwell [60]. The reaction was a gas phase reaction, dehydrogenation of cyclohexane vapour catalysed by platinum supported on alumina The same reaction that was used by Matsen [33].

$$C_6H_{12} \underset{Pt}{\overset{Al_2O_3}{\rightleftharpoons}} C_6H_6 + 3H_2 \qquad 2.12$$

The equipment was slightly bigger than that used by Cho [29]. The annulus was 18 in. long by 10 in. diameter with an annular width of 0.3 in. Although the conversion was not completed as in the case of the batch chromatographic reactor [33], the conversion was about 88% which was 15-20% better than a non-separating reactor. Wardwell [60] reported that the failure to drive the reaction to completion was mainly due to the occurrence of a reverse reaction in the zone where both benzene and cylcohexane remain in contact. This overlapping zone was formed as a result of excessive lateral and axial dispersion in the column. No further developments on the use of continuous rotating annular chromatographs as reactor-separators have been reported.

2.3.3 Counter Current Moving Bed Chromatographic Reactor (CMCR)

2.3.3.1 Theoretical Investigations

Much theoretical work has been carried out on CMCR equipment [61-68]. Visvanathan and Aris [61] were the first to use a CMCR to simulate a first-order irreversible reaction of the type $A \longrightarrow B$.

The CMCR has also been studied by Takeuchi and Urugachi [67-69]. They used a simplified model to investigate the behaviour of a reversible reaction and a consecutive reaction. The model predicts that the selectivity of intermediate products in a first-order consecutive reaction was higher compared to that of fixed-bed reactors. The model also

shows that the conversions of products for reversible reactions can exceed the conversion at chemical equilibrium.

The theoretical work of Visvanathan and Aris was extended by Altshuller [63] to include isotherms of convex form and irreversible kinetics of any order.

Petroulas *et al.* [64,65] also extended the work of Visvanathan and Aris to the reversible first order reaction $A \rightleftharpoons B$ and with a Langmuir adsorption isotherm. The reaction was a first order and occurred on the surface of the catalyst. In equation 2.13 A* and B* are adsorbed on the catalyst surface. k_r and k_r' are the forward and backward rate of reaction.

$$A_{(g)} \rightleftharpoons A^* \underset{k_r'}{\overset{k_r}{\rightleftharpoons}} B^* \rightleftharpoons B_{(g)} \qquad 2.13$$

The CMCR modelled by Petroulas *et al.* [64,65] consisted of a vertical column in which fine catalytic particles are falling downstream. The carrier gas and reactant are fed through the bottom of the reactor as in figure 2.4. An overall mass balance on species A at axial distance x over the column cross section of an isothermal CMCR is given by equation 2.14. A similar equation can be written for species B.

$$\varepsilon \frac{\partial c_A}{\partial t} + (1-\varepsilon)\frac{\partial n_A}{\partial t} - \varepsilon D_x \frac{\partial^2 c_A}{\partial x^2} + \varepsilon U_g \frac{\partial c_A}{\partial x}$$

$$-(1-\varepsilon) U_S \frac{\partial n_A}{\partial x} + (1-\varepsilon) k_r n_A - (1-\varepsilon) k_r' n_B = 0 \qquad 2.14$$

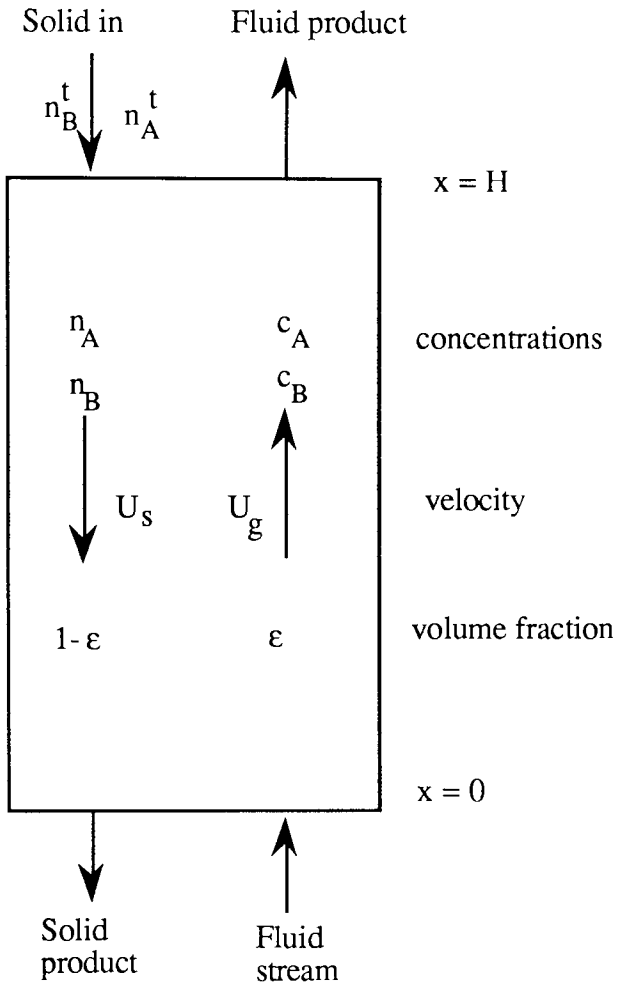

Figure 2.4 Schematic diagram of CMCR

The behaviour of the ideal reactor has been examined for different values of feed concentrations and reactor length. It was shown that under appropriate operating conditions, simultaneous reaction and separation could be achieved. The effect of non-idealities on the behaviour of a CMCR was also studied and the model equations were solved using an orthogonal collocation method.

2.3.3.2 Experimental Investigations

Early experimental studies on CMCR equipment carried out by Takeuchi and Uragachi [69,70] in the oxidation of CO on activated alumina catalyst Al_2O_3 showed the possibility of carrying out simultaneous chemical reaction and separation in a countercurrent moving

bed chromatograph. The chromatograph was similar to the device used earlier by Barker and Critcher [71] for the continuous separation of benzene and cyclohexane.

Other experimental work on CMCR equipment has been carried out by Fish and Carr [72] on the catalytic hydrogenation of 1,3,5 trimethylbenzene (mesitylene, MES) by Pt/Al_2O_3 catalyst to trimethylcyclohexane (TMC) in a laboratory scale reactor. The reactor consisted of a stainless column of 1.3 cm in diameter and 2.24 m long, packed with 30-50 mesh alumnia support material. The system was claimed to be capable of achieving a high conversion in the region of 90% and with a TMC purity approaching 100%. This was a significant improvement compared to the non-separating reactor where the equilibrium conversion was aproximately 50%.

On the other hand, several problems were encountered in operating counter current moving bed columns. There were the difficulties in solid flow control, uneven bed packing, packing attrition, bed fluidisation by the mobile phase and the requirement of a solid recycling unit.

All the previous experimental works on CMCR equipment have been confined to gas-solid systems. No experimental work using a liquid-solid system have been reported to date.

2.3.4 Simulated Counter Current Moving Bed Chromatographic Reactor (SCMCR)

The difficulties associated with the operation of CMCR's can be minimised if the actual counter current movement of the solid and fluid phase is avoided as in the Sorbex technique [73] or the semi-continuous chromatographic refiner (SCCR) system [47-51].

Ray *et al.* [74] carried out numerical studies on SCMCR equipment using the data from the catalytic hydrogenation of 1,3,5 trimethylbenzene (mesitylene, MES) by a Pt/Al_2O_3 catalyst to trimethylcyclohexane (TMC) in a CMCR [20]. For both single column (as in the Sorbex technique) and in the interlinked multicolumn configurations SCMCR, (as in

the SCCR system) the model predicted near complete conversion and high product purity comparable to a CMCR were obtained. However no experimental work to compare with the theoretically predicted results were obtained.

The only experimental work carried out using a simulated countercurrent moving bed chromatographic reactor is in the biochemical field [13,75-79] and will be dealt in the next section.

2.3.5 Biochemical Reaction and Separation in a Continuous Chromatographic Reactor

2.3.5.1 Introduction

Based on published information there are only two research groups engaged in the study of the application of continuous chromatography as biochemical reactor-separators; the Aston University group [13,75-77] and that of Hashimoto *et al.* [78,79]. The former use a flowing eluent stream containing the enzyme whilst the latter used immobilized enzymes.

Hashimoto *et al.* investigated three types of biochemical reaction in three different modes of continuous chromatographic reactor operation:

1. The isomerisation of glucose using an immobilised glucose isomerase in a simulated moving bed counter current system (figure 2.5).

2. The repeated use of free coenzyme adenosine 5-triphospate (ATP) by immobilised hexokinase (HK) and immobilised pyruvate kinase (PK) in a simulated moving bed continuous chromatographic reactor (figure 2.6).

3. The continuous conversion of maltose to glucose by repeated used of the enzyme glucoamylase in a gel chromatographic column (figure 2.7).

The Aston University group used a modified SCCR equipment to carry out the simultaneous biochemical reaction and separation [13,75-77].

1. The continuous inversion of sucrose using the enzyme invertase [13].
2 The biosynthesis of polyglucose dextran from sucrose using the enzyme dextransucrase.were investigated [75].
3. The saccharification of modified starch to maltose and dextrin using the enzyme maltogenase [76].
4. The hydrolysis of lactose to glucose and galactose using the enzyme lactase [77].

2.3.5.2 Hashimoto *et al.* Approach

The first reaction system investigated by Hashimoto *et al.* was the isomerization of glucose to fructose in a simulated moving bed countercurrent chromatographic reactor. The schematic diagram of the experimental apparatus used is shown in figure 2.5. The system consisted of sixteen adsorption columns and seven immobilized glucose isomerase reactor columns. The reactors were 1.38 cm diameter and 10.2 cm long. The adsorption columns were 1.38 cm diameter and 10.2 cm long and were packed with calcium form, Y zeolite (Toyo Soda Mfg, Japan).

The adsorption columns and immobilized reactor columns were connected to form a closed loop as shown by figure 2.5. The countercurrent movement between the liquid stream and the adsorbent was simulated using a multiport rotary valve. The immobilized enzymes reactors were kept stationary. The rotary valve consisted of two stainless steel disks, each bearing 32 holes. The lower disk was stationary, whereas the upper disk was rotated counterclockwise by 22.5^{o} at regular intervals (2 or 3 min).

The system was divided into three zones. In zone 1 the reactor and the adsorption column were connected alternatively, whereas zone 2 and 3 contain only the adsorbent. An equimolar reaction mixture of glucose and fructose was passed through the zone 1. The fructose formed was preferentially adsorbed onto the adsorbent in zone 1. The fructose

was transferred to zone 2 and 3 to be separated from the unreacted glucose and for desorbtion purposes. The glucose was desorbed in zone 2 and the fructose desorbed in zone 3.

In their studies they found that the simulated moving bed process was capable of producing up to 45-65% fructose purities in the product stream. The process was found to require less desorbent than the equivalent fixed bed batch process.

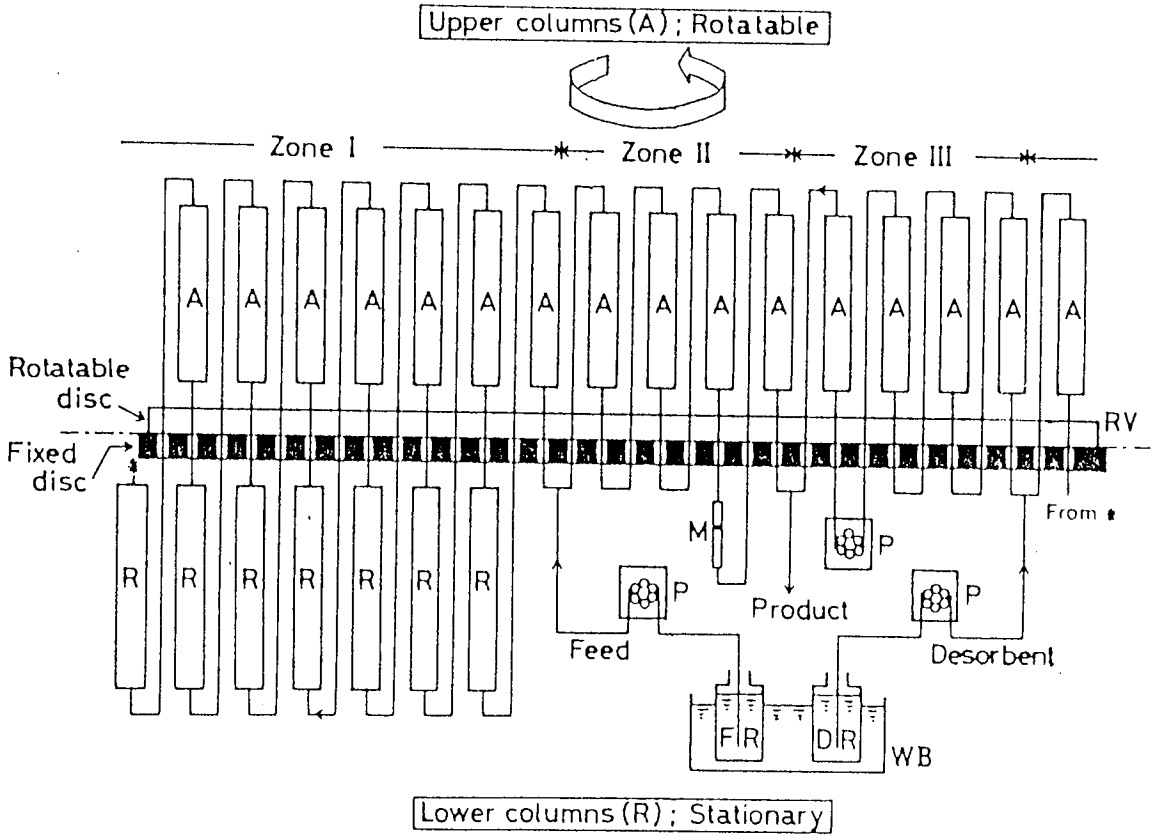

Figure 2.5 Schematic representation of experimental apparatus for producing higher-fructose syrup. RV = rotary valve, A = adsorption columns, R = immobilised glucose isomerase reactors, DR = desorbent reservoir, FR = feed reservoir, M = flow meter, P = constant-feeding pump and WB = water bath.

Although the Hashimoto system as a whole functions as a chromatographic reactor-separator the actual reaction and separation steps have been decoupled due to the use of separate reactor and adsorption columns.

The second biochemical reaction investigated by Hashimoto *et al* [79] is as shown in the following reaction scheme;

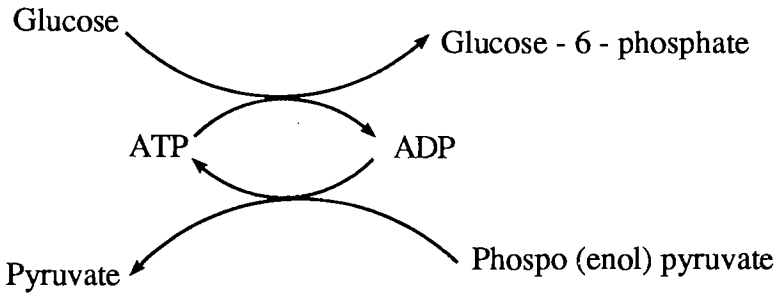

The enzymes were immobilised on to Amberlite XAD-2 by physical adsorption. The resin adsorbed ATP more strongly than the substrates and the products. The column configuration and the principle of operation is shown in figure 2.6.

The system consisted of six columns connected to form a loop. It has one feedstream and two product withdrawal points. Each column is 5 cm long and 1.5 cm in diameter.

The start-up procedures are shown in step (1) and step (2) (see figure 2.6). In theory, once the adsorption of the coenzyme is established, no more addition of the coenzyme is required. The feed point is switched to the next column (step 3) in the same direction as the liquid flow. The switch time is determined by the time taken by the coenzyme to migrate a distance of one column.

The system has been demonstrated to be capable of repeated use of the coenzyme. However more experimental data is needed to evaluate the viability of the system.

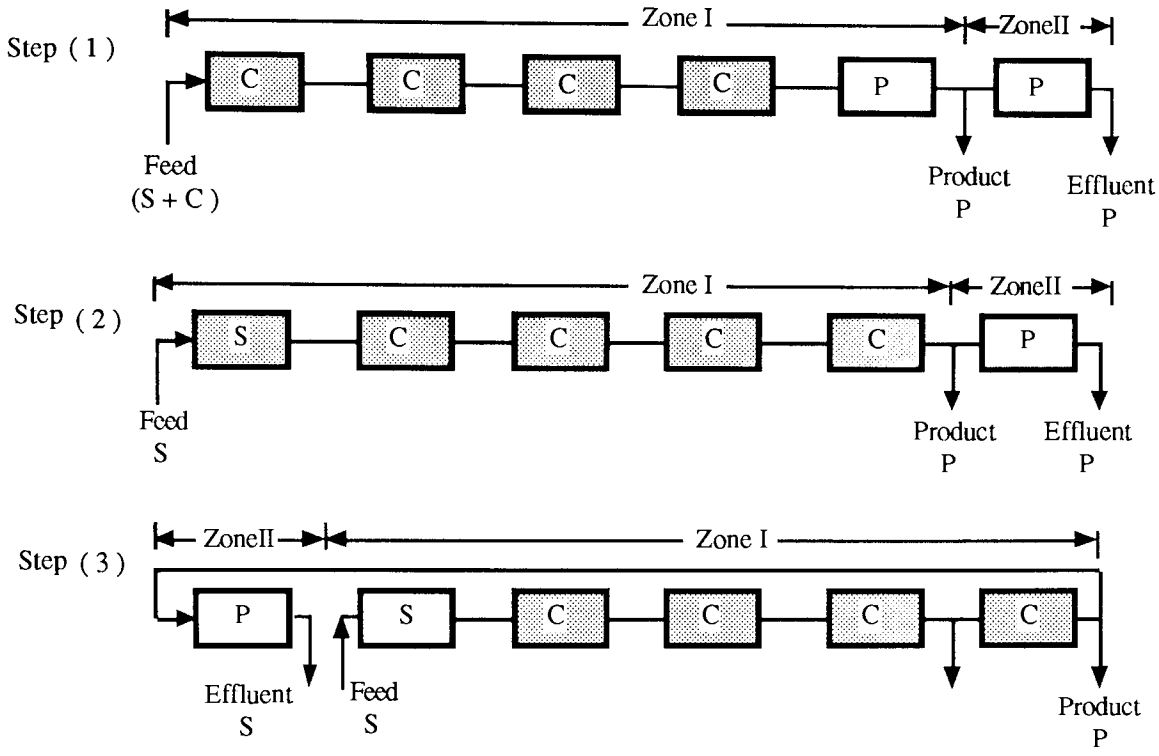

Figure 2.6. Schematic representation of operations repeated use of free enzyme by immobilised conjugated-enzymes reactor of simulated moving type.

The third reaction investigated was the continuous coversion of maltose to glucose using the enzyme glucoamylase. The experimental apparatus was constructed by connecting two chromatographic columns of the same dimension, 1.5 cm diameter and 10 cm in length. The stationary phase used was Bio-Gel P-10.

The reactor principle of operation is shown in figure 2.7. The separation between the enzyme and the product is by a gel permeation mechanism. By changing the position of the feed inlet point and the direction of the flow of the mobile phase (step 1 to step 6) repeated used of the enzyme can be achieved.

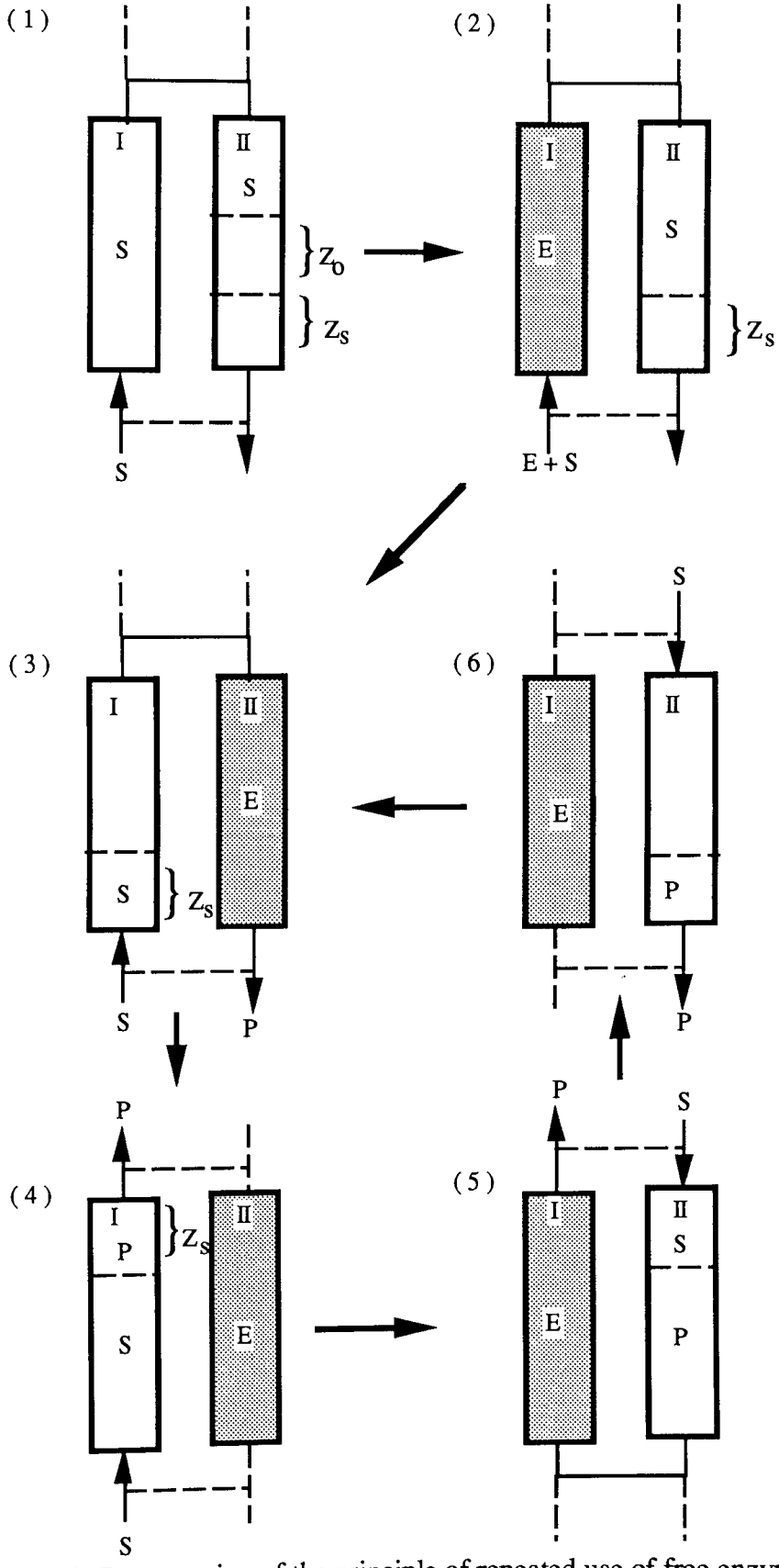

Figure 2.7. Schematic Represention of the principle of repeated use of free enzyme for simultaneous biochemical reaction and separation of maltose into glucose

2.3.5.3 The Aston University Group Approach

Another significant development in simultaneous biochemical reaction and separation in continuous chromatography was contributed by Barker *et al.* [13,75-77] at Aston University. They developed a chromatographic biochemical reactor based on the semi-continuous countercurrent chromatographic separator system, where both reaction and separation take place in the same chromatographic column. The system, semicontinuous counter-current chromatographic reactor-separator (SCCR-S1) was initially used to study the inversion of sucrose to glucose and fructose using the enzyme invertase [13].

The pilot scale system consisted of twelve 5.4 cm internal diameter and 75 cm long stainless steel columns connected at the top and bottom to form a closed loop. The column was packed with an ion exchange resin in the Ca^{2+} form. Six pneumatic poppet valves were connected to each column namely the feed, eluent and purge inlet valves, the glucose rich (GRP) and fructose rich (FRP) product valves and the transfer valve to the next column.

The principle of operation of the SCCR-S1 is shown in figure 2.8. The two diagrams correspond to two consecutive switches. In switch (a) the feed and the eluent is fed to column 7 and 1 respectively and flows a clockwise direction, the less strongly adsorbed component glucose being eluted by the eluent towards the glucose product off-take at column 11. Meanwhile, column 12 is isolated from the loop by closing the indicated transfer valves. A purge stream of a deionised water is fed to the column to desorbed the adsorbed fructose and exits from the column as the fructose rich product.

After a set of time interval known as the switch time, all the port functions are advanced by one column in the direction of the mobile phase as shown in switch position two. This advancement of port function results in a simulated movement of the stationary phase in an opposite direction to the mobile phase flow. Column 1 is then purged and at the same time the feed and the eluent enter column 8 and column 2. The glucose rich product exits from

column 12 and the operation is repeated at the next switching. A cycle of 12 sequences was completed when each column has been used as the feed and purge location. To achieve the separation of the reaction products, the rate of port advancement should be greater than the fructose migration velocity and lower than the glucose and unreacted sucrose migration velocity.

Complete sucrose conversion was obtained for feed concentrations of up to 55 % w/v when using 30% of the theoretical enzyme requirement. Product purities of over 90 % were readily obtained. The product concentration and production throughput of over 5% w/v and 16 kg sugar/m^3 resin/h were achieved. With sucrose inversion using the enzyme invertase, substrate concentrations higher than 12 % w/v have an inhibition effect on the enzyme [82]. SCCR-S1 studies have shown that substrate inhibition can be minimised with this type of processing.

SWITCH (A)

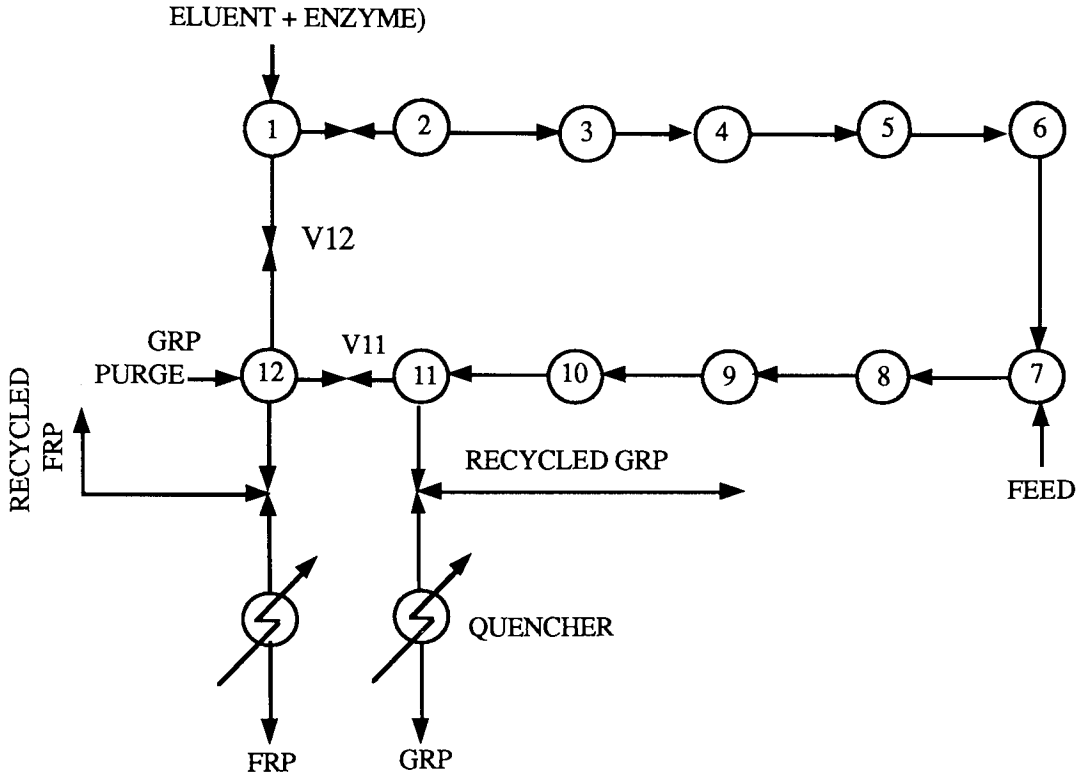

SWITCH (B)

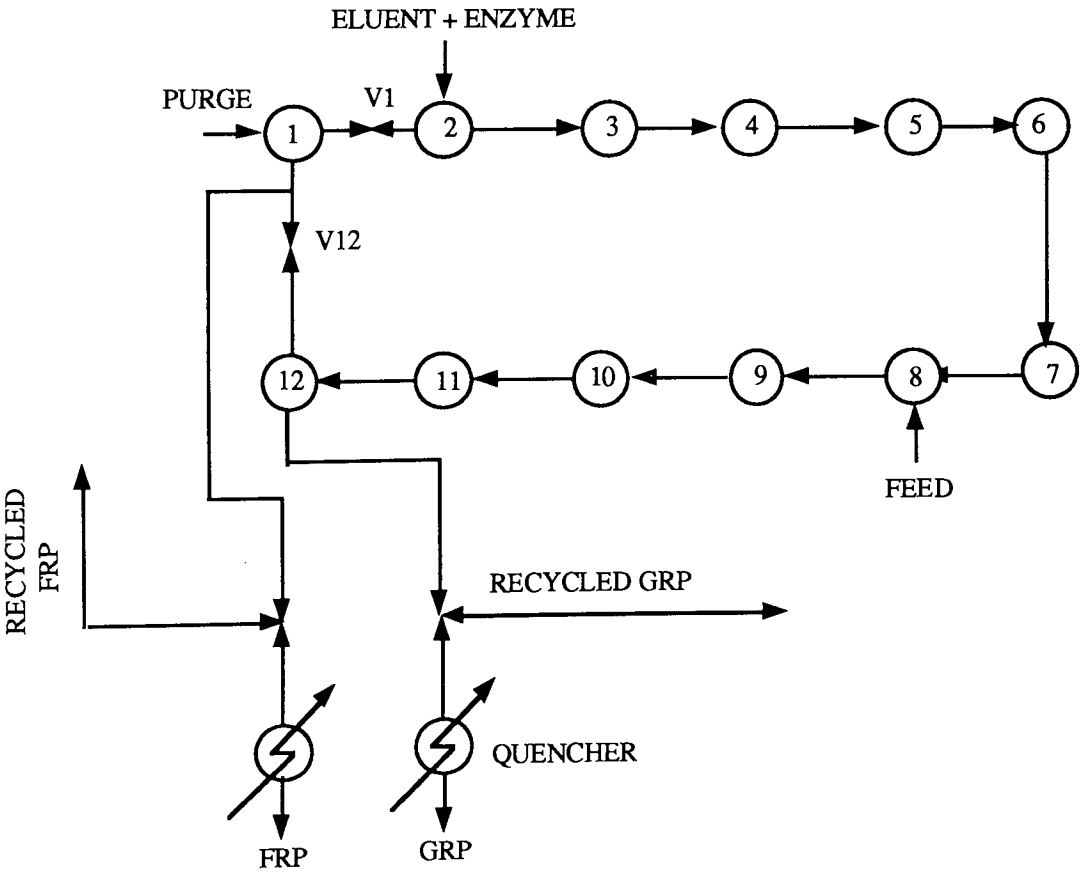

Figure 2.8 Schematic representation of the SCCR-S1 Operating principle.

The second enzyme reaction investigated by the Aston Group was the biosynthesis of dextran using the enzyme dextransucrase. In the biosythesis of dextran the operation was similar. The enzyme was introduced at the required activity in the eluent stream. The dextran formed was the fastest eluted component, due to its size exclusion, while fructose was again retarded by the resin.

At 2-5 % wt/v sucrose concentration, 100 % sucrose conversion was achieved. Over 60% of the dextran produced had molecular weights greater than 2,000,000 daltons.

The third enzyme reaction investigated by the Aston Group was the saccharification of modified starch (Starch C) to maltose and dextrin using the enzyme maltogenase. Using feed throughputs of up to 113g/h, conversion of up to 60% and maltose purities of up to 95.8% were achieved [76].

A mathematical model was also developed to simulate the inversion of sucrose to glucose and fructose on the SCCR-S1 [13]. The mixing cell model [13] was adopted (figure 2.9). In the model, a pseudo-first order reaction kinetic for sucrose inversion was assumed.

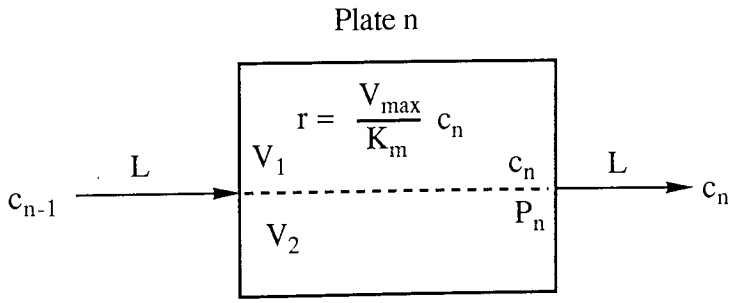

Figure 2.9 Mixing cell model

A mass balance for the reactant over plate n gives:

$$V_1 \frac{dc_n}{dt} + V_2 \frac{dP_n}{dt} = Lc_{n-1} - r V_1 \qquad 2.15$$

Where

V_1 = volume of the mobile phase

V_2 = volume of the stationary phase

P_n = concentration of solute on the stationary phase

c_n = concentration of solute in the mobile phase

Similar equations for the glucose and fructose were obtained. Under linear equilibrium distribution coefficient the linear ordinary differential equations were solved analytically using the Laplace transformation technique. Good agreement between experimental and theoretical predictions were obtained.

2.4 Summary

This review has shown that chromatographic reactors have potentially a wide range of applications. The earlier studies on gas chromatographic reactors demonstrated the potentials of the system for kinetic studies. The later studies on liquid chromatographic reactors has opened up a new area to include the biochemical reaction systems. The Aston University group has successfully demonstrated the use of preparative-scale batch and semicontinuous counter-current chromatographic reactor-separators for biochemical applications. However, there have been only a limited number of applications on preparative scale simultaneous biochemical reaction and separations recorded to date. It is the aim of the thesis to demonstrate for the first time the possibility of carrying out simultaneous biochemical reaction and separation using a preparative scale continuous rotating annular chromatograph.

CHAPTER THREE

EXPERIMENTAL DETAILS

3.1 Experimental Equipments

3.1.1 Continuous Rotating Annular Chromatograph (CRAC)

3.1.1.1 Introduction to CRAC

The continuous rotating annular chromatograph used in this study was constructed by Thirkill [80] based on the design by Scott *et al.* [57]. Details of the design and construction have been previously described by Barker and Thirkill [53]. The chromatograph was originally built to study the separation of carbohydrate mixtures which included the separation of synthetic mixtures of sucrose, glucose and fructose [80], and the separation of sucrose from non-sugars in beet molasses [54,81]

3.1.1.2 Description of the CRAC

The photograph and the schematic view of the CRAC are shown in plate 1 and figure 3.1.

3.1.1.3 The Annulus

The chromatograph was made of two concentric cylinders which formed an annulus (A) 140 cm long, 29.7 cm external diameter and 1.2 cm wide, giving an annular volume of 14.5 dm^3 (figure 3.1). The concentric columns were supported at the top and bottom by two 2.5 cm thick stainless steel (type 316L) flanges. The top stainless steel flange (C) had at its centre a housing for an inlet stationary distributor block.

The outer cylinder (B) was made of a 150 cm long glass pipe and the inner cylinder (S), type 304L stainless steel (RGB Stainless Ltd., Smethwick). The inner stainless steel cylinder was blanked off at its upper end by a flat stainless steel flange (F) to give a 10 cm head space.

To ensure an even eluent flow distribution throughout the annulus, a uniform diameter borosilicate glass pipe (Schott Process Plant Ltd. Stafford) was chosen. This was the best specification available commercially, in the diameter range required (an internal diameter accurate to $\pm$ 4 mm).

Even though the maximum safe working pressure for the glass column was only 101 kNm^{-2}, it allowed visual observation of the column internals (the resin bed, the eluent level and the position of the feed pipe). It was important to observe the column internals, especially during packing of resin into the annulus, so that any inhomogeneity could be detected and rectified by repacking the resin. It was also found that air could get into the chromatographic column and accumulate in the form of air pockets and fissures within the resin bed. The occurrence was more frequent when the chromatograph was operated at elevated temperature (55-60^{o}C). The presence of air in the resin bed would reduced the adsorption capacity of the resin and caused deterioration in the performance of the chromatograph due to maldistribution of the eluent flow. The use of glass allowed these observations to be made.

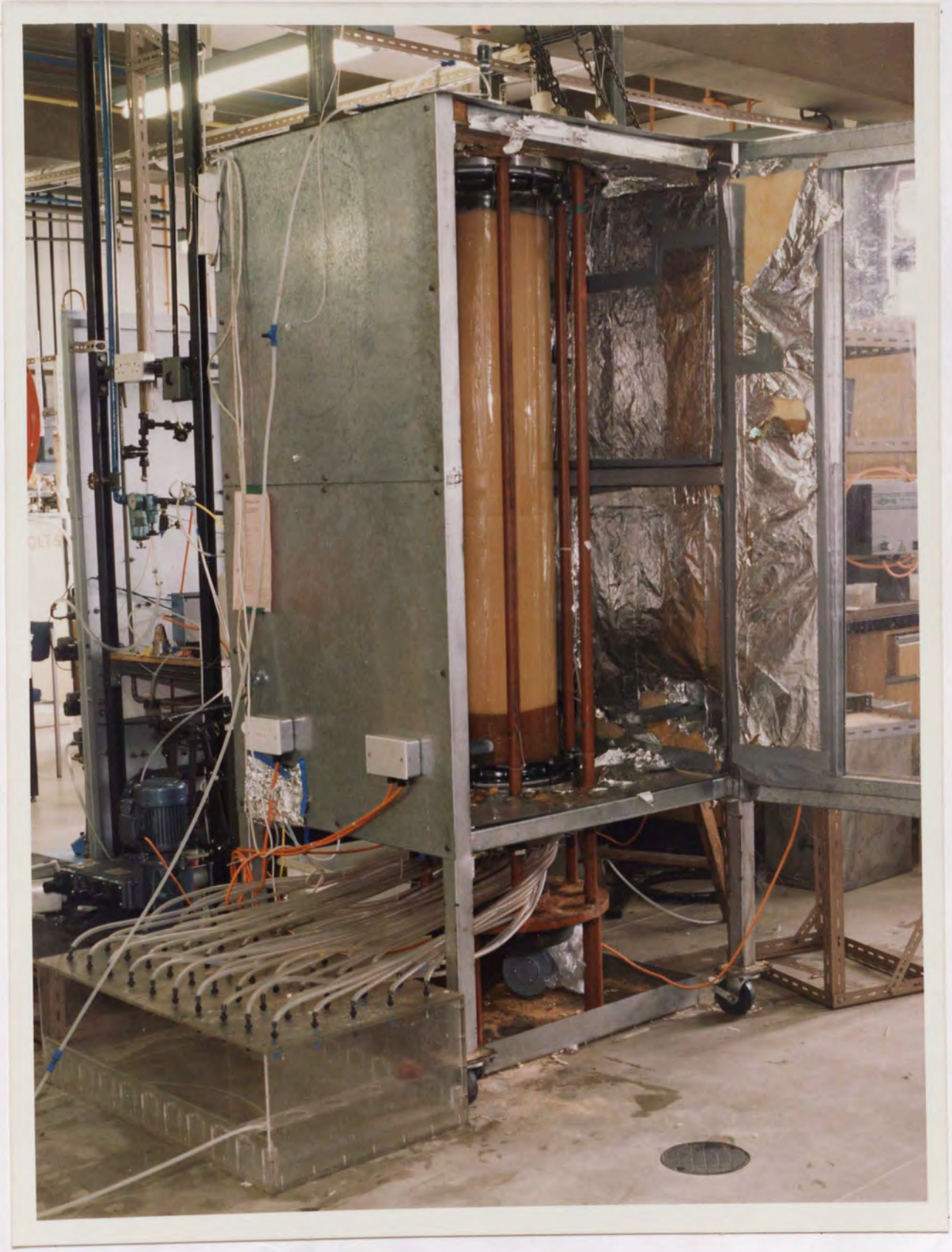

Plate 1. Photograph of the CRAC used in these studies

Key to Figure 3.1

A	The Annulus/ Resin
B	Glass Outer Column
C	Upper Stainless Steel Flange
D	Lower Stainless Steel Plate
E	Inlet Distributor
F	Stainless Steel Blanking Flange
G	Eluent Inlet Point
H	Pressure Relieve Valve Connection Point
I	Pressure Gauge Connection Point
J	Feed Pipe
K	Column Inlet
L	Thermocouple Well
M	Stainless Steel Ring
N	Porous Polyethylene Disc
O	Polyamide Tube
P	Polypropylene Product Collector
Q	Drive Pulleys and Belt
R	The Outer Framework
S	Inner Stainless Steel Column
T	Head Space

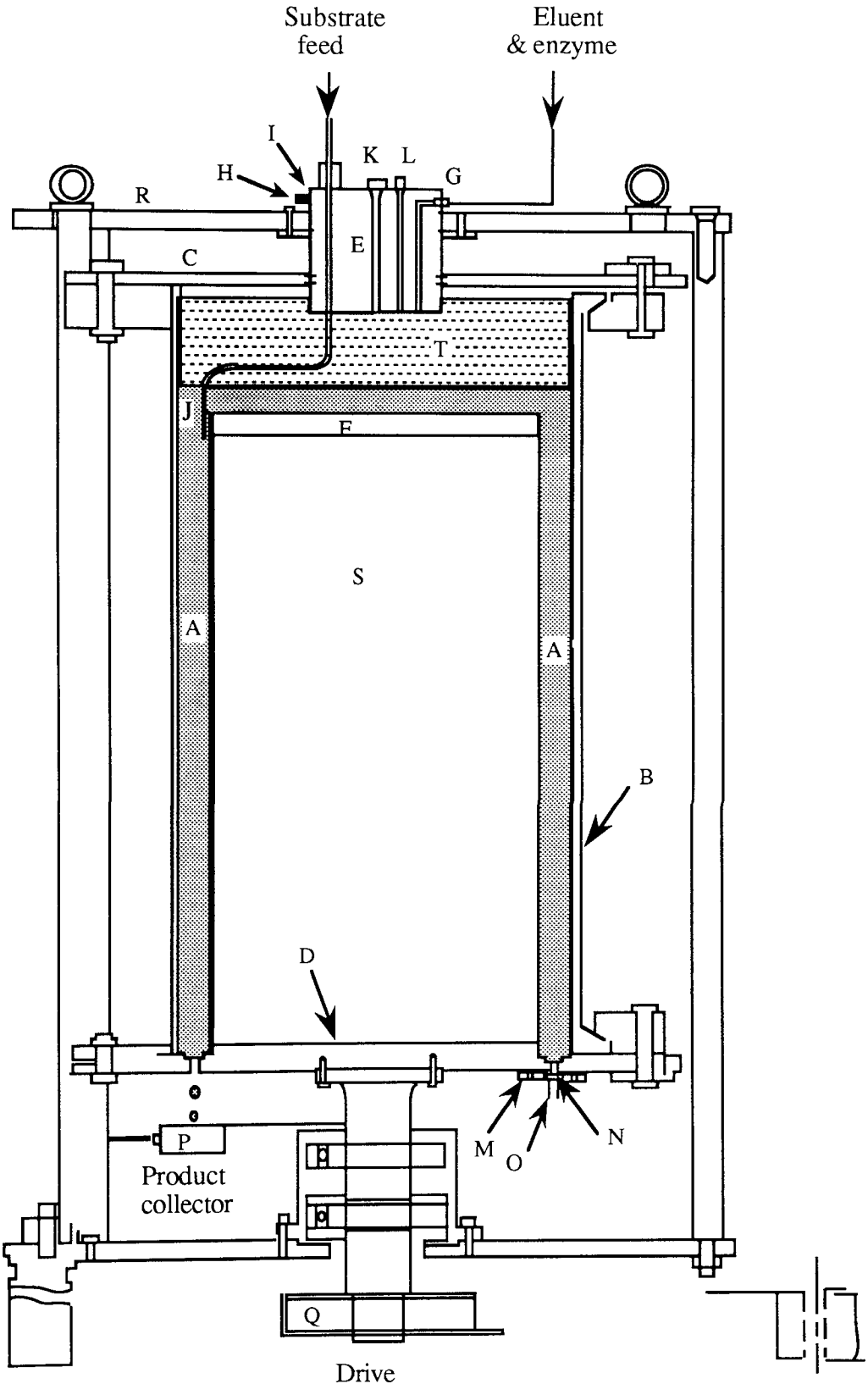

Figure 3.1 CRAC Assembly

3.1.1.4 The Inlet Distributor

The inlet stationary distributor block (E) was located in the top flange by means of two nitrile O-rings fitted into grooves around the distributor. The O-rings acted as a pressure seal and a bearing between the stationary distributor block and the rotating chromatographic column.

The inlet stationary distributor block served as the entry point for the eluent pipe (G), the feed pipe (J), the connection for the pressure gauge (I), the safety relief valve (H) and the thermocouple well (L). The feed pipe was made of thin walled 5 mm outside diameter stainless steel tubing. The feed pipe was adjustable, allowing its height and position of the nozzle in the annulus to be manoeuvred externally. The safety relief valve was set at 95 kNm^{-2} to protect the glass column.

3.1.1.5 The Lower Plate

The lower stainless steel flange (D) retained the two concentric columns at the bottom of the annulus. A stainless steel ring (M) with one hundred evenly spaced exit holes of 0.32 cm diameter was fitted to the lower stainless steel flange. Each of the exit holes were counter-bored to a diameter of 0.7 cm and a depth of 0.3 cm to accomodate a porous polyethylene disc (N). The porous polyethylene discs had a pore size of 60-90 μm which were small enough to retain the resin. Three cm long polyamide tubes (O) were fitted to the exit holes to prevent lateral mixing of the liquid between the adjacent holes.

3.1.1.6 The Motor Drive

The lower flange was mounted on a turn table which was slowly rotated by a variable speed DC motor (DRPM805A Type, Normand Electrical Co Ltd, Aylesbury). The DC motor speed was electronically controlled allowing a range of rotational speeds of 0.4 - 1.44 $revh^{-1}$.

3.1.1.7 Product Collection

The liquid exiting from the polyamide tubes dropped into a stationary plate (P) containing 50 equally spaced collection points covering the circumference of the annulus. Fifty lengths of PVC tubing were attached underneath the collector and these passed to a rectangular perspex tank containing fifty sample bottles (Sterilin, Appleton Woods, Birmingham). Each sample bottle contained 0.2 cm^3 of 1 molar NaOH solution (for sucrose inversion experiments) or 2 cm^3 of saturated $Ca(OH)_2$ solution (for starch saccharification experiments) to bring the pH of the samples to 10-12. In addition, the sample bottles were placed in an ice bath during the sampling to inhibit any further enzymic reaction taking place.

The samples collected from the system were analysed using an HPLC system fitted with a carbohydrate column (Aminex HPX-87C, Biorad UK Ltd.).

3.1.1.8 Temperature Control

The entire CRAC was enclosed in a temperature controlled cabinet, 1.66 x 1.02 x 0.92 m. Four 1 kW heating elements (Eltron Ltd., London) and two fans (Woods of Colchester, Essex) were used to distribute the heat evenly. The inlet process streams were passed through heat exchangers to maintain the desired operating temperature.

3.1.1.9 Metering Pump

A multiple head metering pump (E-range series, MPL Pump Ltd, Middlesex) was used to deliver the eluent, enzyme and feed. The pump was driven by a single-phase 0.45 kW AC motor.

3.1.2 Batch Chromatographic Biochemical Reactor

Before commencing experiments on the CRAC, it was decided to perform preliminary experiments using a conventional batch chromatographic column since the results would be helpful in assessing the likelihood of the successful operation of a CRAC using the same enzyme system.

The preliminary experiments of simultaneous biochemical reaction and separation of modified starch to maltose were carried out in a batch chromatographic column. The schematic diagram of the equipment is shown in figure 3.2.

The reactor column was 1.98 cm diameter and 150 cm long. The chromatographic column was made of a jacketed glass column. The chromatographic resin used was a calcium form of Dowex 50W-X4, a similar resin to that used in the CRAC, the column being slurried packed.

The column was operated at 60°C. The eluent consisted of diluted enzyme maltogenase at a pH 5.3, which was pumped into the reactor column by a peristaltic pump. The modified starch was injected as a pulse and the outlet stream was monitored using a differential refractometer linked to a chart recorder. The detected components in the outlet stream were analysed using an HPLC fitted with a carbohydrate analytical column (Section 3.3.2).

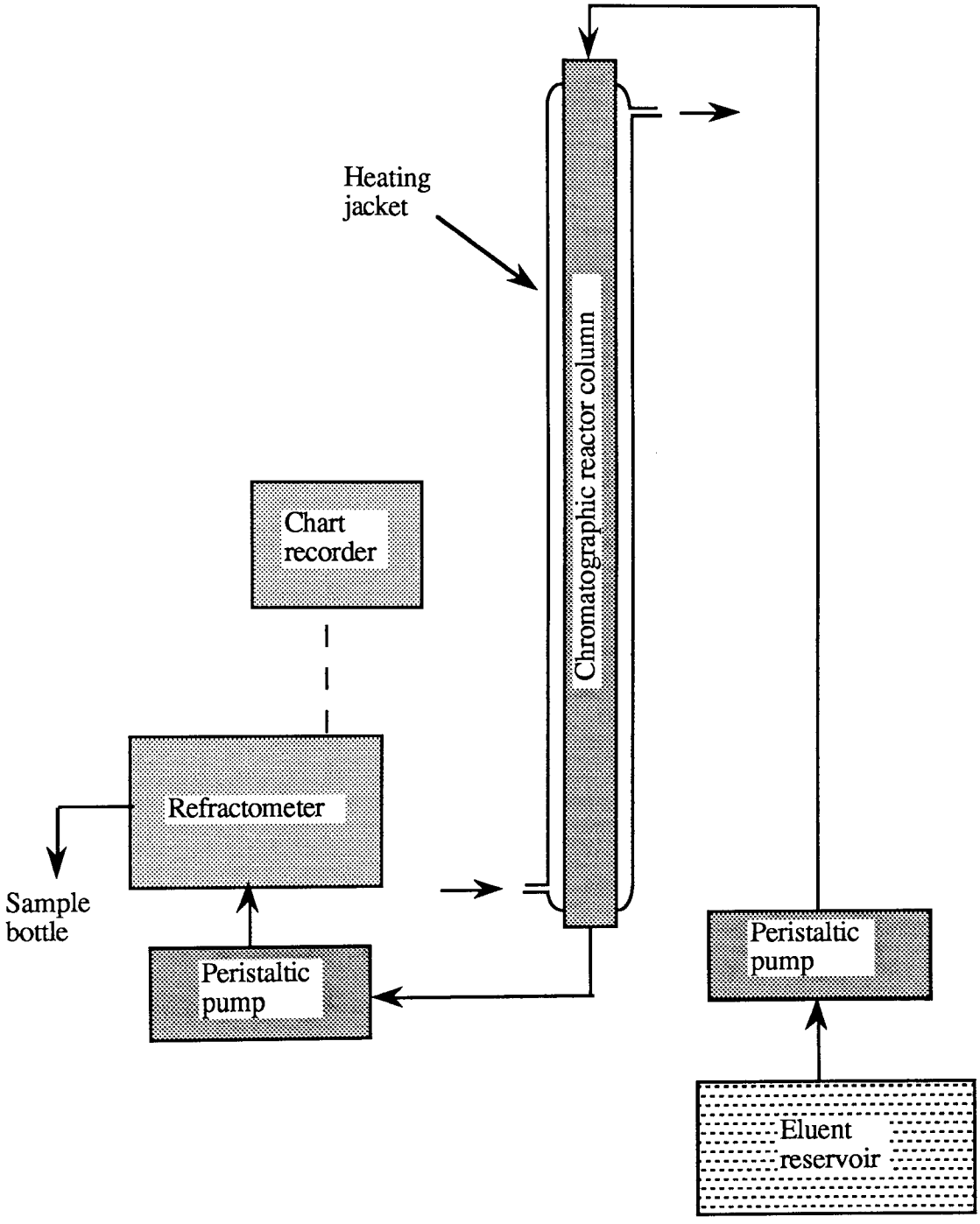

Figure 3.2 Schematic diagram of batch chromatographic reactor

3.2 Experimental Procedure for the CRAC and Batch Chromatographic Reactor

3.2.1 Eluent, Substrate and Enzyme Preparation

3.2.1.1 Eluent Preparation

The deionised water was prepared using an Elgastat B224 water deionisation unit (Elga Water purification, High Wycombe) and stored in a 500 dm^3 overhead tank. The deionised water was first filtered and transferred to a constant temperature deaerator tank where it was heated to 70^oC to remove the dissolved air (see figure 3.3). The deaerated and deionised water was transferred to a constant temperature eluent tank where it was cooled down to 20^oC using a circulating water chiller (Churchill) before being pump into the chromatograph. A constant temperature was required to ensure a constant pumping rate by the eluent pump.

Before entering the chromatographic column the eluent passed through a second 50 micron filter and a heat exchanger to maintain the desired operating temperature.

3.2.1.2 Feed Preparation

A range of feed materials were used in the studies. They were;

1 A pure crystalline fructose (Roche products Ltd. Dunstable, Bedfordshire).

2 Anhydrous crystalline glucose and maltose (Sigma Chemical Co. Ltd. Poole, Dorset).

3 Sucrose (British Sugar, Kidderminster)

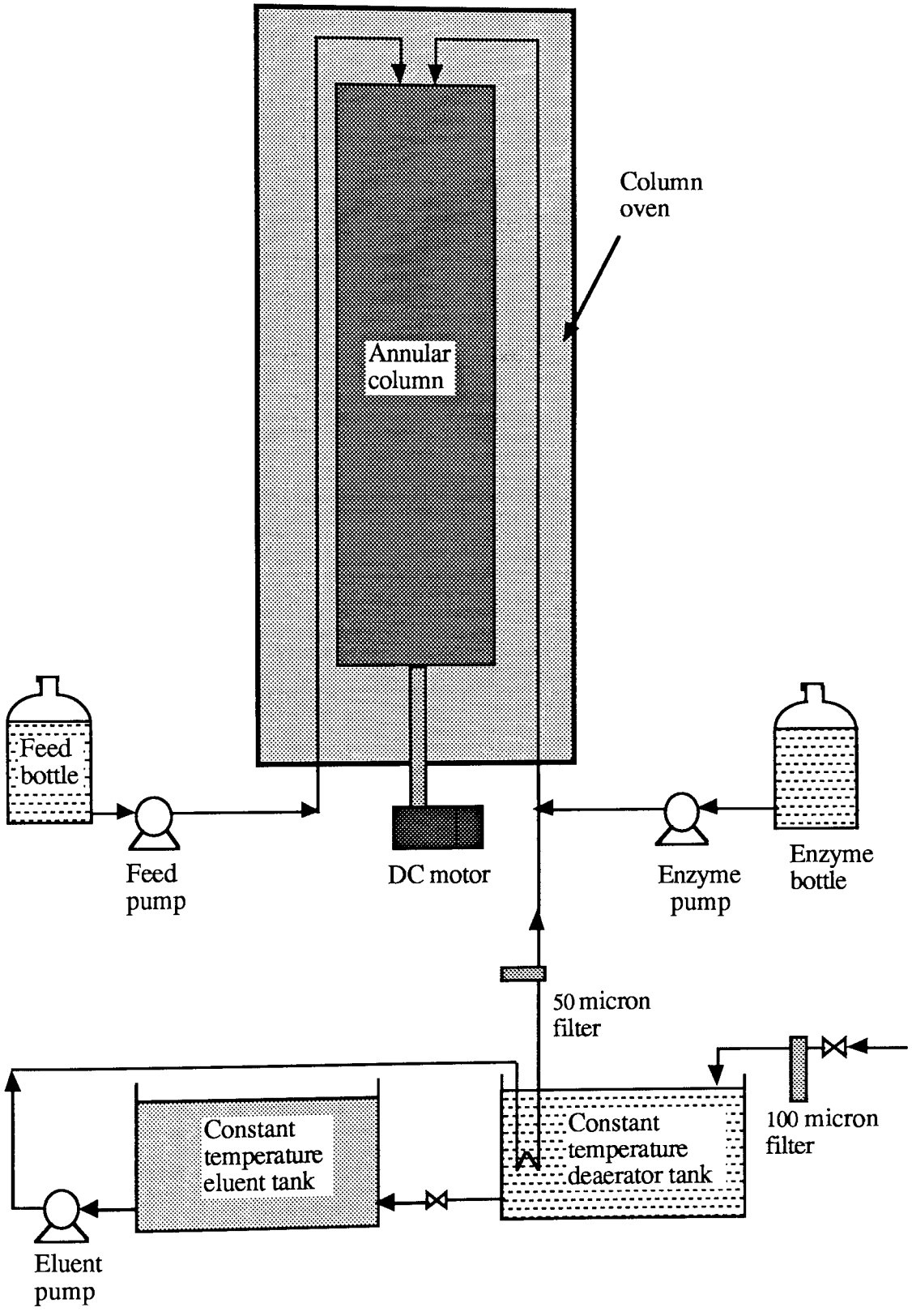

Figure 3.3 CRAC layout

4 Soluble Starch (starch A) and soluble potato starch (starch B) (Sigma Chemical Co. Ltd. Poole, Dorset).

5 Crystal Gum UK^{R} (starch C), a modified tapioca starch (National Starch, Old Trafford, Manchester)

In separation experiments, a feed solution of the required concentration was prepared by dissolving the calculated weight of the sugars in deionised water. Fructose, sucrose and maltose were easy to dissolve. Glucose on the other hand, required rigorous stirring to get it to dissolve.

Inverted feed was prepared by inverting sucrose to glucose and fructose using the enzyme invertase. The inversion reaction was carried out in a batch reaction flask at a sucrose concentration of 50% w/v, pH 5.2 and 50^{o}C and the inversion was completed in 12 hours. The enzyme loading or activity recommended by the manufacturer (Biocon, Tenbury Wells, Worcetershire) was used (0.16 % w/v or 200 U/cm^{3}).

In the experiments of saccharification of modified starch to maltose, the substrate preparation was as follows; a suitable quantity of each type of starch A, B or C was slurried in water and the pH was adjusted to 5.3. The solutions were heated with continuous stirring to 100^{o}C and the volumes were adjusted to give concentrations varying between 5-40% w/v. In the case of starch B, it was thinned using 0.2 % w/v heat labile fungal amylase, Fungamyl 800L^{R} (Novo-Nordisk, Farnham, Surrey) at 60^{o}C for 5 minutes to prevent retrogradation taking place. The feed solution was filtered (sintered glass filter, Whatman) and transferred to a feed flask.

3.2.1.3 Enzyme Preparation

The enzyme invertase containing glycerol as stabiliser was used without purification. The enzyme was stable with only 2% loss of declared activity over a period of six months when stored at 4^{o}C.

On the other hand, the enzyme maltogenase contained maltose as the stabiliser. The maltose had to be removed from the enzyme solution.

A pilot scale ultrafiltation membrane system constructed by Akintoye [82] was used to purify the enzyme. The system consisted of a cold storage compartment, a membrane module fitted with a 30,000MW membrane cassette of 0.464 m^2 area (Milipore) and a peristaltic pump (701 S/R, Watson Marlow, Plymouth). Maltose was completely removed after 8 dialfiltrations. Sodium azide NaN_3 (0.02% w/v) was added to the purified enzyme solution to prevent microbial attack and the enzyme was then stored at 4 ^oC.

3.2.2 CRAC Operating Procedure

Two types of experimental studies were performed on the CRAC;

1 The physical separation of saccharides ;
   - separation of sucrose-glucose-fructose
   - separation of inverted sucrose
   - separation of maltose-dextrin

2 Simultaneous biochemical reaction and separation experiments. Two types of enzymes were used;
   - the invertase for the inversion of sucrose to glucose and fructose.
   - the maltogenase for the saccharification of starch to maltose.

The procedure adopted was as follows:

1 The DC motor drive was switched on and the speed controller set at the speed required, measured in degrees per hour.

2 The column oven heater and the air circulating fan were switched on. The temperature controller was set at the operating temperature (the operating temperatures for glucose-fructose separation and sucrose inversion was 55^oC and for maltose production was 60^oC). The temperature within the oven, the headspace

and eluent exiting from the annulus were monitored using fast response exposed junction thermocouples (Comark Electronics Ltd, West sussex). It took about six to eight hours to heat the CRAC from room temperature up to 55^{o}C. The equipment was therefore maintained at the operating temperature. This helped to prolong the service life of the resin by subjecting the resin to less heating and cooling cycles. Repeated heating and cooling had adverse effect on the resin performance.

A temperature cut-out was incorporated into the temperature control system as a protection against overheating.

3 The eluent was prepared according to the procedure described in section 3.2.1.1. The eluent pump was set to the required flowrate. Time had to be allowed for the internal pressure to reach a steady value. The flowrate was measured using a rotameter which had been calibrated. The rotameter measurement was also checked by directly collecting the eluent discharge in the sample collection tank.

4 A 50 cm^3 burette was used to calibrate the feed pump flow rate. The time for the liquid level to drop from 50 cm^3 to 0 cm^3 was measured and the pump setting adjusted until the required flowrate was obtained.

The feed solution was prepared according to procedures as described in section 3.2.1.2. The feed solution was filtered and placed in a graduated feed flask and fed to the pump using polyamide tubing.

5 After the introduction of the feed solution, the time taken to reach steady state varied with the operating conditions (eluent flowrate and component distribution coefficients). Time had to be allowed for the most strongly retained component to elute from the chromatograph. Steady state was reached when the elution profile was invariant with time. It was determined by repeatedly taking samples from selected positions around the annulus and monitoring their composition changes with respect to time.

For example when using glucose and fructose mixtures at an eluent flowrate of 8 dm^3/h and a rotation rate of $240^o/h$, two column revolutions were required to ensure all components in the feed mixtures had eluted.

6 Samples were taken when equilibrium had been established. Knowledge of the time required to achieve steady state was important to avoid unnecessary repeated sampling. Clean and dried 150 Sterilin sample bottles, were arranged in the collection tank. The samples were filtered into vials and put on the turntable of the autosampler for analysis.

7 In simultaneous biochemical reaction and separation studies a few additional steps were followed;

Enzyme solution was filtered and placed in an enzyme flask. With the invertase-sucrose system the enzyme invertase was mixed on-line with the eluent by mean of a T-connector just before entering the column. In the maltogenase-starch system experiments the enzyme was mixed on-line with the feed stream just before entering the column. The required activity was achieved by controlling the enzyme pumping flowrate.

With the invertase-sucrose experiments the chromatograph was flushed with eluent containing the enzyme equivalent to the head space and one bed void volume. Only then was the sucrose substrate introduced.

3.2.3 CRAC Maintenance Procedure

After an experimental run had been completed, the feed and enzyme pumps were switched off. However the eluent pump was left running continuously. The feed and enzyme containers were rinsed and refilled with a $0.02g/cm^3$ solution of sodium azide. This was pumped through the feed enzyme inlet tubes until they had been flushed out.

During a shut down period, the column oven and the DC motor were switched off. The eluent pump was connected to a timer set to pump the eluent periodically to maintain the liquid level in the head space.

3.3 Analysis

3.3.1 Introduction to Analytical Equipment

The analytical equipment used in this work were high performance liquid chromatography (HPLC) and gel permeation chromatography (GPC). HPLC was used to analyse samples from the chromatograph, the enzyme purification work and the enzyme kinetic studies. GPC was used to obtain the molecular weight (MW) of soluble starch used in the maltose production experiments.

3.3.2 Analytical HPLC

3.3.2.1 System Description

The saccharides (sucrose, glucose, fructose, maltose, maltotriose and dextrin, soluble starch) composition and concentration were determined using an HPLC system fitted with a carbohydrate analysis column (Aminex HPX-87C, Biorad UK Ltd. Watford). The HPLC analytical system (figure 3.4) consisted of;

- A Bio-Rad 1330 Pump (Bio-Rad UK Ltd. Watford)
- A Bio-Rad column heater
- A Bio-Rad differential refractometer type 1750
- A Talbot ASI-3 Autosampler (Talbot Scientific, Alderley Edge, Cheshire)
- A Spectra-Physics Integrator Type SP4270 (Spectra Physics St Albans, Herts)
- An Anachem (Luton, Bedfordshire) debubbler to trap any air bubbles in the eluent delivery tubing.
- A Rheodyne manual sample injection valve model 70-10 for manual injection.

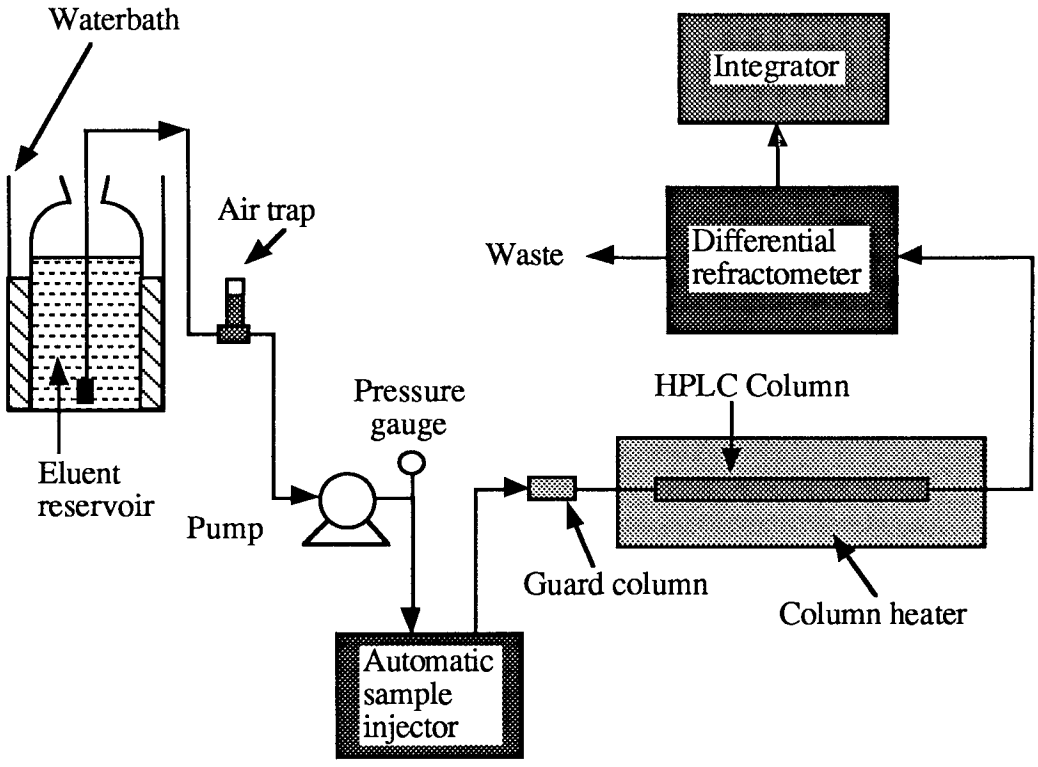

Figure 3.4 HPLC Analytical system

3.3.2.2 The Separation of Saccharides Using an Aminex HPX-87C Column

The Aminex HPX-87C column was 30 cm long and 0.78 cm diameter, packed with 8% crosslinked cation exchange resin in the calcium form. The particle size of the resin was 9 μm. The column is designed to separate saccharides by a number of mechanisms which are called by a generic term " ion-moderated-partitioning" [83]. Ion-moderated-partitioning provided multiple mechanisms for saccharides separation depending on the eluent used and the types of saccharides being separated.

Under the isocratic elution mode with distilled and deionised water as the eluent, the main separation mechanisms are size exclusion and ligand exchange. At present ion-moderated-partitioning remains the best method for saccharides analysis using HPLC [83].

3.3.2.3 HPLC Operation

The analysis samples were filtered through a 5 μm membrane filter (Gelman Science Ltd., Northampton) into 2 cm^3 sample vials (Chromacol Ltd, London). The autosampler was set by selecting the sample position, sampling time, analysis and delay times using the appropriate digital switches. The sampling and injection of a sample was carried out automatically by the autosampler. A turntable on the autosampler could accomodate 60 of these vials. Samples can also be injected into the column by means of a manual injection valve.

The components resolved by the column were detected at the column outlet by a refractive index detector (R.I). The integrator processed the R.I data to give the sample chromatogram. The components on the chromatogram were identified by their retention times while the component concentrations were determined by the areas under the elution profiles.

During analysis, the chromatographic column was maintained at 85°C to avoid the formation of broad peaks due to slow diffusion processes, and doublet formation that result from anomer resolution at room temperature.

3.3.2.4 System Maintenance

To maintain the performance of the HPLC, the following precautions were taken;

- the eluent (distilled deionised water) was filtered using a 10 μm slip-on filter.
- A guard column, Hibar-Lichocart cartridges (BDH Chemical Ltd, Atherstone, Warwickshire) was used as pre column filter.
- 0.02 g dm^{-3} calcium acetate was mixed with the eluent to replace any calcium ions displaced from the resin by other ions.
- The column was reversed if the column pressure drop exceeded 10.1 x 10^4 kNm^{-2}.

- When the separation was poor, the column was cleaned with a 30% acetonitrile/water mixture, followed by regeneration using 0.1M calcium acetate solution.
- The optical cell of the R.I was cleaned with 6M nitric acid if the detection sensitivity dropped significantly.

3.3.3 Analytical Gel Permeation Chromatography

3.3.3.1 Equipment Description

The GPC system was used to obtain the MW of soluble starch. In GPC analysis, the separation mechanism is based on a size exclusion mechanism. The GPC system used shared a common configuration and components with the HPLC system. Therefore, the system will be described only briefly.

Basically, the system consisted of an eluent pump (model 1330, Bio-Rad UK Ltd. Watford), a fractionating column (Lichro sphere diol column, Merck), column heater, differential refractometer (model R401, Waters Associates Ltd, London), Rheodyne sample injection valve, Chart recorder (Venture Servoscribe, RE 541.2, Smith Ltd,) and a PET micro computer (model CBM 4032, Commodore, UK). The micro computer was used for on-line data aquisition and data processing.

The GPC column was calibrated using Pharmacia dextran T-2000 (MW 2,000,000) and glucose (MW 180). The computer program run on a PET micro computer originally written by Vlachogiannis [86] was used in the data aquisition and data processing to calculate the molecular weight of the sample.

3.3.4 Enzyme Assays

3.3.4.1 Introduction to enzyme assay

The activity of the enzyme invertase was determined using the invertase assay [82,84]. For maltogenase, the activity was determined using a chromatographic method [85].

3.3.4.2 Invertase Assay

Invertase (β-fructofuranosidase E.C. 3.2.1.2.6) from *Saccharomyces cerevisiae* was purchase from Biocon (Tenbury wells, Worcetershire). The enzyme was in a soluble liquid form with a declared activity of 11.6 x 10^3 units/cm^3. One unit of activity of the enzyme is defined as the amount of enzyme that will convert 1μmol of sucrose in one minute at pH 5.2 and 55°C.

The enzyme invertase hydrolyses the terminal non-reducing β-fructofuranoside residues of sucrose to yield an equimolar mixture of glucose and fructose (invert sugar). The invert sugar released is then reacted with 3, 5 -Dinitrosalicyclic acid (DNS). The colour change produced is propotional to the amount of invert sugar released, which in turn is propotional to the activity of the invertase present in the sample.

The procedures were as follows; 0.1 cm^3 of suitably diluted enzyme solution was added to 1.4 cm^3 of distilled water and 0.5 cm^3 of acetate buffer (0.05 sodium acetate and acetic acid to adjust the pH to 5.2). The reaction tube was then incubated for 10 minutes at 55°C. 1 cm^3 of 0.3M sucrose was added to the reaction tube and incubated further for exactly 10 minutes. Reaction was stopped by the addition of 2 cm^3 of chilled DNS solution and immersion in a boiling water bath for 10 minutes. The solution was then cooled rapidly in an ice bath and 15 cm^3 of distilled added. The OD_{540} was read against a reagent blank and the micromoles of reducing sugar was determined from a total reducing sugar standard curve.

The activity may be calculated as follows:

$$\text{Activity } (\mu\text{moles/min/cm}^3) = \left(\frac{\mu\text{mole of reducing sugar}}{20}\right) t\, d \qquad 3.1$$

where t = incubation time (min)

d = enzyme dilution factor

3.3.4.3 Maltogenase Assay

Maltogenase is a thermostable exo-acting alpha-amylase and was purchased from Novo-Nordisk (Farnham, Surrey). This enzyme was produced by expressing the maltogenic amylase gene from a *Bacillus stearothermophilus* using recombinant-DNA techniques into a *Bacillus subtilis* host. The enzyme maltogenase catalyses the hydrolysis of 1.4-alpha-glucosidic linkages in amylose and amylopectin. Maltose units are successively removed from the non-reducing chain ends in a stepwise manner until the molecule is degraded or, in the case of amylopectin, until a branch point is approached.

The enzyme activity was determined using a chromatographic method [85]. One unit of activity U/cm^3 is expressed as the amount of enzyme required to produce 1 of maltose in one minute at 60^{o}C and a pH 5.2. In the determination of the maltogenase activity , 2% w/v soluble starch (Sigma Chemical Co. Ltd. Poole, Dorset) in acetate buffer was incubated at 60^{o}C with suitably diluted enzyme solution for 30 minutes. The rate of maltose formation was calculated from the chromatographic data.

3.3.4.4 Other Analytical techniques

The dextrose equivalent (DE) values for starch A, Starch B and Starch C were determined using the reducing sugar method [87] described in section 3.3.4.2. The total reducing sugar standard curve was prepared using glucose.as the standard. DE value was defined as follows;

$$\text{DE value} = \frac{\text{gram of reducing sugar as glucose}}{\text{100 gram of starch}} \text{ X } 100 \qquad 3.2$$

CHAPTER FOUR

SEPARATION AND REACTION SYSTEMS

4.1 Introduction

The feasibility of employing a chromatographic column as a biochemical reactor and separator depends on the nature of the biochemical reaction and the performance of the separation system. This chapter will describe both of these aspects.

The essential components of a biochemical reaction system are the enzyme, the substrate and the medium for the reaction to take place. The two enzymes used in this work were the invertase and the maltogenase. Both enzymes are categorised as hydrolases and can only function in aqeuous medium. The substrates and the products of the two biochemical reactions were carbohydrates (mono, di and higher saccharides).

The separation system consists of the stationary phase and the mobile phase. The choice of the mobile phase is fixed by the nature of the biochemical reaction which require an aqueous medium. The selection of the stationary phase is critical since it must exhibit preferential adsorption for one or more components and does not inhibit the reaction.

4.2 The Separation System

4.2.1 An introduction to Ion Exchangers

The separation of carbohydrate mixtures using liquid chromatography may be carried out using two types of ion exchangers.

1. Silica-based ion exchangers
2. Resin-type ion exchangers

With silica-based ion exchangers, an organic solvent such as acetonitrile/water mixtures are used as the eluent. The requirement of organic solvents for the eluent prohibit their used in preparative scale study and also in industrial applications. Their use are now confined to analytical applications.

Ion exchange resins were developed in parallel with the silica-based ion exchangers. The main advantage of ion exchange resins are that they use mainly deionised water for the eluent. These types of resins have been widely used for the separation of high fructose corn syrup (HFCS) into an enriched fructose stream and enriched glucose stream [88].

There are two types of ion exchange resin, the anion exchanger and the cation exchanger. It is possible to separate saccharides (eg. fructose from glucose) using both types of the resins, but industrial chromatographic applications use only cation exchangers. This is due to cation exchange resins generally being more resistive to thermal and chemical degradation, and less expensive than anion exchange resins.

In this project, strongly acidic polystyrene based cation exchange resins in calcium form were used for the separation of saccharides. A calcium form cation exchange resin was prefered in this work due to their capability to preferentially adsorb a range of saccharides by the formation of a coordination complex. In addition, calcium ions generally act as an activator for most of the hydrolase enzymes [90].

4.2.2 Dowex 50W-X4 Ion Exchange Resin

The chromatographic resin used in this research was Dowex 50W-X4 ion exchange resin (British Sugar, Kidderminster) which is a strongly acidic cation exchanger and had a mean particle diameter of 150 μm. The resin was in the form of spherical beads, light brown in colour and slightly translucent.

Dowex 50W-X4 cation exchange resins are made up of three constituents, namely the basic polymer-forming component, the crosslinking agent and the functional groups [91]. The basic constituent of the resin is styrene. Styrene is crosslinked with divinylbenzene (crosslinking agent) into a polymeric network in the ratio of 96% styrene and 4% divinylbenzene. A strong acidic cation exchange character is due to the anionic functional group SO_3^- covalently bonded to the resin matrix. The resin attains its calcium form by taking Ca^{2+} ions into the anionic functional groups.

The degree of crosslinkage determines the physical structure of the resin matrix and the density of the functional groups. A resin with a high degree of crosslinkage has a smaller pore structure than a low crosslinkage resin. It also has a higher physical resistance to shrinking and swelling, and has more functional groups. However, the resin tends to be brittle and has a slower ion exchange rate.

Ion exchange resins with a low degree of crosslinkage has a more open structure making it permeable to higher molecular weight components. This property is useful for size exclusion purposes. It also has a faster ion exchange rate but it is less selective due to a lower number of ionisable sites per unit volume of resin.

4.2.3 Separation of Saccharides Using Calcium Form Ion Exchange Resins

In a true ion exchange process using the calcium form Dowex 50W-X4 ion exchange resin, Ca^{2+} ions act as the counterions. Ca^{2+} ions will be replaced by sample ions that have the same charge which are, in turn bound to the functional groups. Neutral molecules and those having the same charge as the fuctional groups flow through the column and are separated from the sorbed ions.

The separation of mono, di and higher saccharides using calcium form cation exchange resin and deionised water as the eluent is not a true ion exchange process. The separation is based on the differences between molecular sizes, molecular conformation and the

configuration of the hydroxyl groups. The separation of saccharides are due to two main mechanisms, size exclusion and ligand exchange.

In size exclusion the retention of solutes is based on molecular sizes. Those solute molecules whose molecular sizes are too large to diffuse into the resin matrix move through the column faster than the smaller molecules. The smaller molecules such as monosaccharides (glucose and fructose) diffuse in and out of the resin matrix resulting in a slower movement through the column. Disaccharides such as sucrose and maltose, and higher saccharides are largely excluded from the resin matrix and move faster through the column. Thus separation between mono, di and higher saccharides occur. However size exclusion mechanisms do not explain the differential migration of two monosaccharides or two disaccharides through the column.

Separation of glucose and fructose (monosaccharides isomers), and sucrose and maltose (disaccharides) on calcium form ion exchange resins can be explained in terms of ligand exchange chromatography. Ligand exchange occurs when the water molecules held in the hydration sphere of calcium ions are exchanged for one or more of the hydroxyl groups of the saccharides [92]. A coordination complex results. The strength of the complex with calcium ions depends on the conformation of the saccharides, whether it is in the α- or β-anomeric forms or in the pyranose or furanose ring forms. In aqeuous medium, mono saccharides such as glucose and fructose, exist in five possible forms as indicated by the following scheme [93]:

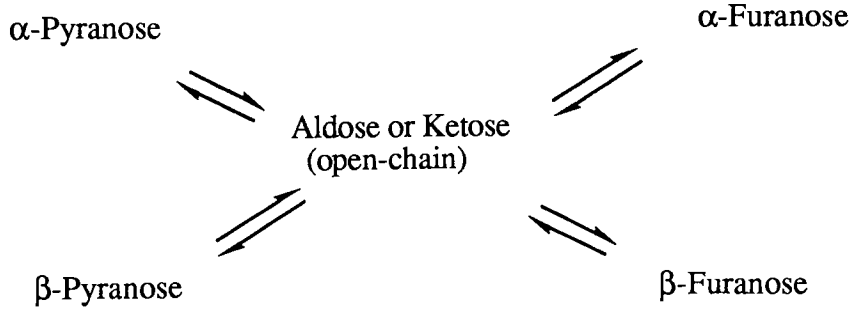

Figure 4.1 Pyranose-furanose interconversions

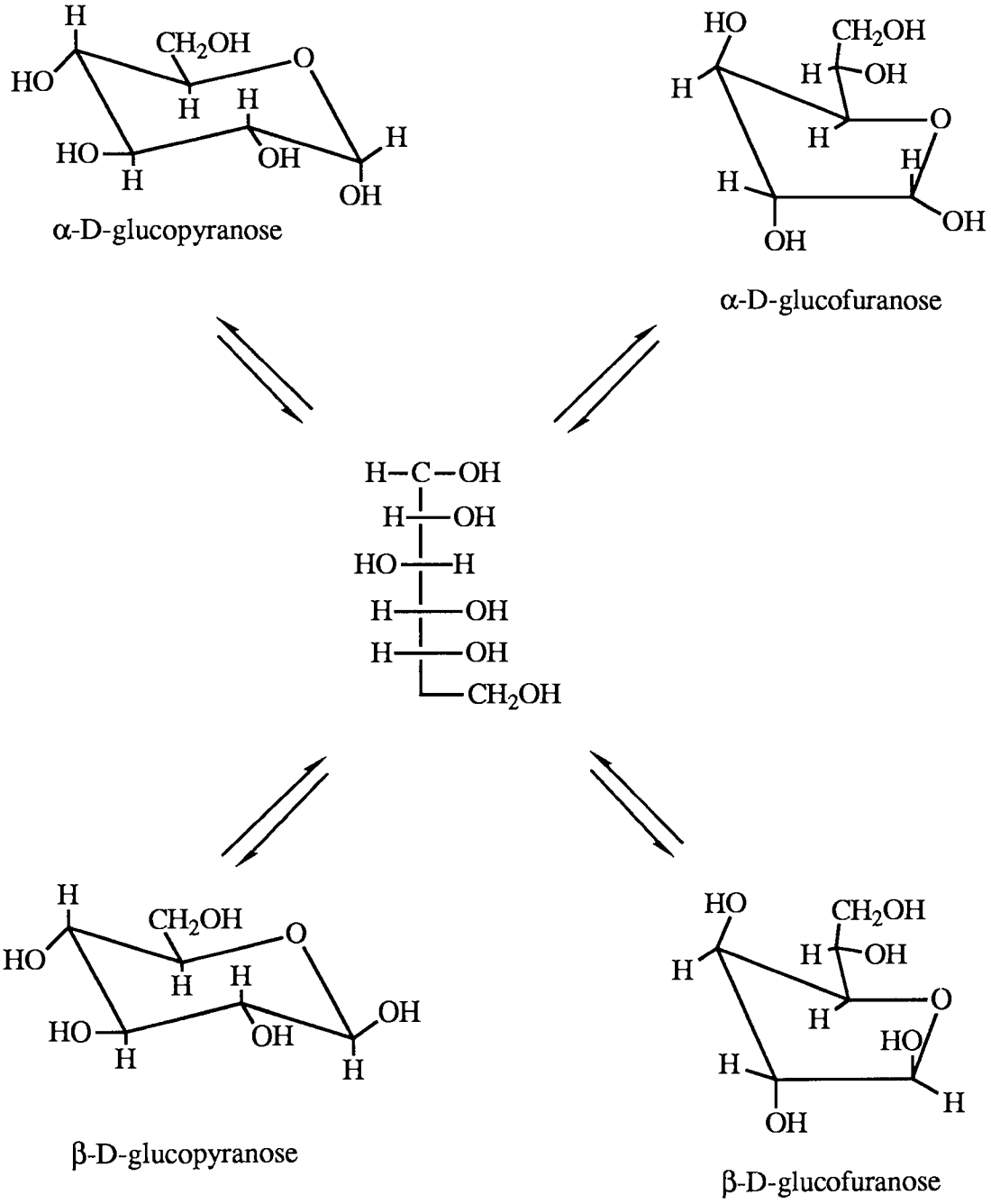

Figure 4.2 Tautomers of glucose

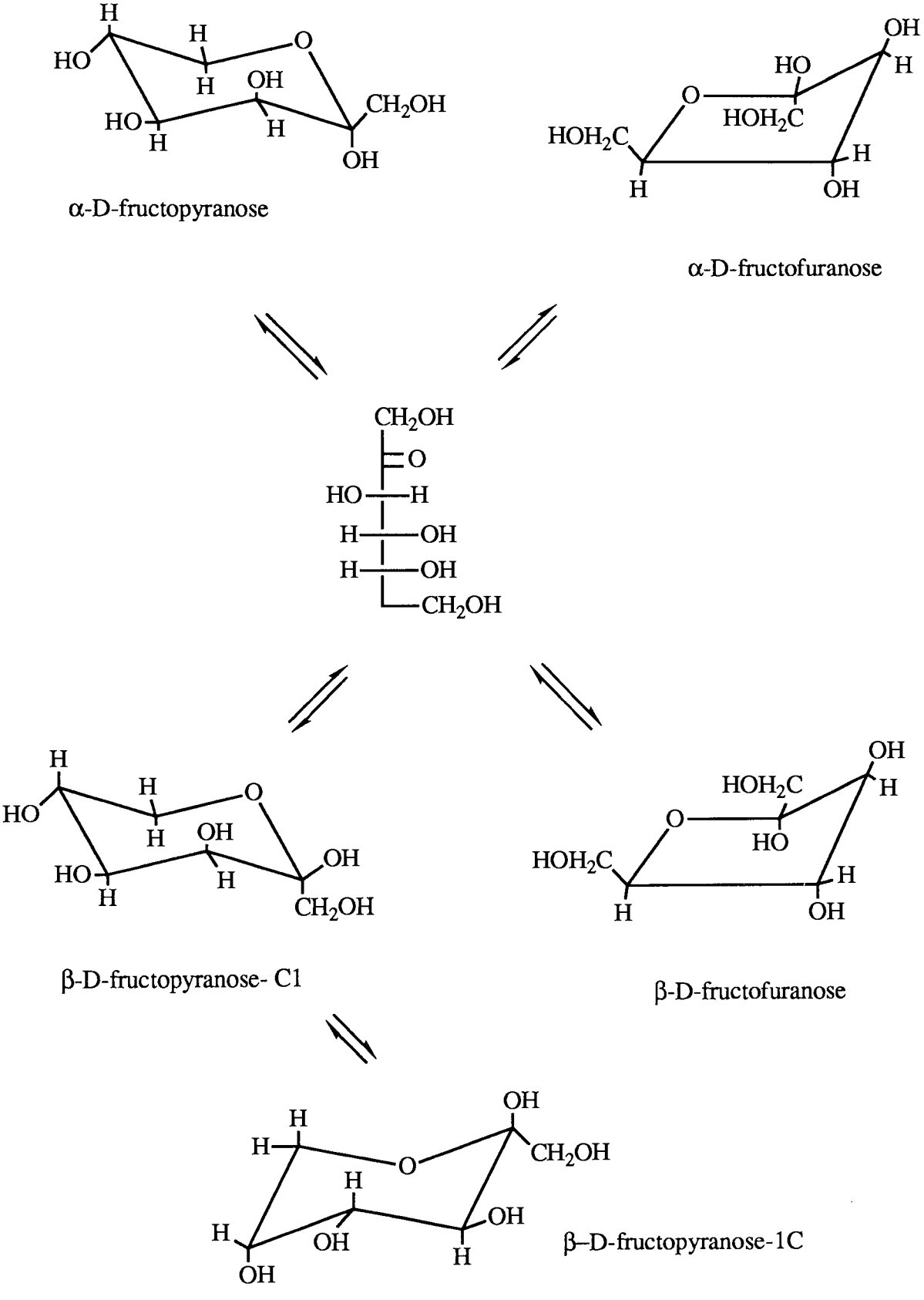

Figure 4.3 Tautomers of fructose

Mutarotation from one tautomeric form to the other occurs through the formation of open-chain forms until an equilibrium is reached. The distribution of of the five possible forms depend in general on the temperature. For glucose (figure 4.2), pyranose forms are the dominant form with one-third as α-anomer and two-thirds as β-anomer [96]. In the case of glucose, the proportion between the two anomers are essentially independent of temperature. Fructose (figure 4.3), on the other hand, undergoes a rapid pyranose-furanose interconversion. At equilibrium, β-fructopyranose and β-fructofuranose are dominant. According to Shallenberger *et al.* [97] the propotion of β-fructopyranose decreases with increase in temperature. At 22°C and 20% w/w concentration, fructose consists of α-D-fructofuranose (6%), β-D-fructofuranose (21%) and β-D-fructopyranose (73%). Whereas at 67°C and at the same concentration fructose consists of α-D-fructofuranose (8%), β-D-fructofuranose (28%) and β-D-fructopyranose (64%).

The ring forms of glucose and fructose cannot be planar because of the tetrahedral geometry of its saturated carbon atoms. Instead they adopt chair, boat or envelope conformations with the hydroxyl groups in axial or equatorial positions. Axial positions refer to the bonds that are perpendicular to the average plane of the ring, whereas equatorial bonds are those parallel to this plane. The most stable conformation is when there is no steric hinderence between adjacent hydroxyl groups. This is achieved if all the hydroxyl groups are in the equatorial positions. However this is not always possible due to the tetrahedral geometry of carbon atoms. Thus separation of two species will occur if one saccharide molecule provides more available sites for ligand exchange than the other.

Goulding [92] reported, the availability of hydroxyl groups in pyranose sugars for ligand exchange with the water molecules held in the hydration sphere of calcium ions dependent on the number of pairs in axial-equatorial positions. α-fructose has one such pair and β-fructose has two pairs. α-glucose, on the hand has one pair while β-glucose has none (all the hydroxyl groups are in equatorial positions). As a result fructose is held more strongly by the resin compared to glucose.

Separation between glucose (monosaccharide) and maltose (disaccharide) are due to both ligand exchange and size exclusion. Maltose has one pair of hydroxyl groups in the axial-equatorial position as in α-D-glucose, however maltose is eluted first because the ratio of a pair of hydroxyl to the total number of hydroxyls in the molecule is half compared with glucose. Also, maltose being the larger molecule has a lesser chance of entering the pores of the resin.

Between sucrose and maltose, sucrose is eluted first since none of its hydroxyl group is in the axial-equatorial position.

On the other hand, the hypothesis proposed by Angyal [98] requires the presence of an axial-equitorial-axial hydroxyl group arrangement for the formation of stable complexes with cations. However, only β-D-Form of fructose has such an arrangement.

4.2.4 Treatment of ion exchange resin

4.2.4.1 Resin Conversion

Dowex 50W-X4 ion exchange resin has been previously used by other workers [81] the in the sodium form for the separation of sucrose from beet molasses. For the separation of glucose, fructose, maltose and higher saccharides, calcium form resin is preferred. Therefore, our resin had to be converted to the calcium form.

The conversion to the calcium form was carried out through an intermediate counterion, namely the hydrogen form. The conversion to the hydrogen form was carried out outside the chromatographic column to prevent chloride corrosion to the stainless steel components.

20 dm^3 resin was mixed with 60 dm^3 10% w/v HCL in a 100 dm^3 polypropylene container and the content was stirred. The mixture was left to equilibriate for 24 hours. The resin was then washed with deionised water until the effluent was neutral. The resin was then in the hydrogen form.

In the second part of the resin conversion to the calcium form, a similar procedure was followed by using 60 dm^3 of 10% w/v $Ca(NO_3)_2$ solution.

The calcium form resin was suspended in deionised water and then slurried into the annular chromatographic column.

4.2.4.2 Column Technique

A uniformly packed resin bed is crucial for efficient chromatographic operation. Any inhomogeneity in the packing will cause uneven eluent flow distribution through the resin bed which leads to channelling.

To facilitate the packing operation, the top plate of the CRAC was removed. The packing method adopted in this work was the continuous slurry packing technique. Column rotation was started and the packing (50% v/v slurry of resin and deionised water) was poured in a continuous stream into the annulus. Excess water was syphoned from the top of the annulus.

The column packing was equilibrated and stabilised by passing deionised and dearated water eluent at 8 dm^3/h for at least 24 h before being used for experimental work.

After several months (3-4 months) of use, the packing became compressed; fines and debris had accumulated within the void between the resin particles. Backwashing in this equipment was not readily possible due to the large number of outlets beneath the column.

It was therefore necessary to unpack the column and this was carried out by removing the top plate of the column, slurrying the resin with water and then syphoning out the resin.

The resin was washed, regenerated using 10% w/v $Ca(NO_3)_2$ solution and repacked into the column using the same procedure as described in section 4.2.4.1

4.2.5 Liquid Distribution Around the Annulus

Before a series of experiments were conducted on the CRAC, the liquid distribution around the annulus was checked. This was carried out by measuring the liquid flow from all 50 collection points. The test was conducted at an eluent flow rate of 10 dm^3/h and a rotation rate of two revolution per hour [80]. The liquid samples were collected for thirty minutes and the bottles were weighed.

The data are shown in table 4.1. The data shows that there was fairly even liquid distribution around the annulus. The mean, mode and standard deviation of the data was 99.46, 100 and 5.32 respectively. The close value between the mean and the mode, and the low value of the standard of deviation indicated that the samples were centrally distributed with a small variability. In simple terms 99.91 % of the collected weights were within ± 10 % of the sample mean value.

4.2.6 Void Fraction Determination

The determination of the resin bed void fraction in the CRAC was carried out using a 2% w/v solution of blue dextran 2000 as feed. Blue dextran has an average molecular weight of 2,000,000 and as such is totally excluded from the resin pores. The conditions used for the voidage determination were; 10 dm^3 eluent flowrate, 150 cm^3 feed flow rate and 240 deg h^{-1} rotation speed. The voidage ε for the resin bed was found to be in the region of 0.38-0.4. Details of the calculation are presented in appendix A1

Table 4.1 Flow distribution around the annulus

Exit positions	Mass of water (g)	Exit positions	Mass of water (g)
1	93	26	103
2	89	27	109
3	88	28	105
4	95	29	104
5	86	30	100
6	94	31	103
7	91	32	101
8	94	33	105
9	98	34	105
10	92	35	102
11	93	36	96
12	95	37	103
13	98	38	105
14	98	39	107
15	102	40	108
16	103	41	103
17	101	42	104
18	100	43	104
19	100	44	104
20	100	45	100
21	101	46	99
22	104	47	97
23	102	48	98
24	100	49	100
25	100	50	99

4.2.7 Physical Separation of Saccharides on the CRAC

The experimental runs are presented in a coded form, 180-25GF-11-240-55, where the code represent feed flow rate 180 cm^3/h, glucose and fructose concentration 25 % w/v, eluent flow rate 11 dm^3/h, column rotation rate 240 degrees/h and temperature 55°C. In table 4.3 the term "50IS" represents inverted sucrose at 50 % w/v concentration and in figure 4.6 the term "30Saccharified Starch C" represents 30% w/v of saccharified Starch C.

The results of the physical separation of saccharides on a CRAC are shown in table 4.2 and table 4.3. Elution profiles for the physical separation of sucrose, glucose and fructose are shown in figure 4.4. Figure 4.5. shows the elution profile of the inverted sucrose feed and figure 4.6 shows the elution profiles of saccharified Starch C feed.

The degree of separation between components was expressed as resolution. It was defined as the ratio of the distance separating the two peaks θ_1 and θ_2 to their average bandwidth W_1 and W_2 measured at the baseline (page 43 reference 81) and as given in equation 4.1.

The determination of the distribution coefficient K_d of the saccharides is given in Appendix A1

$$R_{1-2} = \frac{\theta_1 - \theta_2}{\frac{1}{2}(W_1 + W_2)} \qquad 4.1$$

Table 4.2 Separation of sucrose, glucose and fructose mixtures

Runs	R_{SG}	R_{GF}	K_{dS}	K_{dG}	K_{dF}
180-25GF-11-240-55		0.89	-	0.45	0.78
180-20SGF-11-240-55	0.62	0.7	0.2	0.4	0.7
180-25GF-8-240-55	-	0.75	-	0.42	0.72

Table 4.3 Separation of inverted sucrose

Runs	R_{GF}	K_{dG}	K_{dF}
60-50IS-11-240-55	0.84	0.4	0.68
150-50IS-11-240-55	0.72	0.4	0.74
310-50IS-11-240-55	0.68	0.39	0.7
525-50IS-11-240-55	0.42	0.42	0.74
230-50IS-8-240-55	0.52	0.5	0.7
230-50IS-5-240-55	0.7	0.45	0.72
150-50IS-8-100-55	0.6	0.4	0.65
230-50IS-8-100-55	0.64	0.46	0.78

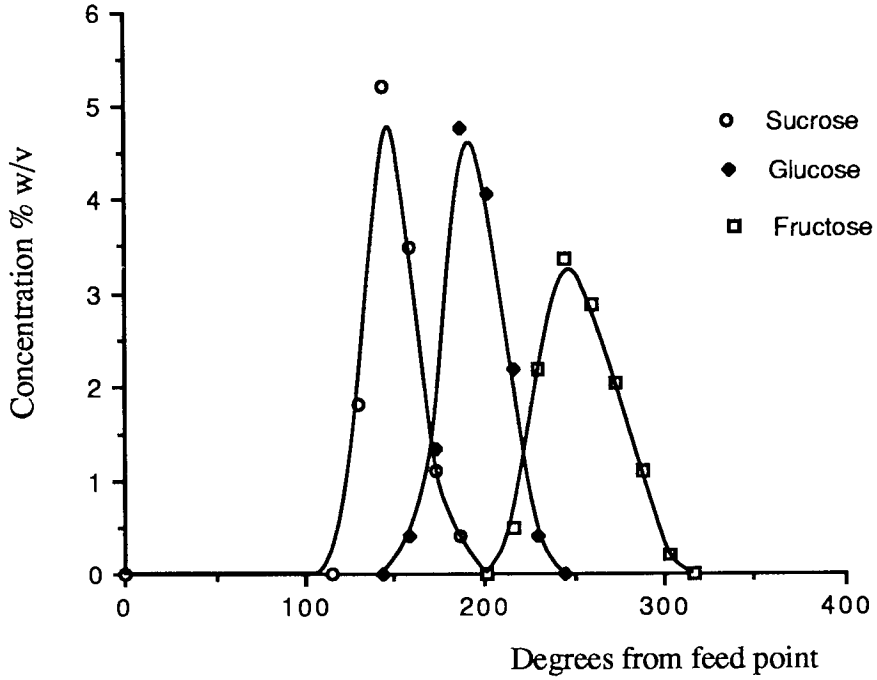

Figure 4.4. Elution profile for run 180-20SGF-11-240-55

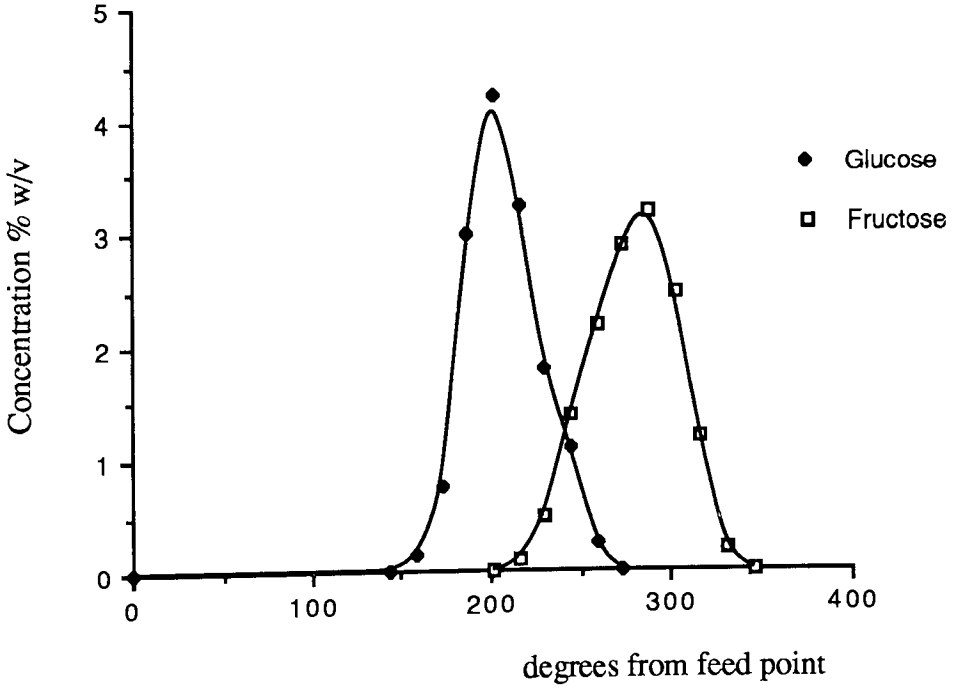

Figure 4.5. Elution profiles for run 310-50IS-11-240-55

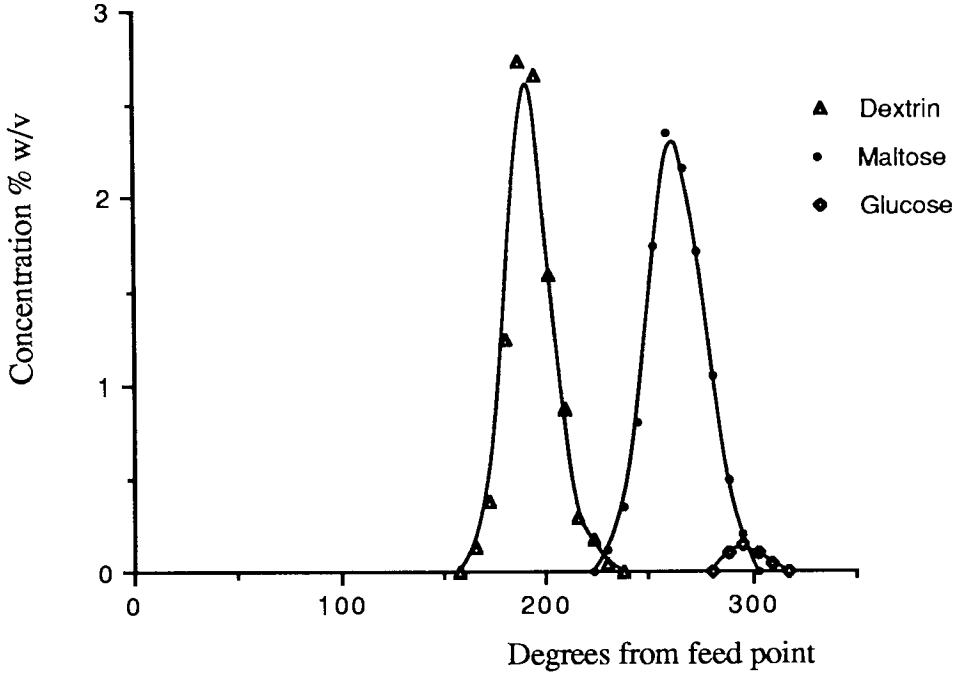

Figure 4.6. Elution profile for run 240-30Reacted starch C-8-240-60

4.3 The Reaction System

4.3.1 Introduction

The suitability of an enzyme catalyst for industrial use depends mainly on four factors:

1. the catalytic activity (rate of reaction)
2. the extent of reaction (equlibrium constant)
3. the enzyme stability
4. the cost of the enzyme

The catalytic activity indicates the quantity of the enzymes needed to achieve the desired product conversion. One unit of activity (U) of any enzyme is defined as that amount which will catalyse the transformation of one micromole of substrate per minute under defined conditions [90]. Wherever possible, the reaction temperature should be 25°C. In practice however, enzymes used in industry do not always react at 25°C and with

chemically definable substrates. Often, it is unavoidable but to ignore the recommended definition and to carry on using one's own convenient unit.

The extent of the reaction or the degree of product conversion are effected by substrate concentrations, general conditions of the reaction (temperature, pH, ionic strength) and the duration of the reaction. This is because the activity and the stability of an enzyme depends on these parameters. The effect of these parameters on the rates and the extent of the product formation can be quantified by carrying out enzyme kinetic studies.

4.3.2 The Kinetics of Sucrose Hydrolysis

Hydrolysis of sucrose to form glucose and fructose (equation 4.2) was carried out experimentally using the enzyme invertase.

SUCROSE FRUCTOSE GLUCOSE

$$C_{12}H_{22}O_{11} + H_20 \xrightarrow{\text{invertase}} C_6H_{12}O_6 + C_6H_{12}O_6 \qquad 4.2$$

The study of the kinetics of sucrose hydrolysis was carried out by measuring the initial rate of reaction for a range of initial sucrose concentrations. Batch reactions were carried out using the procedures as in the invertase assay method (section 3.3.4.2). The activity of the enzyme invertase used was 60 U/cm^3 [82]. Reaction samples were removed from the reaction mixture at 2 minute intervals and placed into a test tube immersed in a boiling water bath to deactivate the enzyme. The samples were then assayed for reducing sugars.

The initial reaction rate data are plotted in figure 4.7. Figure 4.7 indicates a characteristic curve for a substrate inhibited reaction [89]. The curve shows the rate of reaction is at its maximum at 12% w/v sucrose concentration and declines as the sucrose concentration increases.

The determination on the kinetic parameters is reported in Appendix A2

The values of the maximum reaction velocity V_{max} , the Michaelis-Menten constant K_m and the substrate inhibition constant K_I were 0.012 g/cm^3/min, 0.024 g/cm^3 and 0.6 g/cm^3 respectively.

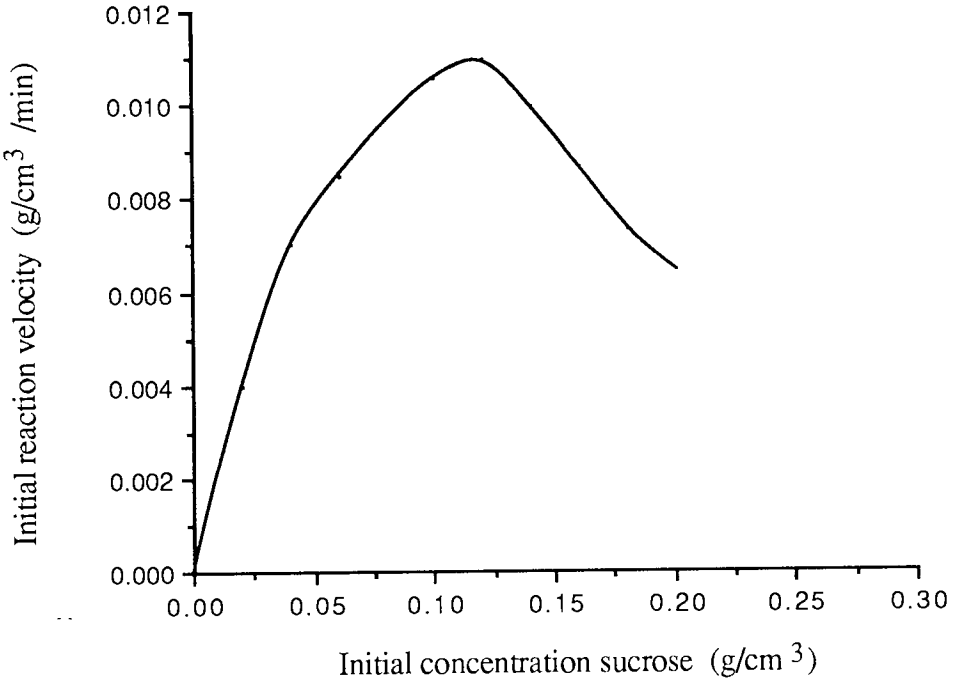

Figure 4.7. Initial rate of reaction of sucrose inversion vs sucrose concentration using the enzyme invertase.

The kinetic constants obtained were comparable to the work carried out by Dickensheet *et al.* [100], Nakajima *et al.* [101] and Akintoye [82]. Most of the other kinetic data of sucrose hydrolysis work were carried out at 25^{o}C [102-104] and are not appropriate for comparison.

The kinetic constants were used in the modelling of simultaneous biochemical reaction and separation on the CRAC (Chapter 7).

4.3.3 Saccharification of Modified Starch to Maltose using the Enzyme Maltogenase

The second biochemical reaction to be carried out on a CRAC was the saccharification of modified starch to maltose using the enzyme maltogenase. The advantages of maltogenase over other maltose producing enzymes are its ability to hydrolyse maltotriose into maltose and glucose, and to hydrolyse a 1,4-α-glucosidic link closer to the branch-points than the soybean β-amylase [105]. Thus under appropriate saccharification conditions, maltose will be the main product together with the unreacted dextrin and a small amount of glucose.

The effects of the type of substrate, substrate concentration, enzyme activity and reaction time on the reaction kinetics were investigated.

4.3.3.1 The Effect of Enzyme Activities

To carry out saccharification of modified starch to maltose in a CRAC, a fast reaction time is required. Therefore, the effect of enzyme concentration on the rate of maltose formation is crucial. Batch reactions were carried out using the procedure as in the maltogenase assay method (section 3.3.4.3).

Starch substrates were prepared according to the procedure in section 3.2.1.2. The average molecular weights (MW) of starch A, starch B and starch C determined by a GPC method (section 3.3.3) were 1.4 x 10^6, 1.05 x10^6 and 5 x 10^5 daltons. The DE values determined by the method described in section 3.6 were 0.2 (starch A), 0.8 (starch B) and 3 (starch C).

Figure 4.8 illustrates the effect of enzyme activity on maltose formation from starch A (5% w/v). The rate of maltose formation increased with the increase of enzyme activity from 20 U/cm^3 to 60 U/cm^3. However raising the enzyme activity to 100 U/cm^3 did not produce a significant extra effect. Similar results were obtained for starch C at 10% w/v and 30% w/v as shown in figure 4.9 and figure 4.10

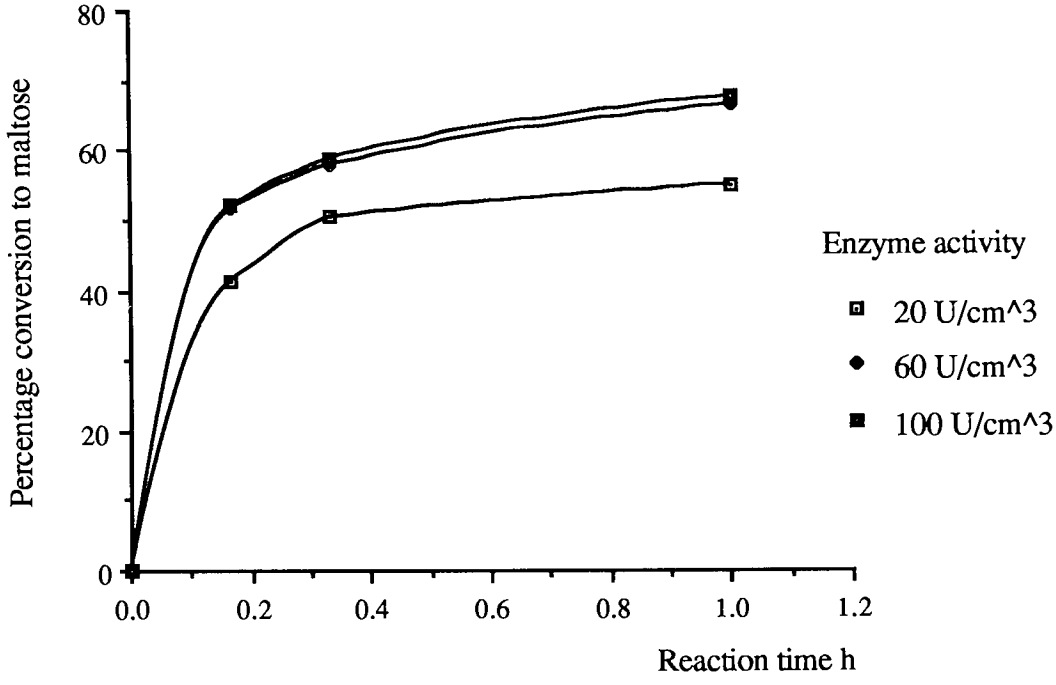

Figure 4.8 The effect of enzyme activity on maltose formation using 5% w/v starch A

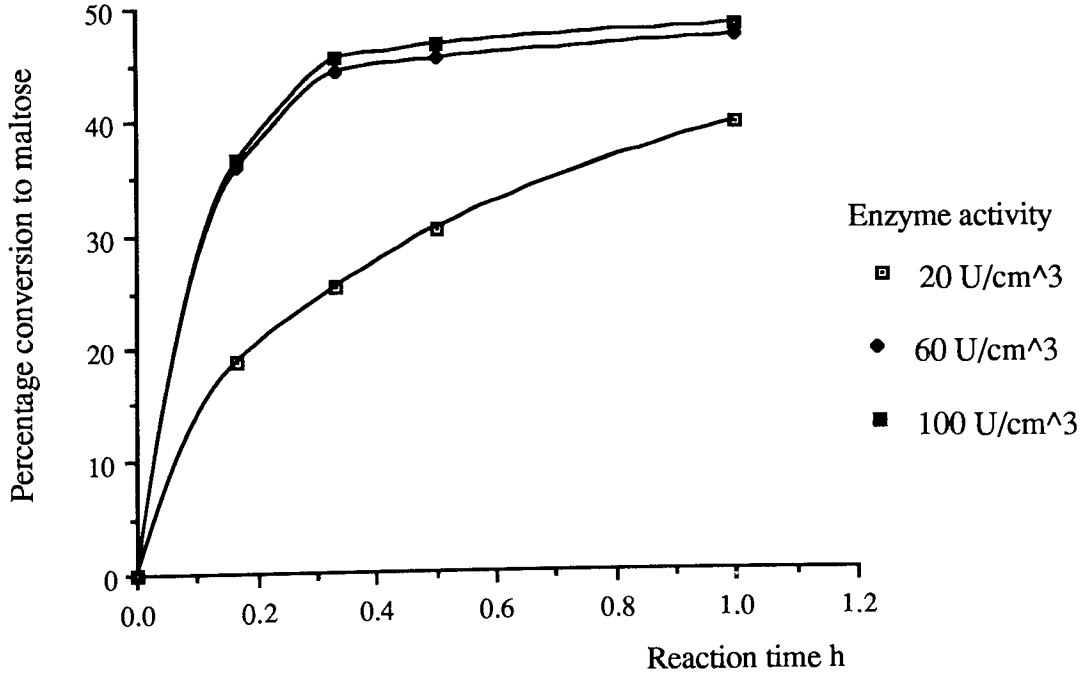

Figure 4.9. The effect of enzyme activity on maltose production using 10% w/v starch C.

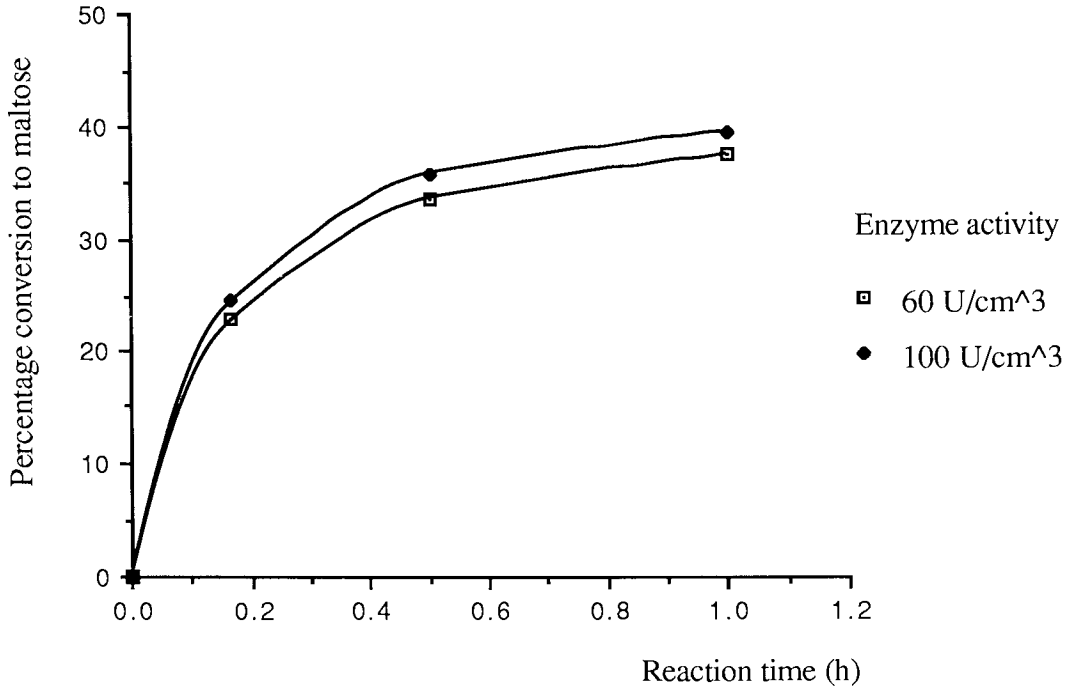

Figure 4.10 The effect of enzyme activity on maltose production using 30% w/v starch C

4.3.3.2 The Effect of Different Starches

Table 4.4 shows the effect of different types of starch on conversion to maltose. The reactions were completed in 10 - 12 h. For 10% w/v initial concentration, Starch A (soluble starch) showed the highest level of maltose production followed by Starch B (potato starch) and Starch C (tapioca starch). Starch A had the lowest DE value and the highest average molecular weight compared to the other two starches. The observation was in agreement with the results reported on maltose production using beta-amylase by Takasaki [106]. Takasaki [106] and Saha [131] showed that, to obtain high maltose conversion, the modified starch should have a DE value as low as possible. However, at a low DE, starch is viscous and could easily retrograde. For starch A, at above 10% w/v concentration, the solution was viscous and retrograded easily at 60^{o}C.

At 30% w/v initial concentrations, Starch B has a higher conversion to maltose than Starch C. Apart from a low DE value and higher MW than Starch C, Starch B contained less

amylopectin in the original starch than Starch C. The average value of amylopectin content is 79% for potato starch and 82% for tapioca starch [107]. The higher the amylopectin content, the greater are the number of α(1-6) linkages and the lower is the equilibrium conversion to maltose.

Table 4.4 Effect of the types of substrate on maltose yield

Substrates	Conc. (% w/v)	Maltose (%)	
		1h	12 h
Starch A	5	68.2	80.4
	10	65.6	79.1
Starch B	10	64.3	76.8
	30	53.1	74.2
Starch C	10	45.4	58.1
	30	41.1	55.2

* Enzyme activity used; 60 U/cm^3

4.3.3.3 The Effect of Substrate Concentration

The effect of initial substrate concentration on the percentage of conversion to maltose for Starch B are shown in figure 4.11. The initial substrate concentration determined the final maltose yield (figure 4.11). The lower the initial concentration the higher was the final percentage of conversion to maltose.

Figures 4.12 and 4.13 show the effect of substrate concentration on the initial reaction rate. The maximum initial rate of reaction for starch B and C occur at initial concentrations in the region of 22-25% w/v.

These results indicate that the initial stage of the reactions did not follow a zero-order kinetic. The reduction of the initial reaction rates and the final product conversion with the increase in the substrate concentration were likely to be due to a substrate inhibition effect.

The variation of the initial rate of reaction for Starch A and Starch B with their concentration were assumed to follow the inhibited Michaelis-Menten kinetic. The values of the kinetic constants were calculated in a similar manner as for the enzyme invertase. The values of the Michaelis-Menten constants are tabulated in table 4.5.

Table 4.5 Michaelis-Menten constants

	K_m (g/cm^3)	V_{max} (g/cm^3/min)	K_I (g/cm^3)
Starch B	0.09	0.01	0.5
Starch C	0.12	0.008	0.52

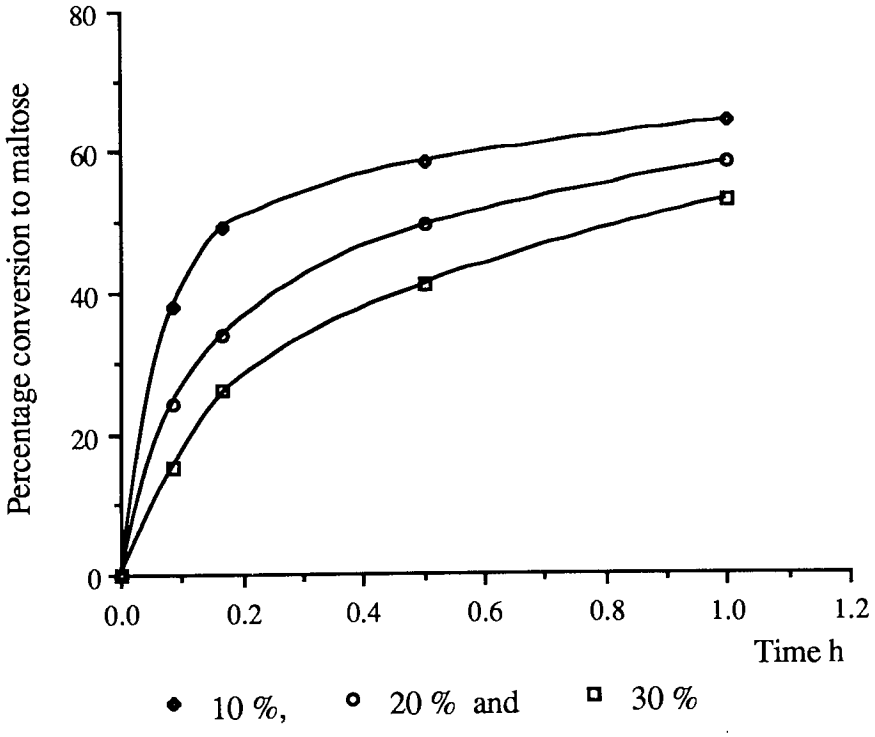

Figure 4.11 maltose formation of starch B vs time

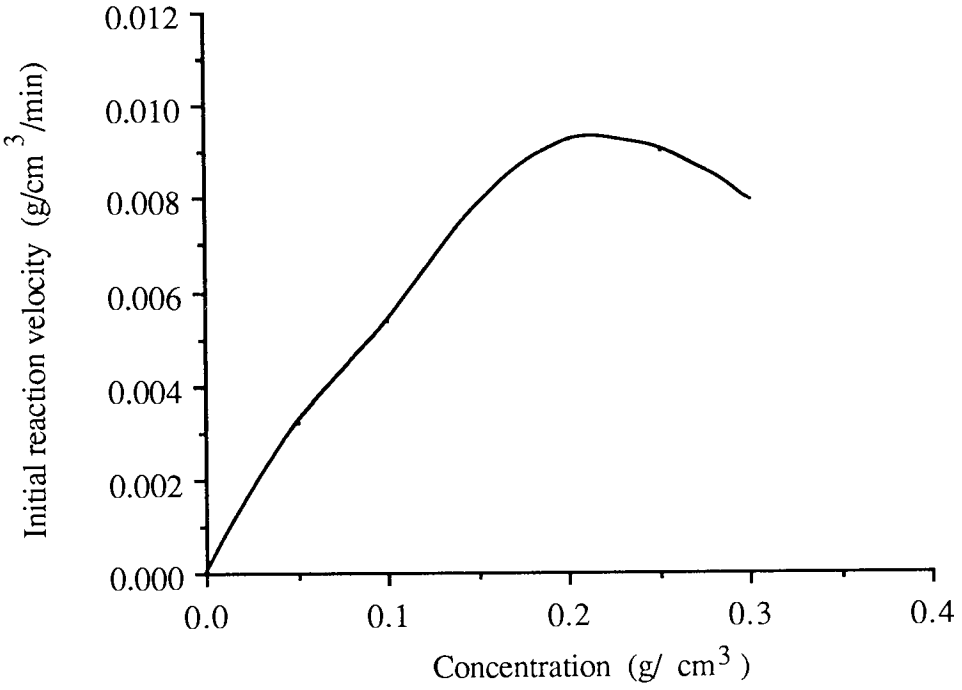

Figure 4.12. Initial reaction velocity of starch B saccharification vs concentration using the enzyme maltogenase

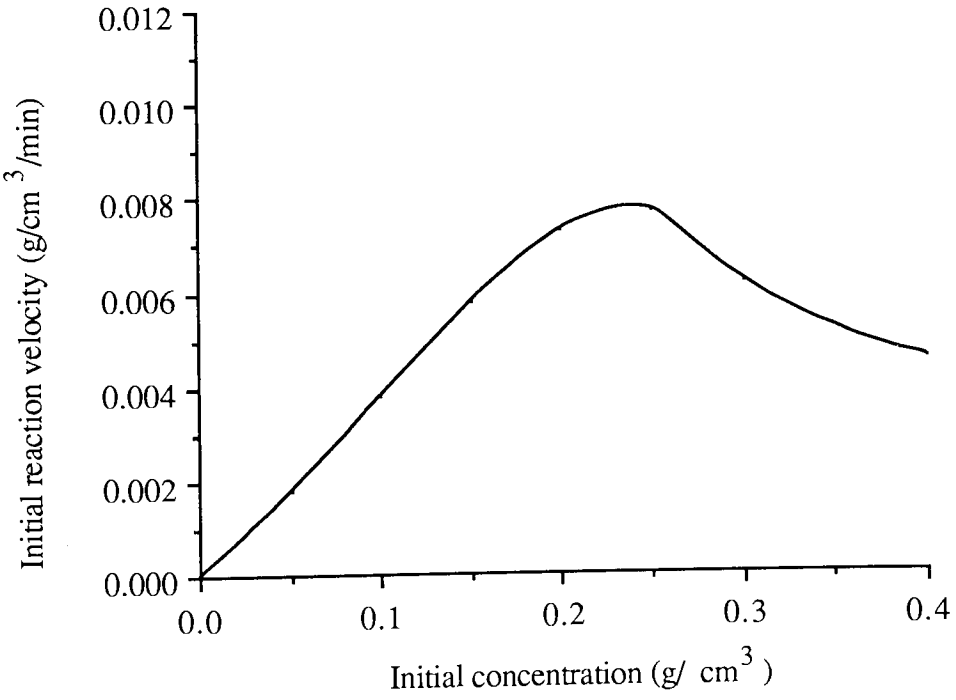

Figure 4.13. Initial reaction velocity of starch C saccharification vs concentration using the enzyme maltogenase

CHAPTER FIVE

STUDY OF A CRAC AS A COMBINED BIOCHEMICAL REACTOR-SEPARATOR USING A SUCROSE INVERSION REACTION

5.1 Introduction

This chapter presents the results of simultaneous biochemical reaction and separation of sucrose to glucose and fructose using the enzyme invertase on a CRAC. The objective of the experiments was to study the behaviour of a CRAC under simultaneous biochemical reaction and separation conditions and also to identify the main operating parameters affecting its performance. The operating parameters considered in the study were the eluent flow rate, feed flow rate, feed concentration, column rotation rate and the enzyme activity.

5.2 Preliminary Experiments

In the preliminary experiments, the eluent flow rate, the feed flow rate and the column rotation rate were based on the work of Bridges [81]. While the enzyme invertase activity, the substrate concentration, the temperature and pH were based on the work of Akintoye on his SCCR-S1 system [82]. Akintoye found out that on SCCR-S1 system, the optimum level of invertase activity was 60 U/cm^3 at substrate concentrations between 25-55 % w/v.

5.2.1 Experimental Results

The parameter settings and the results of the preliminary runs are shown in table 5.1. A run is presented in a coded form 230-25-10-30-240, where the sequence represents

230	=	feed flow rate	cm^3/h
25	=	feed concentration	% w/v
10	=	eluent flow rate	dm^3/h
60	=	enzyme activity	U/cm^3

240 = column rotation rate degrees/h

The concentration elution profiles of the runs are plotted in figure 5.1 and figures A3.1-A3.4. From these figures the percentage of conversion and the degree of separation were calculated.

The percentage conversion of sucrose in the equipment X was calculated using the following equation.

$$X = \left\{ 1 - \frac{W_s Q_T}{360 Q_f} \frac{\sum_{i=1}^{s} c_{Si}}{s c_{So}} \right\} \times 100 \qquad 5.1$$

Where;

X = percentage conversion of sucrose

s = the total number of sampling points distributed at a constant interval

c_{Si} = the sucrose concentration at sampling position i

c_{So} = the initial sucrose concentration in the feed

W_s = sucrose exit bandwidth

Q_T = the total of the eluent and the feed flow rate

The experimental results obtained illustrate for the first time the possibility of carrying out the simultaneous biochemical reaction and separation on a CRAC.

The results tabulated in table 5.1 show that the reaction was incomplete for all the runs. The higher the feed rate and feed concentration the lower was the conversion. It was also observed that higher resolutions between glucose and fructose were obtained in high conversion runs. This could be due to a greater proportion of the products being formed in the upper part of the column. Therefore the products were eluted through a longer distance, thus giving a greater opportunity for them to be separated. Hence for a complete conversion and higher resolution between the products, a higher enzyme activity was required.

Table 5.1 Sucrose inversion and separation

Experimental run	Sucrose Conversion %	Resolution R		
		R_{S-G}	R_{S-F}	R_{G-F}
230-50-8-60-240	65	0.2	0.47	0.39
230-25-8-60-240	82	0.3	0.6	0.41
150-50-8-60-240	70	0.41	0.8	0.42
150-25-8-60-240	91	0.51	0.9	0.48
230-12.5-8-60-240	92	0.3	0.8	0.45

Figure 5.1 shows the elution profiles for run 150-25-8-60-240 as a function of the angular distance from the feed point. In this run the sucrose conversion was 91 %. The elution profiles show there was overlapping between the three peaks. The unreacted sucrose was eluted first, followed by glucose and finally the more retained fructose. The resolution between sucrose and glucose R_{S-G} was 0.51, while the resolution between sucrose and fructose R_{S-F} and the resolution between the product glucose and fructose R_{G-F} were 0.9 and 0.48 respectively.

Figure 5.1 shows that only pure fructose cuts could be obtained. The entire elution profile of glucose contains either sucrose or fructose. Therefore, to obtain a pure glucose cut, a complete sucrose inversion was required.

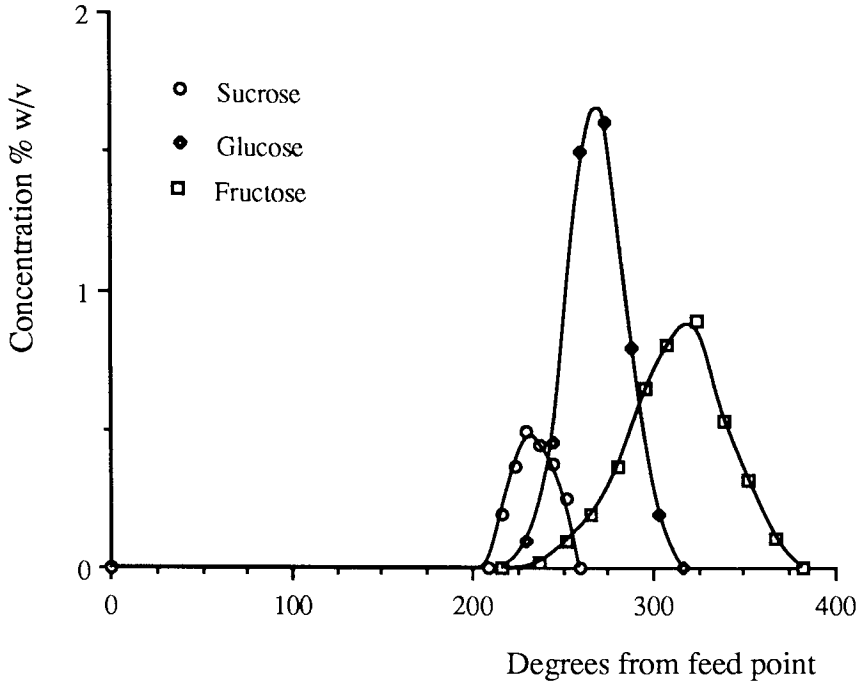

Figure 5.1 Elution profile for run 150-25-8-60-240

The chromatographic figures of merit [83,110-112], peak concentration, bandwidth (W), asymmetry factor (As) and overall shape of the elution profiles were also evaluated. These are some of the important parameters in characterizing the elution profiles.

The peak asymmetry factor is a measure of the deviation from a Gaussian shape and is defined as the ratio of the width of the two halves of the bandwidth measured at 10 % of the peak height as shown in figure 5.2. A chromatogram having an asymmetry factor value between 0.9-1.2 is considered to be reasonably symmetrical [83].

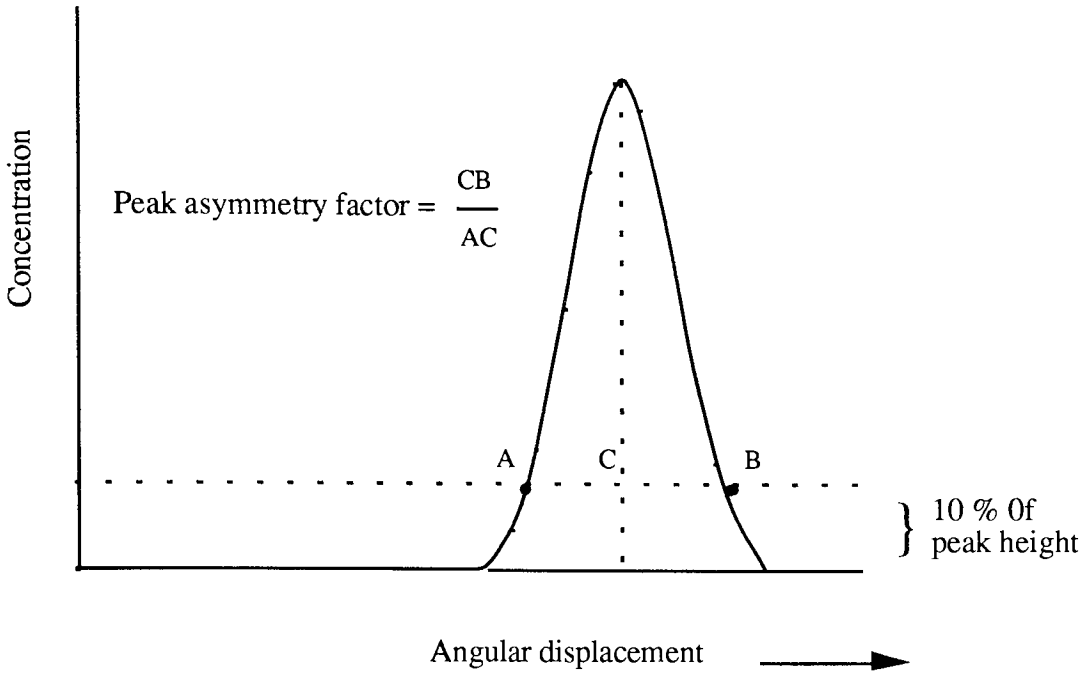

Figure 5.2 Definition of peak asymmetry factor

The elution profile of the unreacted sucrose has a narrow triangular shape. The elution profile for the product glucose, is narrower than that of fructose and is almost symmetrical (As_G =0.94) with a small amount of band broadening on each side of the peak base, while the elution profile of the fructose shows a significant asymmetry (As_F=0.75) with a negative skew towards the glucose and sucrose peak. As a result the bandwidth is broader and the peak height is reduced considerably compared to the glucose peak.

The formation of a narrow and a symmetrical elution profile for glucose reduces the degree of overlapping between peaks and thereby enhances the separation. Furthermore, the separated components can be recovered at a higher concentration. It is therefore desirable to obtain a narrow symmetrical elution profile in chromatographic reaction and separation to enhance the resolution between peaks and the product recovery.

Separation studies of glucose and fructose on the same equipment were carried out by Thirkill [80]. It was establised that at a higher feed concentration, the fructose elution profile exhibited a slight positive skew. In liquid chromatography, a positive skew elution profile is an indication of the presence of a convex shape adsorption isotherm. Therefore,

the negative skews shown in figure 5.1and figures A3.1-A3.4 are not due to adsorption isotherm nonlinearity but rather due to the simultaneous reaction and separation effect.

The effect of simultaneous reaction and separation on the development of the product elution profiles can be explained as follows. At the beginning of the process, small amounts of the fructose and glucose were formed and they co-eluted under the unreacted sucrose peak. This situation caused a tag-along effect [133] to occur. As the reaction proceeded and the separation developed, the concentration of the peak front for glucose increased more than that of fructose due to its lower affinity for the resin. Under this condition, the tag along effect on the fructose peak front increased. Thus, the higher affinity of fructose for the resin coupled with the tag-along effect and insufficient column length for the separation to develop was believed to contribute to the shape of the fructose elution profile.

The reaction and separation would have developed fully if the column was longer. Since the length of the CRAC was fixed, the obvious way to improve the performance was to increase the level of the enzyme activity.

5.2.2 Performance of a CRAC as a Biochemical Reactor Separator

The performance of the CRAC as a biochemical reactor separator was further analysed in terms of peak concentration, product throughput enzyme usage and the percentage of recovery of a pure product.

The same definition of enzyme usage used by Akintoye [82] and Zafar [41] was employed in this work. The enzyme usage was related to the theoretical amount of enzyme required to convert the same amount of sucrose in a batch reactor over the same time period. The details of the calculation are cited in Appendix A5.

These performance indicators were also obtained from figure 5.1 and figures A3.1-A3.4 and the values are tabulated in table 5.2. The enzyme usage and product throughput were based on a single feed stream. However in practice two feed streams can be used since

most of the elution profiles from a single feed occupied less than half of the circumference of the annulus.

Table 5.2 Performance of the CRAC

Experimental run	Enzyme usage	Peak concentration % w/v		Fructose at 100 % purity	
		Glucose	Fructose	Throughput (g/h)	% recovered %
230-50-8-60-240	1.43	3.8	2.9	8.67	15
230-25-8-60-240	2.86	1.9	1.4	0.32	0.11
150-50-8-60-240	2.2	2.75	1.68	8.83	23.55
150-25-8-60-240	4.4	1.62	0.52	6.54	34.9
230-12.5-8-60-240	5.74	1.5	1.2	4.89	34.1

Results in table 5.2 indicate that a higher product peak concentration and a greater product throughput were obtained when using high substrate concentrations. The enzyme usage was also the lowest. However, a high substrate concentration reduced the degree of conversion which in turn reduced the resolution and the percentage of recovery of pure fructose.

From these preliminary experimental results, it was found that the conditions for optimum reaction and separation were different from the conditions for high product throughput. Under a constant enzyme activity, the reaction and separation duty preferred a low feed concentration and a low feed flow rate.

On the other hand, the product throughput was better at a higher feed flow rate and feed concentration. Therefore, as was mentioned in section 5.2.1, an obvious way to increase the productivity is to increase the level of the enzyme activity used. However, this in turn will increase the value of the enzyme usage. Interdependence between the operating parameters needed to be established.

5.3 Factorial Experiment

It was decided to investigate the performance of the system in a more systematic manner by using the factorial experiment technique. In this technique the number of experiments required to assess a given number of factors is less than one-factor-at-a-time, experimental technique. It is also capable of assessing the effect of changing any one factor independently of any other factors. Furthermore, factorial experiments permit the evaluation of the interactions effects between the factors involved.

5.3.1 Choice of Factors and Factor Variables

The choice of factors and factor variables for the factorial experiments were based on the preliminary experiments (Section 5.2). These factors were the feed flowrate, the feed concentration, the enzyme activity and the eluent flowrate. Each factor was studied at two levels, giving a total of 16 different sets of experimental conditions. The level of the factors were:

A = Feed rate cm^3/h	$A_1 = 150$	$A_2 = 230$
B = Feed concentration % w/v	$B_1 = 25$	$B_2 = 50$
C = Enzyme activity U/cm^3	$C_1 = 75$	$C_2 = 100$
D = Eluent rate dm^3/h	$D_1 = 8$	$D_2 = 10$

In factorial experiment, the 16 different sets of experimental conditions are called the treatment combinations and the results of the treatment combinations are called the response.

A convenient way to write a treatment combination is as follows. A factor is denoted by a capital letter and the two levels of the factor are represented by the subscript 1 or 2 to the capital letter. Thus a treatment combination $A_1B_1C_1D_1$ refers to all factors being at lower level while a treatment combination $A_2B_2C_2D_2$ represents all factors being at the higher level. All the possible treatment combinations and the order of the experiments are

tabulated in table 5.3. Each of the treatment combinations was performed once in a random manner, to eliminate any possible time dependent trend. The number in bracket represents the order of in which the treatment combination was carried out in the experimental programme.

Table 5.3 The order of treatment combinations in the experimental programme

A Feed rate cm^3/h	B Feed concentration % w/v	Eluent rate D			
		8 dm^3/h		10 dm^3/h	
		Enzyme activity U/cm^3		Enzyme activity U/cm^3	
		75	100	75	100
150	25	(3) $A_1B_1C_1D_1$	(9) $A_1B_1C_2D_1$	(2) $A_1B_1C_1D_2$	(11) $A_1B_1C_2D_2$
	50	(6) $A_1B_2C_1D_1$	(15) $A_1B_2C_2D_1$	(7) $A_1B_2C_1D_2$	(14) $A_1B_2C_2D_2$
230	25	(8) $A_2B_1C_1D_1$	(12) $A_2B_1C_2D_1$	(16) $A_2B_1C_1D_2$	(13) $A_2B_1C_2D_2$
	50	(5) $A_2B_2C_1D_1$	(1) $A_2B_2C_2D_1$	(10) $A_2B_2C_1D_2$	(4) $A_2B_2C_2D_2$

5.3.2 Results and Statistical Analysis

The results of the factorial experiments showed that carrying out the experiment at enzyme activities of 75 U/cm^3 and 100 U/cm^3 significantly increased the percentage of conversion of the substrate sucrose compared to the preliminary experiment at 60 U/cm^3. Most of the treatment combinations achieved 100% sucrose conversion, except for treatment combination $A_2B_2C_1D_2$ where the conversion was 98%.

For each of the 16 treatment combinations there were 7 responses of interest. Response (1) is the resolution between glucose and fructose $R_{G\text{-}F}$, responses (2) and (3) are the peak

concentrations of glucose $\hat{C}_G$ and frucrose $\hat{C}_F$, and responses (4) and (5) are the percentage of the products recovered at 100 % purity Y_G and Y_F and responses (6) and (7) are the pure product throughputs P_G and P_F. However, responses (6) and (7) were not analysed statistically since they were derived from responses (4) and (5). These responses are presented in table 5.4.

Table 5.4 The 2^4 factorial experiment results

Response	1	2	3	4	5	6	7
Runs	R_{G-F}	$\hat{C}_G$ %w/v	$\hat{C}_F$ %w/v	Y_G %	Y_F %	P_G	P_F
$A_1B_1C_1D_1$	0.76	1.32	1.22	24.5	37.6	4.59	7.05
$A_2B_1C_1D_1$	0.5	2.2	1.6	0.59	5.3	0.17	1.52
$A_1B_2C_1D_1$	0.65	3.4	2.96	27.6	26.8	10.35	10.05
$A_2B_2C_1D_1$	0.3	3.55	3.1	2.1	4.67	1.21	2.69
$A_1B_1C_2D_1$	0.71	1.42	1.32	16.67	25.76	3.1	4.83
$A_2B_1C_2D_1$	0.57	2.4	1.6	2.4	27.3	0.69	7.85
$A_1B_2C_2D_1$	0.62	3.65	2.9	27.6	37.92	10.35	14.22
$A_2B_2C_2D_1$	0.52	4.3	3.9	11.3	18.62	6.5	10.71
$A_1B_1C_1D_2$	0.7	1.46	1.37	19.4	21.2	3.64	3.98
$A_2B_1C_1D_2$	0.76	2.75	2.33	53.6	25.2	15.41	7.24
$A_1B_2C_1D_2$	0.7	1.9	1.76	8.4	25.1	3.15	9.4
$A_2B_2C_1D_2$	0.64	4.1	3.2	1.17	23.89	0.67	13.74
$A_1B_1C_2D_2$	0.72	1.5	1.3	20.8	51.8	3.9	9.71
$A_2B_1C_2D_2$	0.63	2.88	2.4	23.47	31.9	6.74	9.14
$A_1B_2C_2D_2$	0.65	2.5	2.15	33.9	25.0	12.7	9.38
$A_2B_2C_2D_2$	0.7	3.1	2.75	8.3	17.4	4.77	10.0

In factorial experiments, the effect of a factor, say A, on a response is calculated as the difference between the average responses with factor A at higher level A_2 and at lower level A_1. While the interaction effect between factor A and B, is calculated as the difference between the effects of changing from A_1 to A_2 with B at the high level and with B at the low level.

Davies [113] has outlined a systematic tabular method for these calculations. The method is called the Yate's method and is reported in Appendix A4. To decide whether the effects of the factors or factor interactions were significant, a statistical test of significance was required. The most appropriate statistical test in this case was the F-test [113-115].

In order to apply the F-test an estimate of error variance is needed. However, the experimental error variance could not be calculated directly at two levels with single replicate factorial experiments. An alternative approach to estimate the experimental error variance is to add to the 2^4 factorial design replicated centre point experimental runs [116]. This centre point is designated as $A_0B_0C_0D_0$. The pure error sum of squares was determined by computing the sum of squares between the observations at the centre of the design [116]. The values of the factors at the centre of the 2^4 factorial design were;

Feed fow rate	A_0	= 190 cm^3/h
Feed concentration	B_0	= 37.5 % w/v
Enzyme activity	C_0	= 87.5 U/cm^3
Eluent flow rate	D_0	= 9 dm^3/h

Table 5.5 shows the responses and the corresponding error variance of the replicated centre point experimental runs.

Table 5.5. Responses for the replicated centre point

Runs	R_{G-F}	$\hat{C}_G$ %w/v	$\hat{C}_F$ %w/v	Y_G %	Y_F %
$(A_oB_oC_oD_o)_1$	0.55	3.0	2.74	24.97	32.1
$(A_oB_oC_oD_o)_2$	0.58	3.5	2.85	28.2	27.3
$(A_oB_oC_oD_o)_3$	0.52	3.2	2.61	25.5	42.8
$(A_oB_oC_oD_o)_4$	0.68	3.1	2.8	40.1	29.8
$(A_oB_oC_oD_o)_5$	0.62	3.3	2.5	32.6	30.3
Sum of square	0.016	0.159	0.082	157.19	145.41
error variance	0.004	0.039	0.021	39.3	36.35

Using the values of error variance in table 5.5 the corresponding F-ratio could be calculated. The F-value is the ratio of a response variance of a treatment combination divided by the error variance of that particular response. As either positive or negative changes in the effects were of interest, a double-sided test was appropriate [113].

The critical F-values obtained from standard F-tables [113] based on 1 and 4 degrees of freedom and at the 10 % level of significance was 7.71. If any of the F-values obtained from the treatment combination was greater than 7.71, the value was considered to be significant. On the other hand, if the F-value was less than 7.71, then there was a greater than 10 % chance that the observed variance was due to background variation and therefore was not significant. However, discretion must be made for F-values close to the critical value.

5.3.3 Discussion of Statistical Results

In the 2^4 factorial experiment, there were fifteen estimated effects, four were the main effects, six were two-factor interactions and five were of higher order interactions for each response. The effects and the F-values for the responses are given in tables 5.6-5.9. The feed rate was found to be the most significant factor affecting the performance of the CRAC as a combined reactor separator.

Refering to table 5.6, a value of -0.111 for the estimate of the main effect of feed rate on the resolutions, implied that the effect of increasing the feed rate from 150 cm^3/h to 230 cm^3/h was to decrease the resolution by 0.111. As was mentioned in section 5.3.3, this value refered to the difference between the average effect of resolutions from 8 treatment combinations at a feed rate of 230 cm^3/h and 8 treatment combinations at a feed rate of 150 cm^3/h.

Accordingly, from table 5.9 a value of 0.108 for the estimate of the main effect of eluent rate on resolution implied that an increase in resolution by 0.108 was obtained by increasing the eluent rate from 8 dm^3/h to 10 dm^3/h.

5.3.3.1 Effect of Feed Rate

The effects of increasing the feed rate from 150 cm^3/h to 230 cm^3/h on the responses are discussed in more detail in this section. The direct effect of increasing the feed rate could be visualised by comparing the elution profiles of all its treatment combination pairs (Appendix A4).

A pair of treatment combinations was defined as the two treatment combination which differ at the level of one of the factors only. In 2^4 factorial experiments, for each factor, the treatment combinations could be arranged into 8 corresponding pairs. An example of a pair of treatment combinations for the effect of feed rate are $A_1B_1C_2D_1$ and $A_2B_1C_2D_1$. The only difference between these treatment combinations $A_1B_1C_2D_1$ and $A_2B_1C_2D_1$ was

that the former was set at the lower feed rate level while the latter was set at the higher feed rate level.

Table 5.6 summarises the effects and F-values for all the responses.

Table 5.6 F-values for the effect of feed rate

Response		Effect	F-Value
Resolution Glucose - Fructose (1)	R_{G-F}	-0.111	12.25
Peak concentration of glucose (2)	$\hat{C}_G$	1.016	103.6
Peak concentration of fructose (3)	$\hat{C}_F$	0.737	103.5
Yield of pure glucose (4)	Y_G	-9.5	9.17
Yield of pure fructose (5)	Y_F	-12.11	16.14

The results of the statistical analysis in table 5.6 showed that the feed rate significantly reduced the performance of the biochemical reaction and separation in a CRAC. Although the effect on the peaks in the concentration of glucose and fructose was positive, the effect was not large enough to produce a positive effect on the yield.

Increasing the feed flow rate from 150 cm^3/h to 230 cm^3/h at a constant concentration, has the effect of increasing the mass of sucrose fed into the column by about 50%. In terms of the actual mass flow rate, the change corresponds to an increase of 20 g/h at the lower substrate concentration and 40 g/h at the higher substrate concentration. These have the effect of decreasing the value of the enzyme usage. In other word less enzyme was available per unit mass of the substrate.

Increasing the amount of substrate also increased the time for the enzyme to mix and react. Accordingly, less time was available for the separation of the formed glucose and fructose. In addition, increasing the feed flow rate, increased the initial feed bandwidth. The

following empirical relationship [80] relates to the initial feed bandwidth θ_f for a feed flowrate of Q_f and an eluent flowrate of Q_e.

$$\theta_f = \frac{2\pi Q_f}{Q_f + Q_e} \qquad 5.3$$

According to equation 5.3 at the lower eluent flow rate of 8 dm^3/h, an increase in flowrate from 150 cm^3/h to 230 cm^3/h caused the initial band width to change from 6.6° to 10.1°. While at the higher eluent flow rate of 10 dm^3/h, an increase in flowrate from 150 cm^3/h to 230 cm^3/h caused the initial bandwidth to change from 5.3° to 8.1°. A larger initial bandwidth caused the products to have a larger exit bandwidth and thus increased the degree of bands overlapping. The combinations of these effects reduced the resolution between the products.

The statistical analysis of the effect of the peak concentration indicated that there was 1.01 and 0.7 % w/v significant increase for glucose and fructose respectively. This significant difference was mainly attributed to the shape of the elution profiles of glucose and fructose. The effect of increasing the feed rate could also be demonstrated by comparing elution profiles of one of the treatment combinations pairs, figure 5.3 for the treatment combination $A_1B_1C_2D_1$ and figure 5.4 for the treatment combination $A_2B_1C_2D_1$. From figures 5.3 and 5.4, increasing the feed rate, raised the concentration of both glucose and fructose peaks. The rise in concentrations for both cases were not in the same order of magnitude. There was a 70% rise in the peak concentration of glucose while there was only a 21% increase in the fructose peak.

As mentioned in section 5.2.1, fructose tends to have a broader elution profile. The increase in flow rate caused a greater increase in the peak bandwidth for the fructose peak than the glucose peak. As a consequence the rise in the peak concentration for fructose was less than that of glucose.

From figure 5.4, the formation of a broad and negative skew elution profile for fructose towards the glucose peak caused a greater band overlapping. This is also shown by the difference in the asymmetric factor values, 0.95 for glucose and 0.8 for fructose. In fact, the significant gain in the peak concentration of glucose was offset by this greater band overlapping.

Accordingly, the overall effect on the percentage of recovery of pure glucose and fructose dropped by 9.5 % and 12.11% respectively.

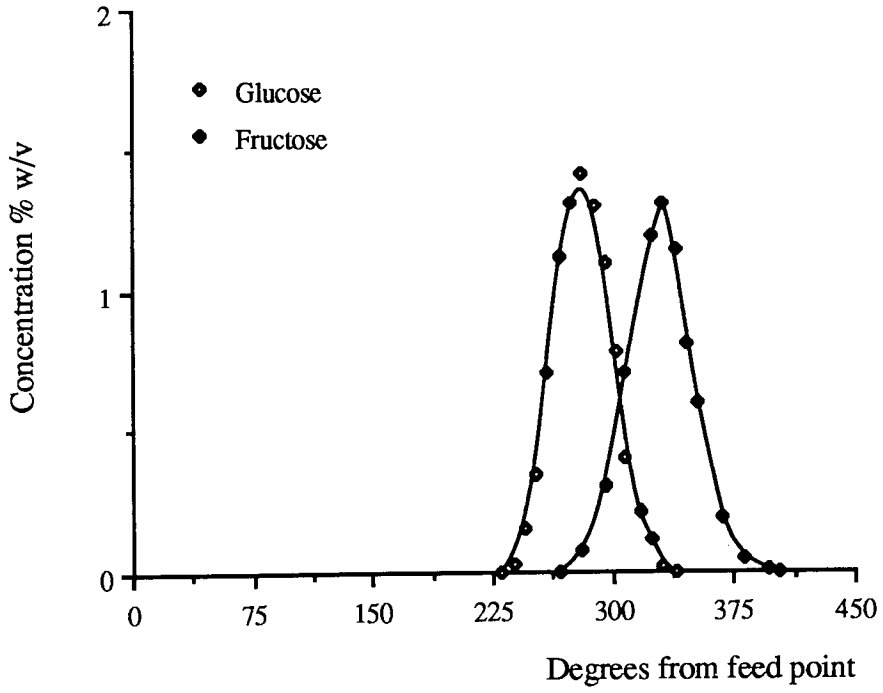

Figure 5.3 Elution profile for treatment combination $A_1B_1C_2D_1$ (Run 150-25-8-100-240)

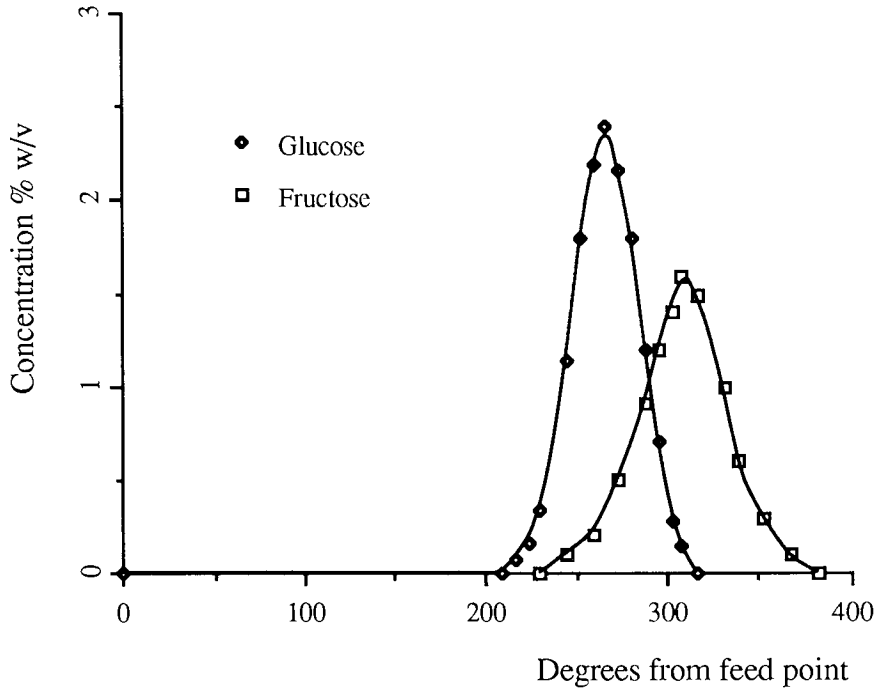

Figure 5.4 Elution profile for treatment combination $A_2B_1C_2D_1$ (Run 230-25-8-100-240)

5.3.3.2 Effect of Feed Concentration

Table 5.7 shows the effects and F-values on the responses when the substrate concentration was changed from 25 % w/v to 50 % w/v. The analysis indicated that, the effects on the peak concentration of glucose and fructose were statistically significant.

Table 5.7 F-values for the effect of feed concentration

Response		Effect	F-Value
Resolution Glucose - Fructose (1)	R_{G-F}	-0.071	5.0
Peak concentration of glucose (2)	$\hat{C}_G$	1.32	174.9
Peak concentration of fructose (3)	$\hat{C}_F$	1.19	273.1
% of pure glucose recovered (4)	Y_G	-5.13	2.68
% of pure fructose recovered (5)	Y_F	-5.83	3.74

The effect of the feed concentration on the elution profiles is shown by one of its treatment combinations pairs, $A_1B_1C_1D_1$ and $A_1B_2C_1D_1$ in figures 5.5 and 5.6.

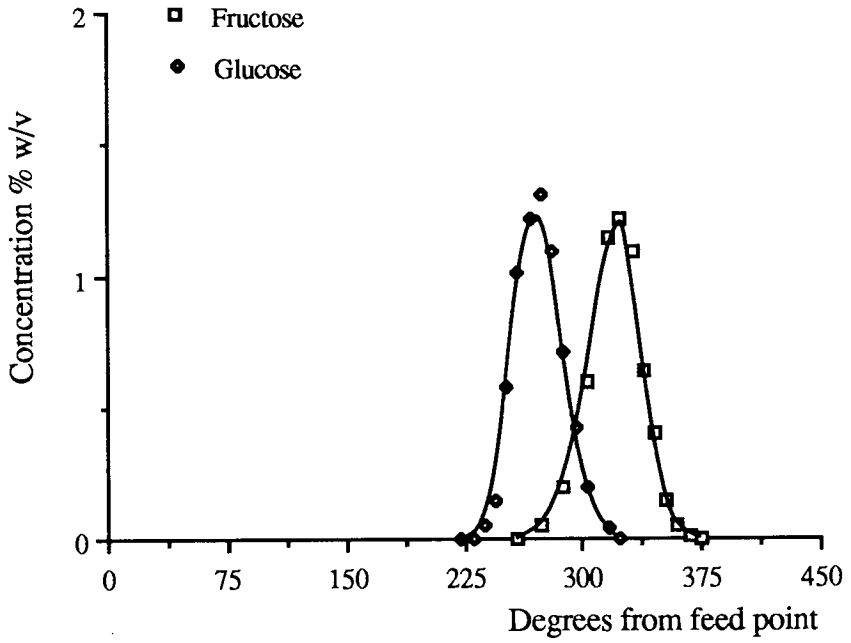

Figure 5.5 Elution profile for treatment combination $A_1B_1C_1D_1$ (Run 150-25-8-75-240)

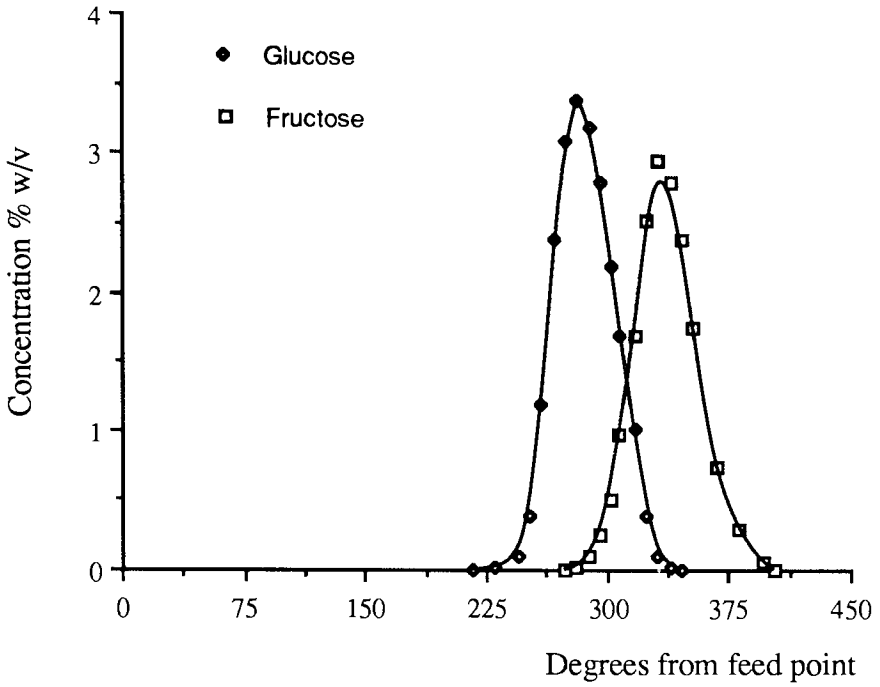

Figure 5.6 Elution profile for treatment combination $A_1B_2C_1D_1$ (Run 150-50-8-75-240)

The change from low feed concentration to high feed concentration resulted in an increase in the actual mass flow rate from 37.5 g/h to 57.5 g/h. This increase was relatively much higher compared to the increase due to changing the feed rate. Despite this greater increase, the effect of feed concentration on the resolution was considerably less (-0.07) compared to the effect of feed rate (-0.11). In fact, the effect on the resolution was statistically insignificant. This observation was of great interest since it conclusively pointed out that mass overload was preferred over volume overload in high conversion runs.

A relatively higher positive effect on the products peak concentrations was also noted. Unlike the effect of feed rate, the effect of feed concentration on the percentage of pure products recovered was not significant. This result indicated that, a higher throughput of the products could be obtained from a higher substrate concentration. However, this was at the expense of more impure products being wasted.

5.3.3.3 Effect of Enzyme Activity

Increasing the enzyme activity from 75 U/cm^3 to 100 U/cm^3 did not produce any significant effect on the responses. Compared to the preliminary experiment at 60 U/cm^3 enzyme activity, the effect of increasing the enzyme activity to 75 U/cm^3 was considerable. However, increasing the enzyme activity beyond 75 U/cm^3 did not significantly improve the performance of the system. It was also noted by Akintoye [82] working on the SCCR-S1 sytem, that there was an optimum level of enzyme activity in the system (60 U/cm^3). No further improvement in the performance of the system was obtained by increasing the enzyme activity above this level.

This limit was probably due to the phenomena of mixing. For the substrate to react in the column, it has to mix with the enzyme. The mixing process in the column is governed by the interstitial eluent velocity, the feed rate and the feed concentration. The efficiency of the enzyme is therefore dependent on these factors. It will be shown in section 5.3.3.5 that the increase of enzyme activity did have an interaction effect with the other factor.

As mentioned in section 5.3.2, the treatment combination $A_2B_2C_1D_1$ did not achieve a 100 % conversion. Since only one treatment combination which did not achieve a complete conversion, statistical analysis was not carried out for the percentage of conversion response. This was more likely to be due to an experimental error rather than a random error.

The elution profiles for this treatment combination is shown in figure 5.7 and its corresponding treatment combination pair ($A_2B_2C_2D_1$) is shown in figure 5.8. The differences in the responses between these two treatment combinations are tabulated in table 5.4. As a result of incomplete reaction the resolution between glucose and fructose dropped considerably below the average value.

The results once more indicated that to obtain a higher performance in a simultaneous biochemical reactor separator a fast reaction rate was desirable.

Table 5.8 F-values for the effect of enzyme activity

Response		Effect	F-Value
Resolution Glucose - Fructose (1)	R_{G-F}	0.014	0.19
Peak concentration of glucose (2)	$\hat{C}_G$	0.133	1.8
Peak concentration of fructose (3)	$\hat{C}_F$	0.097	1.81
% of pure fructose recovered (4)	Y_G	0.89	0.08
% of pure fructose recovered (5)	Y_F	8.22	7.43

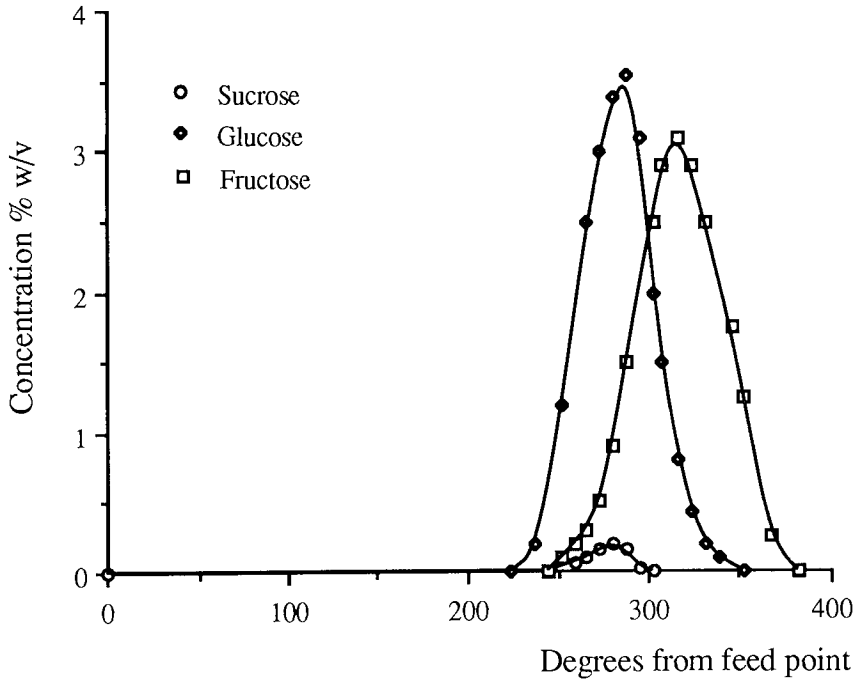

Figure 5.7 Elution profile for treatment combination $A_2B_2C_1D_1$ (Run 230-50-8-75-240)

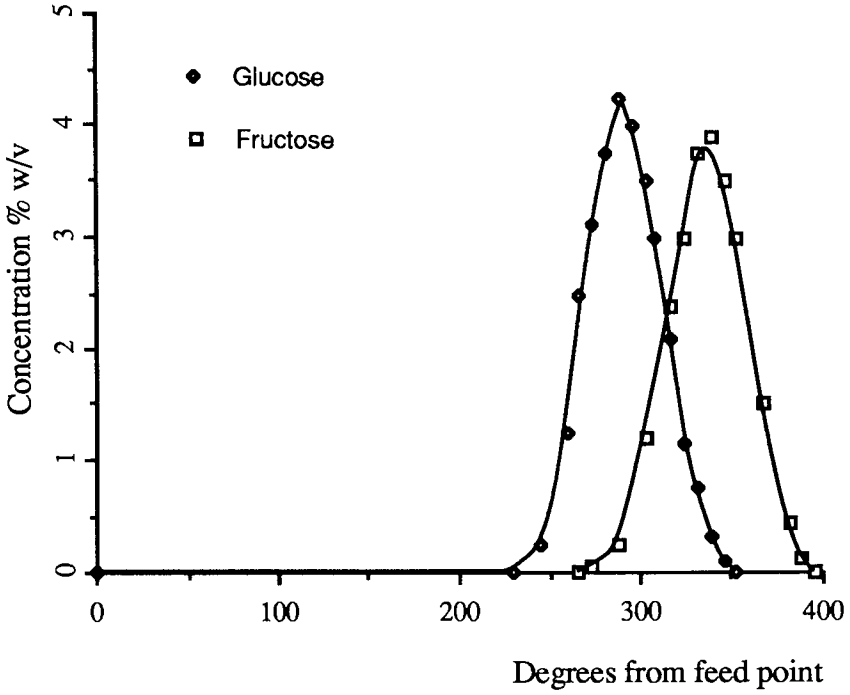

Figure 5.8 Elution profile for treatment combination $A_2B_2C_2D_1$ (Run 230-50-8-100-240)

5.3.3.4 Effect of Eluent Rate

The statistical analysis showed that increasing the eluent rate from 8 dm^3 to 10 dm^3 significantly improved the resolution. The increase in the eluent rate effectively increased the interstitial velocity from 3.11 cm/min to 3.89 cm/min and thereby decreased the residence times of the solutes. The reduction in the residence times was apparently compensated for by the gain in faster mixing between the enzyme and the substrate. This faster mixing between the enzyme and the substrate, helps to bring down the substrate concentration to below the inhibition level more quickly.

Table 5.9 F-value for the effect of eluent rate

Response		Effect	F-Value
Resolution Glucose - Fructose (1)	R_{G-F}	0.108	11.83
Peak concentration of glucose (2)	$\hat{C}_G$	-0.26	6.59
Peak concentration of fructose (3)	$\hat{C}_F$	-0.167	5.33
% of pure glucose recovered(4)	Y_G	10.5	11.22
% of pure fructose recovered (5)	Y_F	4.71	2.44

The sucrose inversion reaction was assumed to follow the inhibited Michelis-Menten kinetics. The maximum rate of reaction V_{max} occurs at 12% w/v sucrose concentration. Above this value, the reaction rate is inhibited.

Dilution of the substrate to a concentration where V_{max} occurs helped to increase the reaction rate and as a result, more of the products were formed in the upper section of the column, giving a greater possibility for them to be separated. This explained the effect of eluent flow rate on the experimental results obtained.

Also at a higher eluent rate, the degree of dispersion and band broadening were reduced which in turn reduced the band overlapping. However, more enzyme was required to maintain the enzyme activity due to an increased eluent rate. There is however a limit to this statement since chromatographic theory predicts that higher eluent rates will cause the performance to fall.

The effect of eluent rate on the elution profiles on a pair of treatment combinations are shown in figure 5.9 and 5.10. The elution profiles for both glucose and fructose are sharper and their exit bandwidths are smaller in comparison to the low eluent rate run. The resolution between glucose and fructose R_{G-F} is 0.76 and the asymmetry factors As_G and As_F are 1.29 and 1.2 respectively for the high eluent rate treatment. These asymmetry factor values indicate that the chromatograms are nearly symmetrical. As a result the

percentage of pure glucose and fructose recovery increases from 0.59 to 53.6 % for glucose and 5.3 to 25.2% for fructose (table 5.4). In fact this is the only treatment combination pair where the percentage of recovery of pure glucose is greater than that of fructose. This again demonstrates the effect of the eluent flow rate on the shape of the elution profile which in turn affects the performance of the chromatograph.

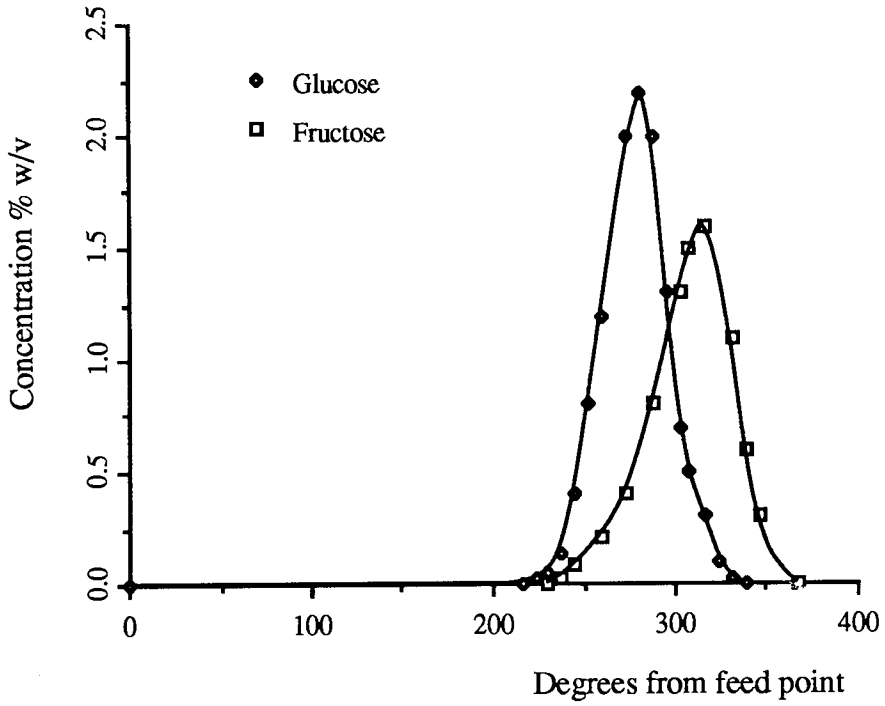

Figure 5.9 Elution profile for treatment combination $A_2B_1C_1D_1$ (Run 230-25-8-75-240)

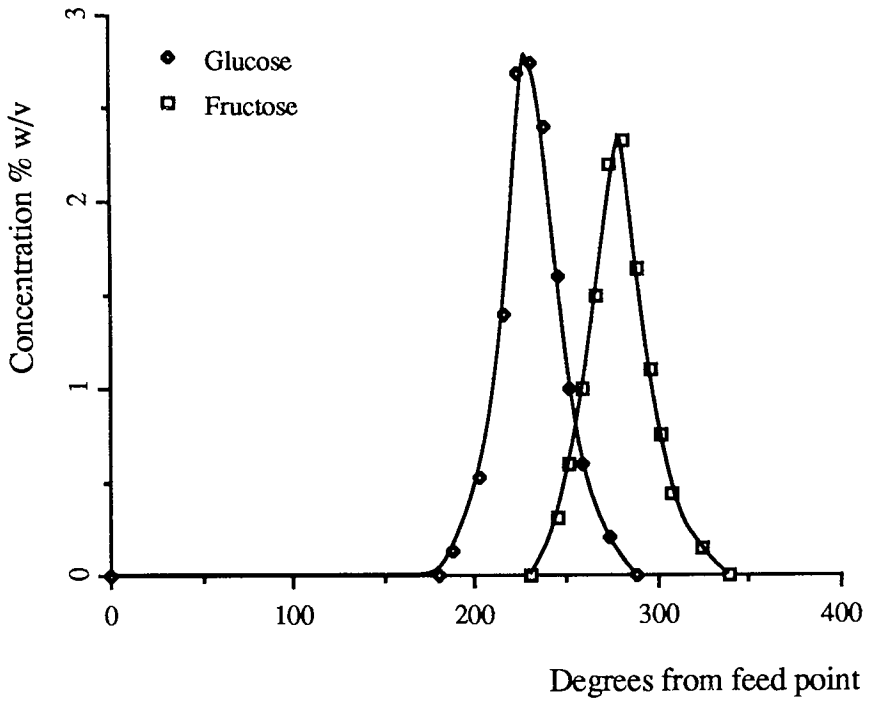

Figure 5.10 Elution profile for treatment combination $A_2B_1C_1D_2$ (Run 230-25-10-752-40)

5.3.3.5 The Effect of Interaction

The summary of the interactions effects are given in table 5.10. Table 5.10 indicates that the feed rate and the eluent rate interact to produce the most positive significant effects on the responses.

It was shown in table 5.6 that the increase in feed rate alone can significantly decrease the resolution. A positive interaction with eluent rate and feed rate indicated that the decrease is greater at lower eluent rates. This further suggests that dilution of the feed at higher eluent rate helps to reduce the inhibition effect on the enzyme.

In the case of the peak concentration of glucose and fructose, the positive interaction effect between feed rate and eluent rate means that the loss in increasing the eluent rate is lower than the gain due to the high feed rate.

The individual effects of increasing the feed rate and the eluent rate resulted in the increased percentage of glucose recovery as shown in tables 5.6 and 5.9. Increasing both of these factors will enhance the percentage of glucose recovery further.

The increase in factor feed concentration alone was found to produce a positive effect on peak concentration and an insignificant effect on percentage of recovery of the product. While the increase in eluent rate alone has a negative effect on the peak concentration and a positive effect on the percentage recovery of glucose. However, table 5.10 shows that these two factors interacted to produce a negative effect on all the responses. This means that the effect contributed by the eluent rate produced more useful result at the lower substrate concentration.

Other interaction effects are between factors A and C to produce significant effect on the percentage of recovery of glucose. This positive interaction effect indicated that the effect of enzyme activity was greater at higher substrate concentrations.

Table 5.10 F-value of the major interactive effect

Treatment combination	R_{G-F} (1)	$\hat{C}_G$ (2)	$\hat{C}_F$ (3)	Y_G (4)
$A_1B_2C_2D_1$	—	—	—	9.62
$A_2B_1C_1D_2$	10.25	12.38	15.76	11.22
$A_1B_2C_1D_2$	—	32.33*	64.62*	12.82*

* Negative effect

5.4 Further Study on the Effect of Feed Rate on the Biochemical Reaction and Separation in a CRAC

From the results of the statistical analysis, feed rate was found to have the most significant effect on the bioreaction and separation in an annular chromatograph. It was decided to

investigate this factor further. Five runs were carried out and the results are presented in table 5.11.

Table 5.11 shows that a complete conversion for feed rates of up to 350 cm^3/h was obtained. The resolution between glucose and fructose and the percentage of pure product recovered decreased as the feed rate was increased. On the other hand, the product throughput increased as the feed rate was increased and reached a maximum value at feed rate of 350 cm^3/h.

Increasing the feed flow rate to 400 cm^3/h as in run 400-50-7.5-240 did not achieve 100 % conversion. There was still about 5 % of unreacted sucrose in the product stream. In table 5.11 the percentage of pure fructose recovered was always greater than for glucose. This observation was almost true in the factorial experiment in section 5.3.2. The main reason for this observation was that the elution profile of the more retained component (fructose) was always skewed towards the faster moving component (glucose). Since the two components were in equal amount, then a higher throughput will always be obtained from the more retained component.

Table 5.11 Effect of feed rate data

Response	1	2	3	4	5	6	7
Runs	R_{G-F}	$\hat{C}_G$ %w/v	$\hat{C}_F$ %w/v	Y_G %	Y_F %	P_G g/h	P_F g/h
150-50-7.5-75-240	0.6	3.14	2.82	22.1	30.9	16.5	23.12
200-50-7.5-75-240	0.58	3.42	3.15	18.6	18.8	18.6	18.8
250-50-7.5-75-240	0.67	3.95	3.43	14.5	34.2	18.12	42.5
350-50-7.5-75-240	0.42	5.25	4.16	13.8	25.8	24.15	45.15
400-50-7.5-75-240	0.36	6.13	5.42	3.12	5.8	6.24	11.6

5.5 Comparison of Biochemical Reaction and Separation Performance in a CRAC and SCCR-S1 System

The comparison of reaction and separation performance on a rotating annular chromatograph and SCCR-S1 system [82] was based on three main operating parameters namely the feed throughput T_{Feed}, product concentration and enzyme usage. The comparison was based on two feed streams for the CRAC.

In terms of feed throughput and product purities both systems are comparable (tables 5.12 and 5.13). In the SCCR-S1 system only one of the product fractions could be obtained at high purity. The only product available at greater than 95% purity was glucose. The fructose fraction was only 85% pure. In the case of the CRAC, the equipment can handle multicomponent mixtures and the products can be collected into any number of fractions. However, the SCCR-S1 enzyme usage was lower than the enzyme usage in the rotating annular chromatograph (table 5.12). At the same feed throughput of about 16 kg/m^3 resin/h the enzyme usage for the SCCR-S1 system was half that of the enzyme usage for the rotating annular chromatograph with two feed points.

In terms of the equipment construction, the SCCR-S1 system was more complex than the CRAC system. Although the capital cost for each type of equipment was similar, the bed length for the CRAC was 1.35 m whereas the SCCR-S1 had a separating bed length of 6.6 m. This longer bed length and thus a higher separation performance of the SCCR-S1 enabled higher concentrations of products to be obtained.

The main advantage of a CRAC over the SCCR-S1 system was that, the former operates under steady state conditions. In the SCCR-S1 system a psuedo steady state could only be achieved after about 60 hours of operation. However in a CRAC a steady state could be achieved in about 2 hours. A steady state process is simpler to operate and control than the unsteady state process.

Table 5.12 Simultaneous biochemical reaction and separation performance on the CRAC

Runs	Feed throughput (kg sugar/m^3 resin/h) T_{Feed}	Glucose throughput at 95% purity (kg sugar/m^3 resin/h) T_G	Glucose concentration % w/v $\overline{C}_G$	Fructose throughput at 95% purity (kg sugar/m^3 resin/h) T_F	Fructose concentration % w/v $\overline{C}_F$	Enzyme usage
150-50-7.5-75-240	10.4	2.28	1.37	3.13	1.38	1.28
200-50-7.5-75-240	13.8	2.55	1.24	2.37	1.27	0.96
250-50-7.5-75-240	17.2	2.71	1.87	4.82	2.12	0.78
350-50-7.5-75-240	11.4*	1.68*	1.66	2.39*	2.11	1.10*

* Single feed point

Table 5.13 Simultaneous biochemical reaction and separation performance on a SCCR-S1system (data from reference 82).

Feed throughput (kg sugar/m^3 resin/h)	Glucose throughput at 95% purity (kg sugar/m^3 resin/h) T_G	Glucose concentration % w/v $\overline{C}_G$	Fructose throughput at 85% purity (kg sugar/m^3 resin/h) T_F	Fructose concentration % w/v $\overline{C}_F$	Enzyme usage
6.19	3.31	2.42	2.07	0.93	0.345
9.27	3.62	2.85	2.92	1.75	0.397
12.94	4.38	3.54	5.9	2.85	0.337
16.32	5.3	4.34	6.95	3.69	0.338

CHAPTER SIX

FURTHER STUDY OF A CRAC AS A COMBINED BIOCHEMICAL REACTOR-SEPARATOR USING MALTOGENIC ENZYME AND MODIFIED STARCH

6.1 Introduction

The results of the simultaneous saccharification and separation of liquefied starch to maltose experiments are presented in this chapter. Preliminary simultaneous saccharification and separation experiments were carried out in a batch liquid chromatographic column. In the preliminary experiments on a batch chromatographic column soluble starch (starch A) was used while in the main experiments on the CRAC soluble potato starch (starch B) and modified tapioca starch (starch C) were used. The enzymic reaction conditions established in chapter 4 were used throughout the experiments.

The main objective of the work has been to evaluate further the performance of a CRAC under simultaneous biochemical reaction and separation conditions and also to establish the upper limit of the equipment performance. In this study, the degree of substrate conversion, the resolution of the product maltose and the percentage of pure maltose recovered were used as the performance indicators.

6.2 Simultaneous Biochemical Reaction and Separation in a Batch Chromatographic Reactor

The experimental runs are presented in the coded form, 5-5A-200-60, where the code represent pulse size 5 cm^3, substrate A concentration 5 % w/v, eluent flow rate 200 cm^3/h and enzyme activity 60 U/cm^3. The results in table 6.1 indicated that it was possible to carry out simultaneous saccharification of liquefied starch and separation of the product maltose in a chromatographic reactor. The results also indicated that the conversion was

comparable to the steady-state value obtained under batch reaction conditions (table 4.4, Chapter 4).

Table 6.1 Batch chromatographic reactor-separator results

Experimental Run	Starch conversion to maltose %	Resolution R_{M-D}	Starch conversion to glucose %
5-5A-200-60	81.1	1.5	5.4
10-5A-200-60	79.1	1.1	3.18
5-10A-200-60	76.8	1.3	3.0

The elution profiles of the runs are plotted in figure 6.1 through to figure 6.3. From figure 6.1 (run 5-5A-200-60), the liquefied starch conversion to maltose was 81.1 %. The elution profiles indicated that there is a complete separation between dextrin and the product maltose and glucose. Dextrin was eluted first, followed by maltose and small amount of the more retained glucose. The absence of any maltotriose and the presence of a small amount of glucose indicated that it had been converted to maltose and glucose.

The elution profile of the unreacted starch exhibited a triangular shape with a mild skew. The maltose peak shows a narrow symmetrical elution profile. The formation of narrow symmetrical elution profiles was desirable as they allow the product to be collected at a higher concentration and reduces the degree of overlapping between peak. A small amount of glucose appeared as a broad peak under one side of the maltose peak base. The inability of glucose to separate was probably due to a tag-along effect. This phenomena occured as a result of a faster speed of migration of the more retained solute (maltose) when the two solutes co-eluted in a significantly different proportion. The removal of the small amount of glucose from the maltose peak was more of a purification problem rather than a separation problem.

Doubling feed pulse size as in run 10-5A-200-60 increased the elution profiles bandwidths (figure 6.2). As a consequence the resolution R_{M-D} decreased from 1.5 to 1.1. However good conversion and separation were still achieved.

Comparing the elution profiles in figure 6.2 and figure 6.3 for run 10-5A-200-60 and run 5-10A-200-60, a higher resolution R_{M-D} and a higher maltose peak were obtained for the higher concentration run. In term of the actual amount of substrate injected, the value was equal in both runs. This result further confirmed the finding in section 5.3.3.2 that mass overload was better than volume overload in a high conversion run.

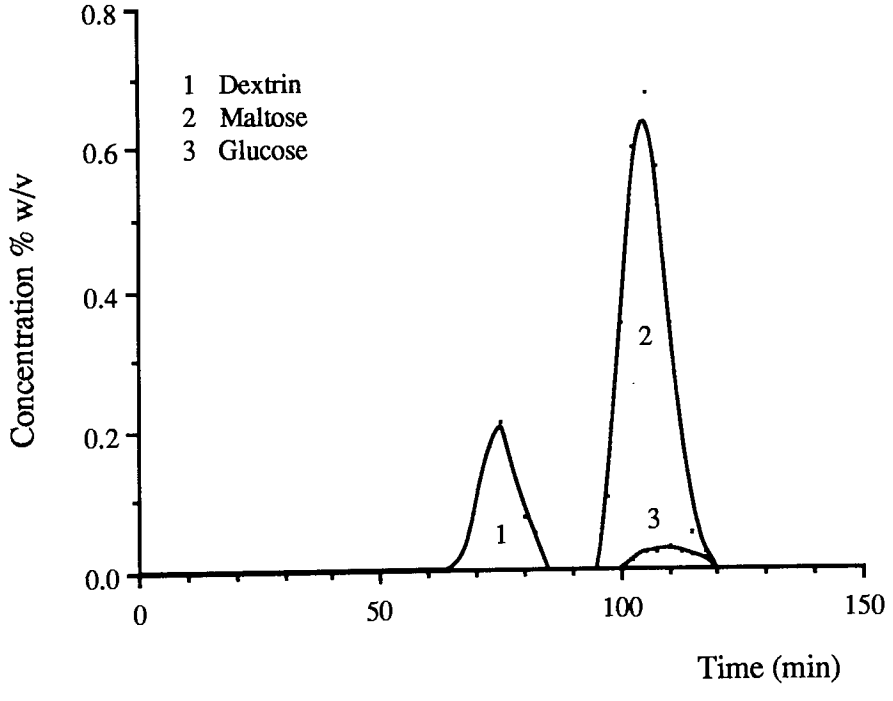

Figure 6.1 Elution profile for run 5-5A-200-60 on a batch chromatgraphic reactorseparator

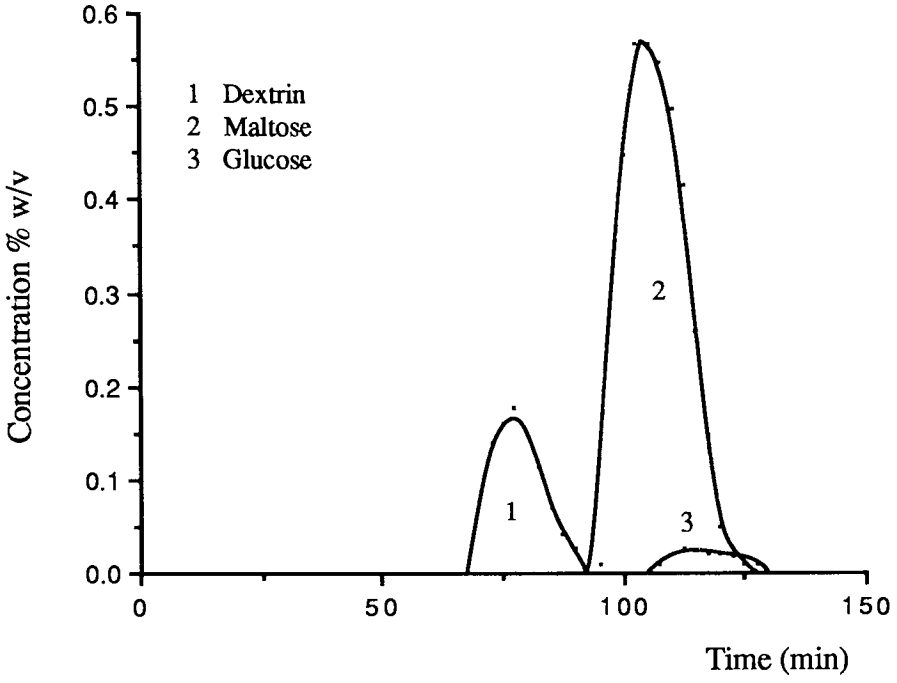

Figure 6.2 Elution profile for run 10-5A-200-60 on a batch chromatgraphic reactor-separator

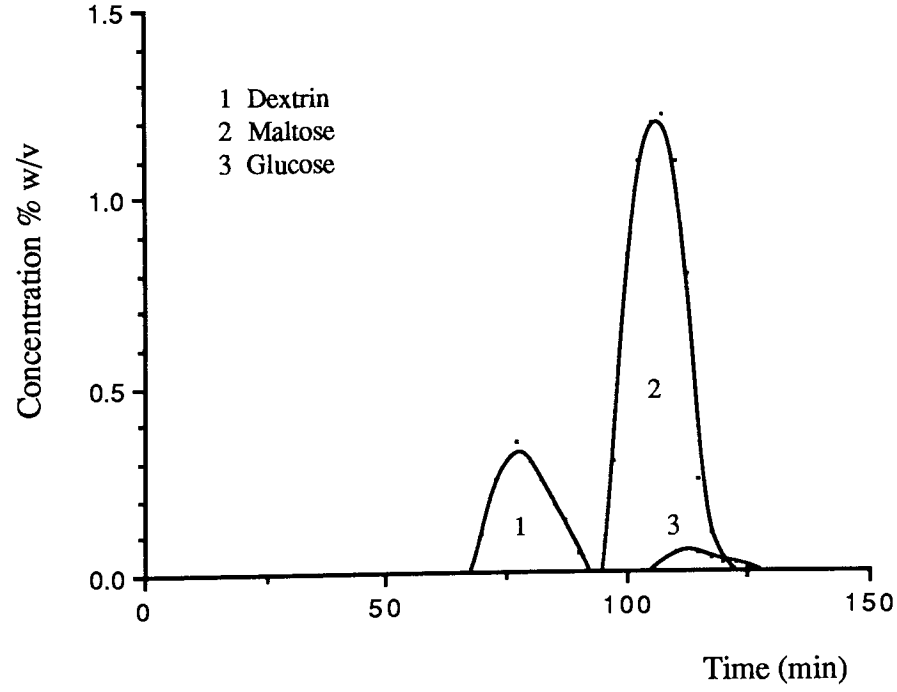

Figure 6.3 Elution profile for run 5-10A-200-60 on a batch chromatgraphic reactor-separator

6.3 Simultaneous Biochemical Reaction and Separation In a CRAC

In chapter 5, the factors which determined the performance of a CRAC under simultaneous reaction and separation conditions had been established. In this section the effect of feed flow rate and feed concentration under a constant eluent rate and enzyme activity will be investigated further.

The linear flow eluent velocity used in the batch chromatographic reactor was maintained. The corresponding eluent flow rate on the CRAC was 8 dm^3/h. The annular column rotation rate was set at 240 degrees/h.

The study was carried out by using a simple experimental programme. The programme involved operating the CRAC under a volume overload followed by a concentration overload condition [43,132]. The first part was carried out by using a constant low substrate feed concentration and gradually increasing the substrate feed flow rate until a volume overload condition was approached. The second part of the experiment was carried out by operating the CRAC near the volume overload and gradually increasing the feed concentration until the performance of the CRAC had deteriorated.

In the preliminary experiment on the CRAC it was found that by directly mixing the enzyme and the feed solution on line just before entering the column, the amount of the enzyme used could be reduced considerably. Compared to the batch chromatographic reactor, only about one third of the enzyme activity based on the total eluent flowrate was required to perform the reaction.

This procedure was possible since both the enzyme and the liquefied starch were not retarded by the resin. Another advantage of this procedure was that as the liquefied starch underwent stepwise degradation to dextrin, it started to be held back by the resin. As a result there was a relative separation between the substrate and the enzyme as they moved through the column. The separation between the degraded starch molecules, maltose and the enzyme ensured that the reaction occurred mainly in the upper part of the column where

the reaction rate was fastest thus giving sufficient column length for the separation to take place.

It was noted by other workers [117] when studying the saccharification of modified starch to maltose using the enzyme β-amyase, the reaction velocity decreased with a decrease in molecular weight of the starch and with the accumulation of the saccharification products.

6.3.1 Volume Overload Experiment

The results of volume overload experiments are shown in table 6.2. The experimental runs were coded in the same manner as for the batch chromatographic reactor where the first term represented the feed flowrate cm^3/h, followed by type of substrate and its concentration % w/v, eluent flowrate dm^3/h, enzyme activity U/cm^3 and column rotation rate degrees/h respectively.

Table 6.2. Effect of feed flow rate on CRAC performance

Experimental Run	Starch conversion to maltose %	Resolution R_{M-D}	Maltose exit bandwidth	% of maltose recovered
220-6.8B-8-14-240	81.9	1.73	86.4°	80.4
330-7.25B-8-20-240	79.1	1.33	100.8°	74.1
440-8.4B-8-20-240	72.6	0.81	115.2°	72.2

From table 6.2 at low feed concentration and feed flow rates as in the run 230-7.25B-8-20-240, a high substrate conversion to maltose was achieved. This is comparable to the steady-state value obtained under batch reaction conditions (see table 4.4). The resolution R_{M-D} between the product maltose and dextrin was 1.33. The value indicated that there was a complete separation between the two components as shown by figure 6.4.

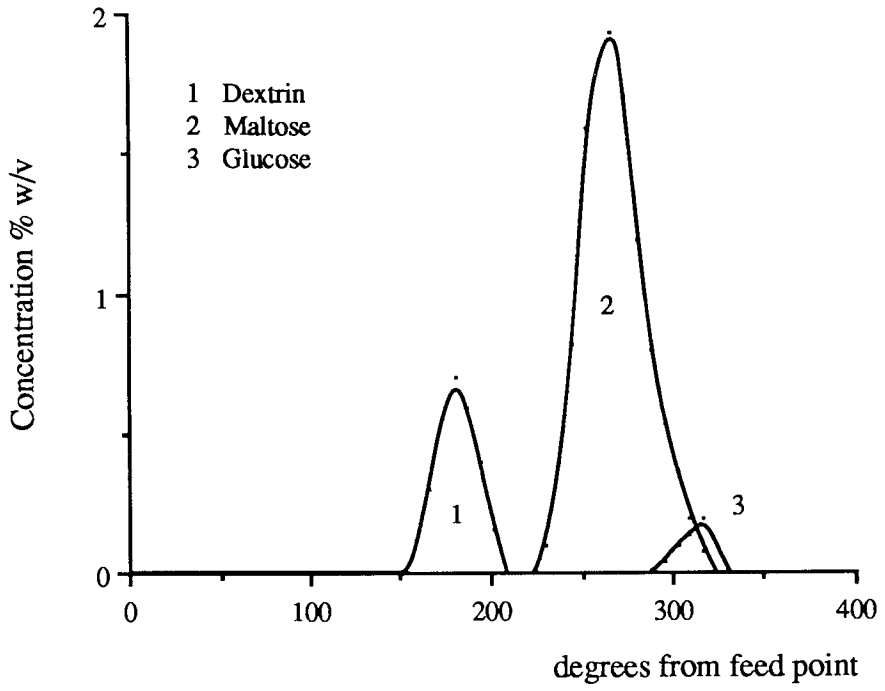

Figure 6.4. Elution profiles for run 330-7.25B-8-20-240

From figure 6.4 the overall elution profile is similar to the profile obtained from the batch chromatographic reactor (see figures 6.1-6.3). Dextrin was eluted first as a completely separated peak followed by the maltose peak. Both the maltose and dextrin elution profiles appear to be nearly symmetrical. As in the batch chromatographic reactor-separator, the small amount of glucose was not separated fully from the maltose peak.

Table 6.2 also indicated, as the feed flow rate was increased both the conversion and resolution $R_{M\text{-}D}$ decreased. However, as their values indicated, a good conversion and separation were still obtained. Increasing the feed flow rate further beyond 450-500 cm^3, caused the column to be overloaded. Under this condition the resin bed at the vicinity of the feed inlet was disturbed and cavity formation was observed. The cavity formation may eventually cause the feed to escape to the surface of the resin bed. For practical purposes under the present operating conditions the maximum feed flowrate was set at 400 cm^3/h.

6.3.2 The Effect of Concentration Overload

Setting the feed flowrate at a constant 400 cm^3/h, a further series of experiments at an increasing feed substrate concentration were carried out. The experiments were carried out using two types of starch, starch B and C. The results of the experiments are tabulated in table 6.3

Table 6.3. Effect of substrate concentration on CRAC performance

Experimental Run	Starch conversion to maltose %	Resolution R_{M-D}	Maltose exit bandwidth	% of pure maltose recovered
400-7.75B-8-20-240	82.3	1.3	122.4°	78.2%
400-15.5B-8-20-240	79.1	0.91	129.6°	74.6%
400-24.4B-8-20-240	67.9	0.85*	187.2°	51.1%
400-7.75C-8-20-240	63.3	0.9	108°	56.3%
400-15.5C-8-20-240	53.1	0.82	115.2°	28.1%
400-23.25C-8-20-240	51.4	0.74	122.4°	21.2%

* Resolution Between maltose and maltotriose

The results from table 6.3 indicated that, as the concentration of substrates B and C were increased, the performance of the CRAC decreased. The elution profiles for the substrate B are shown in figures 6.5-6.7. From figures 6.5-6.7, increasing the substrate concentration from 7.75 to 24.4 % w/v increased the exit banwidth. As a result, the resolution and the percentage of pure maltose recovered decreased with the increase in the substrate concentration. The increase in exit bandwidth was probably caused by the viscosity effect of the substrate. It is well known that higher viscosity tends to promote the

spreading of the chromatographic band. As a result of the band spreading, the product was obtained at a lower concentration.

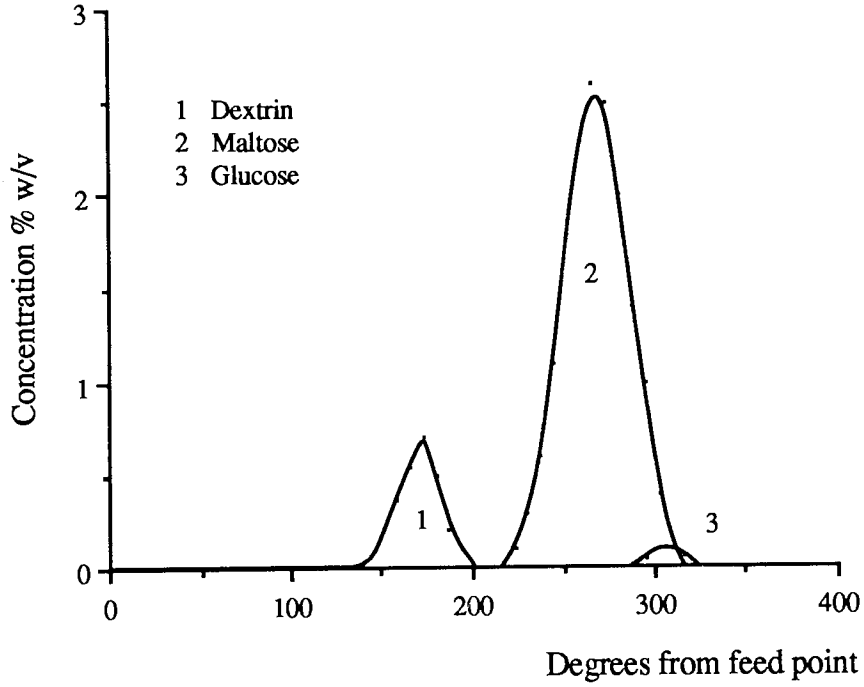

Figure 6.5. Elution profiles for run 400-7.25B-8-20-240

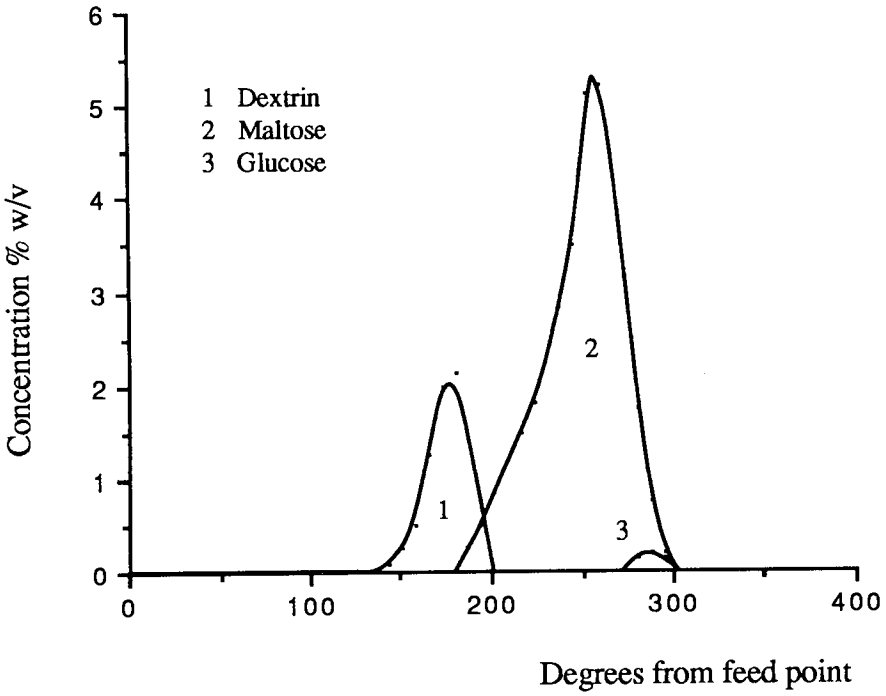

Figure 6.6. Elution profiles for run 400-15.5B-8-20-240

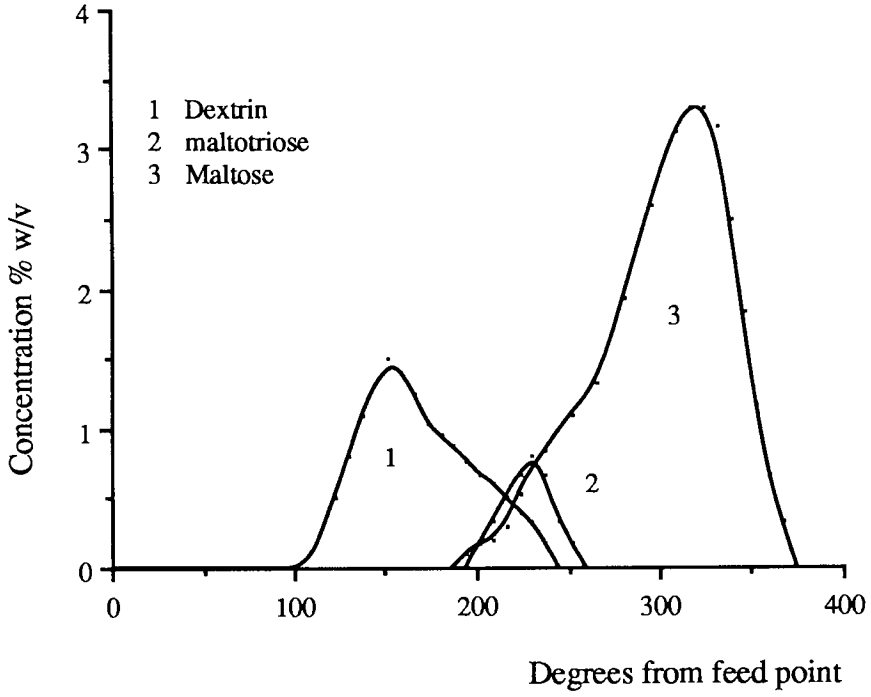

Figure 6.7. Elution profiles for run 400-24.4B-8-20-240

For the highest substrate concentration experiment, as shown in figure 6.7, the elution profiles indicate broad exit bandwidths and a gross asymmetry for both the dextrin and maltose peaks. The two peaks were skewed toward each other with the maltotriose peak in between. The presence of maltotriose suggested that the reaction had not reached completion. This is shown by a considerable reduction in the conversion to maltose (table 6.3).

It was also noted, the percentage of pure maltose recovered decreased with the increase in subsstrate concentration. The percentage of the pure maltose recovered was expressed as the mass flow rate of pure maltose in the product stream per unit mass flow rate of substrate in the feed stream. However, in term of chromatographic throughput, a higher value was obtained from the high concentration run. The maltose throughput for runs 400-7.75B-8-20-240, 400-15.5B-8-20-240 and 400-24.4B-8-20-240 were 1.62, 3.2 and 3.4 kg maltose m^{-3} resin/h respectively. In a practical situation, the choice between a high

percentage of pure product recovered and a high product throughput has to be decided on the economic of the process. One side of the argument is that there would be no point in increasing the amount of substrate if most of the products are to be recycled or wasted. However, if the objective is to maximise the throughput, a lower percentage of product recovery is then acceptable.

In the case of substrate C the degree of conversion was comparable to that obtained in the batch reaction (table 4.4). The results also indicated that a similar trend for substrate B was observed. The percentage of pure maltose recovered decreased with the incerease of substrate concentration. In term of the pure maltose throughput, the values were 1.2, 1.25 and 1.36 kg maltose m^{-3} resin h^{-1} for run 400-7.75C-8-20-240, 400-15.5C-8-20-240 and 400-23.25C-8-20-240. Increasing the substrate C concentration above 25% w/v caused cavity formation in the resin bed and the experiment was concluded.

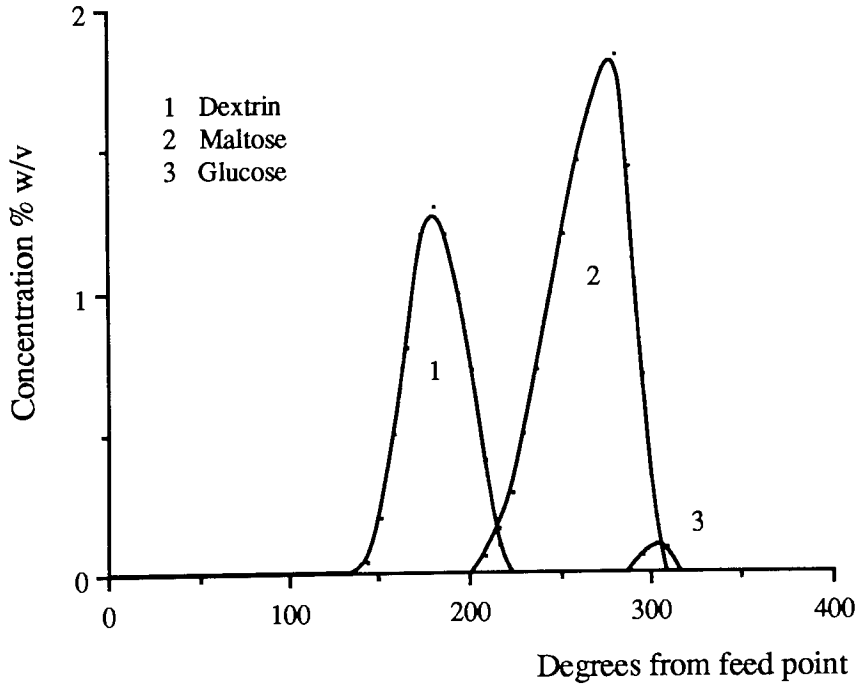

Figure 6.8. Elution profiles for run 400-7.75C-8-20-240

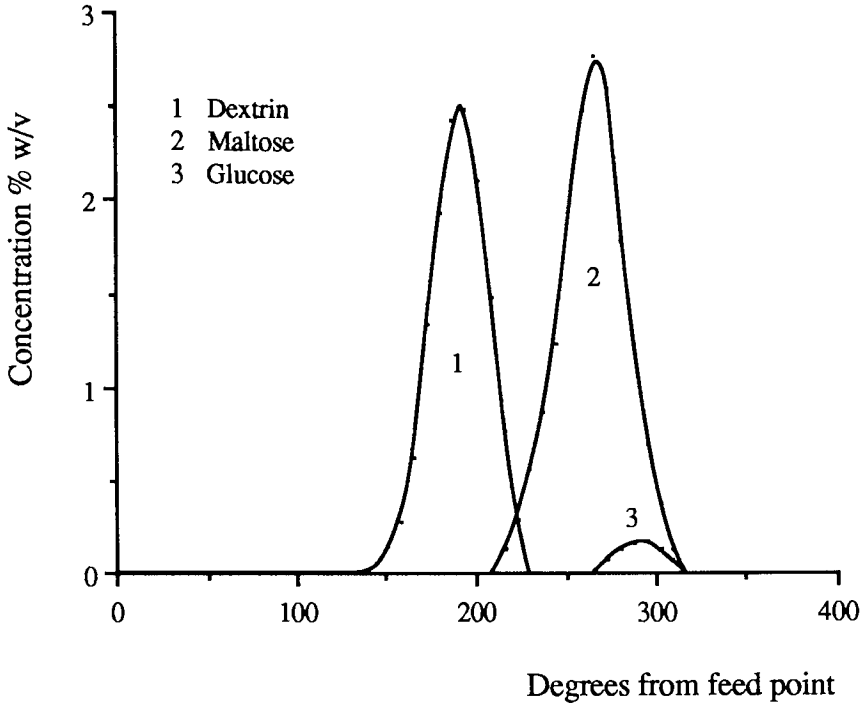

Figure 6.9. Elution profile for run 400-15.5C-8-20-240

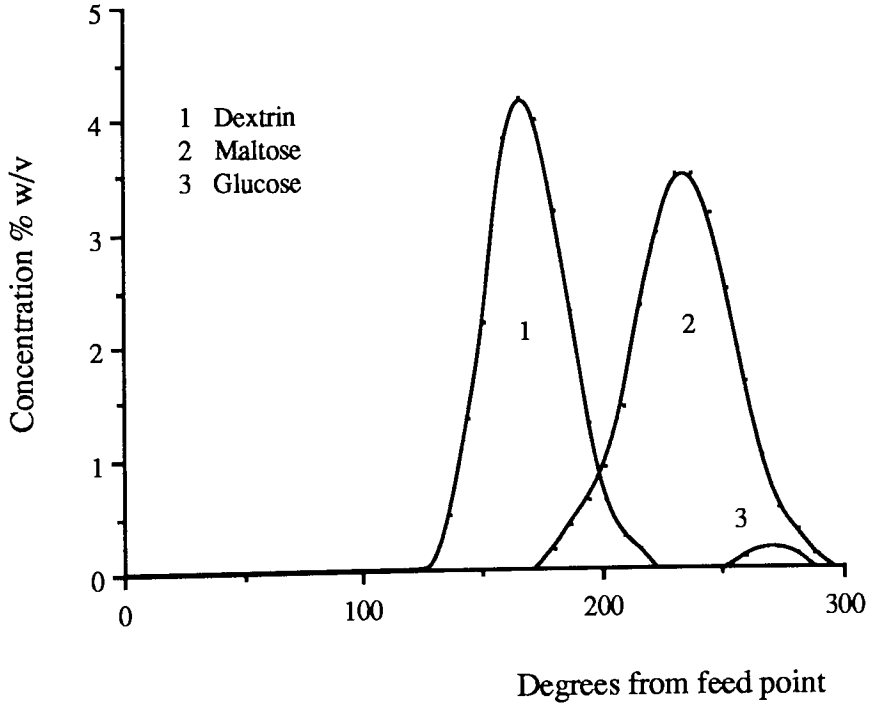

Figure 6.10. Elution profile for run 400-23.25C-8-20-240

CHAPTER SEVEN

MATHEMATICAL MODEL AND NUMERICAL SIMULATION

7.1 Introduction

Modelling of a CRAC in a physical separation mode has been carried out using three approaches; the theoretical-plate model [53,57], the equilibrium stage model [118] and the differential model [55,119-121].

The modelling of simultaneous chemical reaction and separation in a continuous rotating annular chromatograph has been carried out by Cho *et al* [29] for acid catalysed hydrolysis of aqueous methyl formate to formic acid and methanol. No work has been reported previously on experimental work or the modelling of biochemical reaction and separation in a CRAC. In their work Cho *et al.* used a differential model and employed Freundlich isotherms. The model did not explicitly include the axial dispersion term. However, the Lax's method used to solve the equations has a built-in psuedo dispersive effect which can be manipulated by a proper mesh strategy to simulate the dispersion.

7.2 Mathematical Model

The modelling of simultaneous biochemical reaction and separation on a CRAC has to consider the physical, thermodynamical and biochemical aspects of the process. At present it is not possible to state how these different phenomena interact in the process. Since this was the first attempt to the model simultaneous biochemical reaction and separation on a CRAC, severals simplifiying assumptions were made in developing the model.

The main aim in developing the model was to study the effect of biochemical reaction on the performance of the system. A semi-ideal differential model was considered to be

appropriate for this purpose. Moreover, this approach could still accomodate the various chromatographic phenomena that were thought to be present.

The model was based on the continuity equations for the flowing mobile phase in a conventional chromatographic column [122]. It was then applied to an annular chromatographic column [123] by translating the time dimension t to angular position θ, by the following relationship:

$$t = \frac{\theta}{\omega}. \qquad 7.1$$

The assumption made are as follows [132]:

- The annular column was assumed to be uniformly packed and under an isothermal operating condition.
- The annular space was considered to be small compared to the outer and inner cylinder so that the curvature effect could be ignored .
- The reaction takes place only in the mobile phase and follows the inhibited Michaelis-Menten kinetic. For every mole of sucrose reacted, equimolar amounts of fructose and glucose are formed.
- The adsorption process of each solute is non-interacting and the equilibrium distribution coefficient between the solute i in the mobile and stationary phase can be described by $K_{di} = \frac{q_i}{c_i}$
- There is a negligible radial gradient in velocity and concentration.

For the substrate sucrose balance in the mobile phase the following phenomena were considered:

Solutes accumulation in liquid and packing	=	Solutes dispersion in - out	+	Solutes convection in - out	+	Substrate consumed or products formed

– accumulation in the mobile phase: $\omega\frac{\partial c_S}{\partial \theta}$

– accumulation in the stationary phase: $\omega\left(\frac{1-\varepsilon}{\varepsilon}\right)\frac{\partial q_S}{\partial \theta}$

– transport by axial dispersion: $D_z\frac{\partial^2 c_S}{\partial z^2}$

– convective transport in the mobile phase: $v\frac{\partial c_S}{\partial z}$

– substrate consumed in the mobile phase: $\frac{c_S V_{max}}{c_S + K_m + \frac{c_S^2}{K_I}}$

Based on the continuity equation [123] a steady-state mass balance for sucrose in the mobile phase results in a second order non-linear partial differential equation. The resulting equation (equation 7.2) is categorised as a mixed system, since it contains both hyperbolic and parabolic characters [124]. Without the reaction term, equation (2) is similar to the equation described by Begovich *et al.* [55], Bridges et al [121], Howard *et al.* [119] and Bratzler *et al.* [120] for the operation of a CRAC in a physical separation mode.

$$\omega\frac{\partial c_S}{\partial \theta} + \omega\left(\frac{1-\varepsilon}{\varepsilon}\right)\frac{\partial q_S}{\partial \theta} + v\frac{\partial c_S}{\partial z} + \frac{c_S V_{max}}{c_S + K_m + \frac{c_S^2}{K_I}} = D_z\frac{\partial^2 c_S}{\partial z^2} \qquad 7.2$$

The interstitial eluent velocity v in the convective transport term in equation (7.2) is directly proportional to the eluent rate Q_e, where $v = Q_e/A_a\varepsilon$. A higher eluent rate increases the

interstitial velocity v. As a result, it decreases the residence time of a solute and increases the degree of mixing between the enzyme and the substrate. The eluent rate also determined the quantity of enzyme needed to maintain the required enzyme activity in the eluent.

Sucrose inversion to glucose and fructose was assumed to follow the inhibited Michaelis Menten-kinetic. The value of V_{max} is directly related to the enzyme concentration E_O by a proportionality constant k_3, where $V_{max} = k_3 E_O$ [90]. The value of k_3 obtained from a batch reaction experiment was 9.7×10^{-3} μmol $U^{-1}s^{-1}$.

Introducing the term $\phi = \frac{\theta}{2\pi}$, $x = \frac{z}{L}$, axial peclet Number $Pe = \frac{Lv}{D_Z}$, the distribution coefficient $K_{dS} = \frac{q_S}{c_S}$ and $V_{max} = k_3 E_O$ into equation (7.2) yields

$$H_S \frac{\partial c_S}{\partial \phi} + \frac{\partial c_S}{\partial x} + \frac{L}{v} \frac{c_S k_3 E_O}{c_S + K_m + \frac{c_S^2}{K_I}} - \frac{1}{Pe} \frac{\partial^2 c_S}{\partial x^2} = 0 \qquad 7.3$$

$$\text{Where } H_S = \frac{\omega L}{2\pi v}\left(1 + \left(\frac{1-\varepsilon}{\varepsilon}\right) K_{dS}\right)$$

A correlation developed by Chung and Wen [125] was used to estimate Pe_z.

$Pe_z = \frac{L}{2R}(02 + 0.011 Re^{0.48})$ where the Reynolds number (Re) is defined as

$$Re = \frac{2R\rho v\varepsilon}{\mu}$$

A similar mass balance for the products glucose and fructose results in the following equations:

$$H_G \frac{\partial c_G}{\partial \phi} + \frac{\partial c_G}{\partial x} - \frac{L}{v} \frac{c_S k_3 E_O}{c_S + K_m + \frac{c_S^2}{K_I}} - \frac{1}{Pe} \frac{\partial^2 c_G}{\partial x^2} = 0 \qquad 7.4$$

$$H_F \frac{\partial c_F}{\partial \phi} + \frac{\partial c_F}{\partial x} - \frac{L}{v} \frac{c_S k_3 E_O}{c_S + K_m + \frac{c_S^2}{K_I}} - \frac{1}{Pe} \frac{\partial^2 c_F}{\partial x^2} = 0 \qquad 7.5$$

$$\text{where } H_G = \frac{\omega L}{2\pi v}\left(1+\left(\frac{1-\varepsilon}{\varepsilon}\right)K_{dG}\right) \text{ and } H_F = \frac{\omega L}{2\pi v}\left(1+\left(\frac{1-\varepsilon}{\varepsilon}\right)K_{dF}\right)$$

To solve these equations appropriate initial boundary conditions have to be specified. The initial conditions were determined by the way the feed was introduced. The size of the initial feed bandwidth θ_f was determined using an empirical relationship [80] relating the feed flowrate Q_f and eluent flowrate Q_e

$$\theta_f = \frac{2\pi Q_f}{Q_f + Q_e} \qquad 7.6$$

Prior to the introduction of the feed, the column was equilibrated with eluent containing the enzyme invertase. The model assumed that the sucrose solution contained the same enzyme activity as in the mobile phase. In practice, the enzyme mixed with the substrate sucrose in the column gradually by an elution mode. The variation of enzyme concentration within the substrate was described by equation (7.7) [41].

$$E_O^{'} = E_O\left(1-\frac{c_S}{c_{SO}}\right) \qquad 7.7$$

The boundary conditions used were based on the work by Begovich *et al* [55] in his modelling of a rotating annular chromatograph for continuous separations.

for $\phi = 0$, at all x $c_S = c_F = c_G = o$

for $x = 0$, at $0 < \phi \leq \phi_{feed}$ $c_S = 1, c_G = c_F = 0$

$\phi_{feed} < \phi < 2\pi$ $c_S = c_F = c_G = 0$

at $x = \infty$, at all ϕ $c_S = c_F = c_G = 0$

7.3 Numerical Solution

An analytical solution is not available at the present time, therefore an appropriate numerical method should be used. A finite difference method was used to approximate equations (7.3), (7.4) and (7.5). The first order partial derivative with respect to the dimensionless axial distance x and dimensionless space ϕ were estimated using a forward difference and backward difference scheme, while the second order axial partial derivative was converted into a central difference type [124,128].

$$\frac{\partial c_S}{\partial \phi} = \frac{c_S(i,j) - c_S(i-1,j)}{\Delta \phi} \qquad 7.8$$

$$\frac{\partial c_S}{\partial x} = \frac{c_S(i,j+1) - c_S(i,j)}{\Delta x} \qquad 7.9$$

$$\frac{\partial^2 c_S}{\partial x^2} = \frac{c_S(i,j+1) - 2\,c_S(i,j) + c_S(i-1,j)}{\Delta x^2} \qquad 7.10$$

Denoting the position of the node in the numerical grids along ϕ and x coordinates as i and j, respectively, equation (7.3) becomes

$$c_S(i,j+1) = c_S(i,j) - \frac{\Delta x H_S}{\Delta \phi}\left[c_S(i,j) - c_S(i-1,j)\right]$$

$$- \frac{\Delta x L}{v} \frac{c_S(i,j)\, V_{max}}{c_S(i,j) + K_m + \dfrac{c_S(i,j)^2}{K_I}}$$

$$+ \frac{1}{Pe\,\Delta x}\left[c_S(i+1,j) - 2c_S(i,j) + c_S(i-1,j)\right] \qquad 7.11$$

Equation (7.4) and (7.5) were transformed into finite difference forms in the same manner. For glucose:

$$c_G(i,j+1) = c_G(i,j) - \frac{\Delta x H_G}{\Delta\phi}[c_G(i,j) - c_G(i-1,j)]$$

$$+ \frac{0.5\Delta x L}{v} \frac{c_S(i,j)\, V_{max}}{c_S(i,j) + K_m + \frac{c_S(i,j)^2}{K_I}}$$

$$+ \frac{1}{Pe\,\Delta x}[c_G(i+1,j) - 2c_G(i,j) + c_G(i-1,j)] \qquad 7.12$$

and for fructose:

$$c_F(i,j+1) = c_F(i,j) - \frac{\Delta x H_G}{\Delta\phi}[c_F(i,j) - c_F(i-1,j)]$$

$$+ \frac{0.5\Delta x L}{v} \frac{c_S(i,j)\, V_{max}}{c_S(i,j) + K_m + \frac{c_S(i,j)^2}{K_I}}$$

$$+ \frac{1}{Pe\,\Delta x}[c_F(i+1,j) - 2c_F(i,j) + c_F(i-1,j)] \qquad 7.13$$

The stability criterion [124] was bounded by the value h,

$$\text{where } h = \frac{\Delta x\, H_F}{\Delta\phi} \leq 1.0$$

The value H_F was chosen as it represent the slowest moving component through the column and to ensure numerical stability the value of h was kept below 0.35 throughout the simulation work.

7.4 Computer Program

A FORTRAN program was written to solve the difference equations and was implemented on a VAX 8650 computer. The listing of the program is given in appendix A6.

The calculations begin at x = 0 or jth row in the mesh formulation [128] (figure 7.2). Equation 7.11 gives a formula for the unknown concentration c_S at the (i-1, j+1)th mesh point in terms of the known concentrations along the jth row, c_S(i-1, j), c_S(i, j) and c_S(i+1,j). The next c_S value to be calculated was the (i, j+1)th mesh point and so on until the (i+n, j)th mesh point. The calculation then proceeded to the x = x + Δx value. The mesh points on the j+1th row were then calculated using the computed values on the previous jth row. The procedure was repeated until all the required concentration values were computed. A similar procedure was used on different grids to calculate the concentration of the products glucose and fructose using equations 7.12 and 7.13.

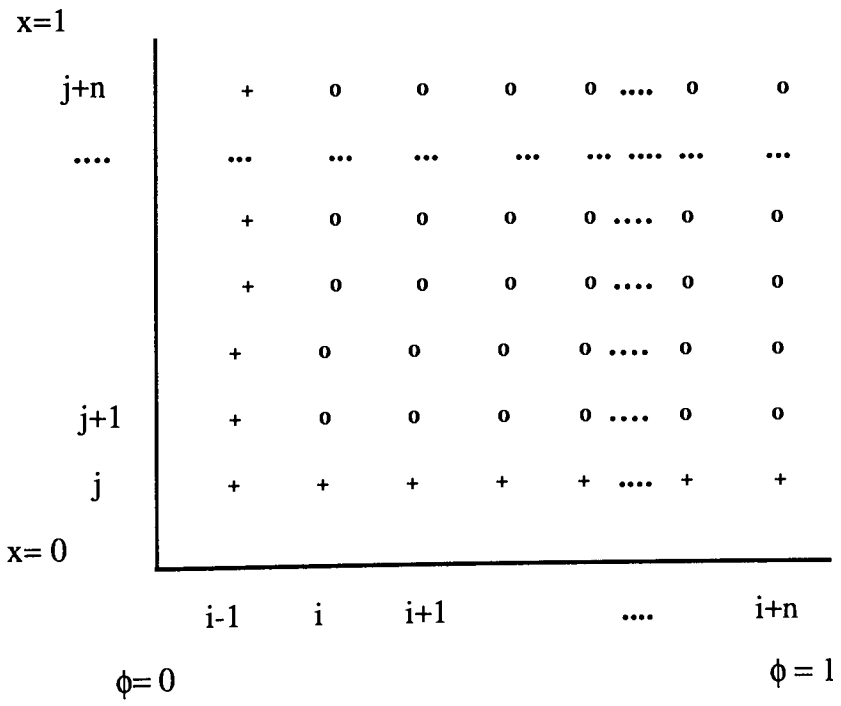

Figure 7.1 Computational mesh formulation

Key: + Known values

o Solution values

Typical operating data for the simulation work are given in table 7.1. In the initial simulation work at the low enzyme activity of 60 U/cm^3 the degrees of conversion obtained did not match with that obtained experimentally. Similar observations were also made by Zafar [41] on a batch chromatographic reactor and by Akintoye [82] on a SCCR-S1 system. Some degree of physical adsorption or denaturation of the enzyme might have taken place in the column which lowered the on column rate of reaction. In this work the proportionality constant k_3 (refer to page 139) was corrected to match the percentage of conversion obtained at an enzyme activity of 60 U/cm^3. The corrected k_3 value was 7.25 x 10^{-3} μmol $U^{-1}s^{-1}$ and this value was used throughout the simulation runs.

Table 7.1 Operating parameters for the simulation

Parameters	
K_{ds}	0.14
K_{dG}	0.42
K_{dF}	0.68
V_{max} (μmol cm^{-3} s^{-1})	variable
K_m (mmol cm^{-3})	0.07
K_I (mmol cm^{-3})	1.75
Pe_z	variable
L (cm)	135
Voidage (ε)	0.4

The main aim of the model was to elucidate the effect of biochemical reaction on the performance of a CRAC. Even though the model did not explicitly include the mass transfer effect, the effect was circumvented by using the appropriate mesh size in the numerical simulation [118,126,127]. A high mass transfer resistance will have a dispersive effect on the elution profiles. The other dispersive effect was due to the axial

dispersion. The axial dispersion was estimated from the column axial Peclet number. This was calculated from a standard correlation [125] and the values were between 5,000 - 6,000. The values indicated that the axial dispersion on the column was small.

In the numerical simulation, discretisation of dimensions x and ϕ in equations (7.3), (7.4) and (7.5) introduced numerical dispersion effects [126]. The numerical dispersion was controlled and used to match the dispersion in the experimental elution profiles. The experimental elution profile of sucrose was used to estimate the dispersion effect due to mass transfer resistance since sucrose has the lowest mass transfer coefficient compared to glucose and fructose [119]. By trial and error, at $\Delta x = 0.0009$, the simulated elution profile of sucrose fitted quite well with the experimental elution profile (figure 7.2) and this discretised value was used in the simulation works.

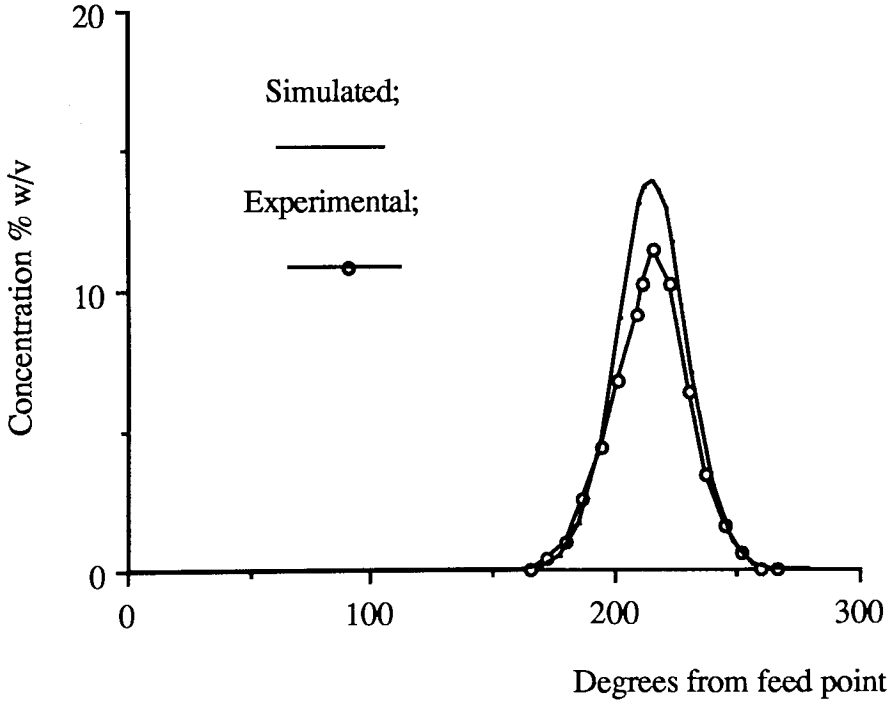

Figure 7.2 Experimental and simulated elution profiles (z = 135 cm) of sucrose for run 230-25-8-240

7.5 Simulation Results

The simulation results were compared with the experimental elution profiles under various operating conditions. The model was also used to investigate the effect of enzyme activity and the effect of the column length on the behaviour of the chromatograph.

7.5.1 The Overall Picture of the Simultaneous Biochemical Reaction and Separation

The simulated concentration profiles for run 230-50-10-100-240 at various axial distances from the feed point are plotted in figure 7.3. The overall development of the simultaneous biochemical reaction and separation could be clearly seen in this figure 7.3. At an axial distance z=25 cm the substrate, sucrose, has been rapidly diluted to about two thirds of its original concentration and eluted at a peak position of 35°. The substrate conversion at this axial distance was 27%. The products formed started to separate from the unreacted sucrose however, they appeared as one elution profile.

Further down the column at z=75 cm the substrate conversion increased to 76%. The unreacted substrate and the products formed started to separate into three distinct peaks. Sucrose was eluted first, followed by glucose and fructose. The unreacted sucrose peak appeared as a sharp triangular peak, while both the glucose and fructose peaks were broader and asymmetrical with a significant amount of tailing.

At z=135 cm the reaction was completed and the separation between glucose and fructose was further developed. Their elution profiles appear to be nearly symmetrical. The simulated and experimental elution profiles compared reasonably well. As expected the glucose peak was sharper and had a smaller bandwidth than the fructose peak.

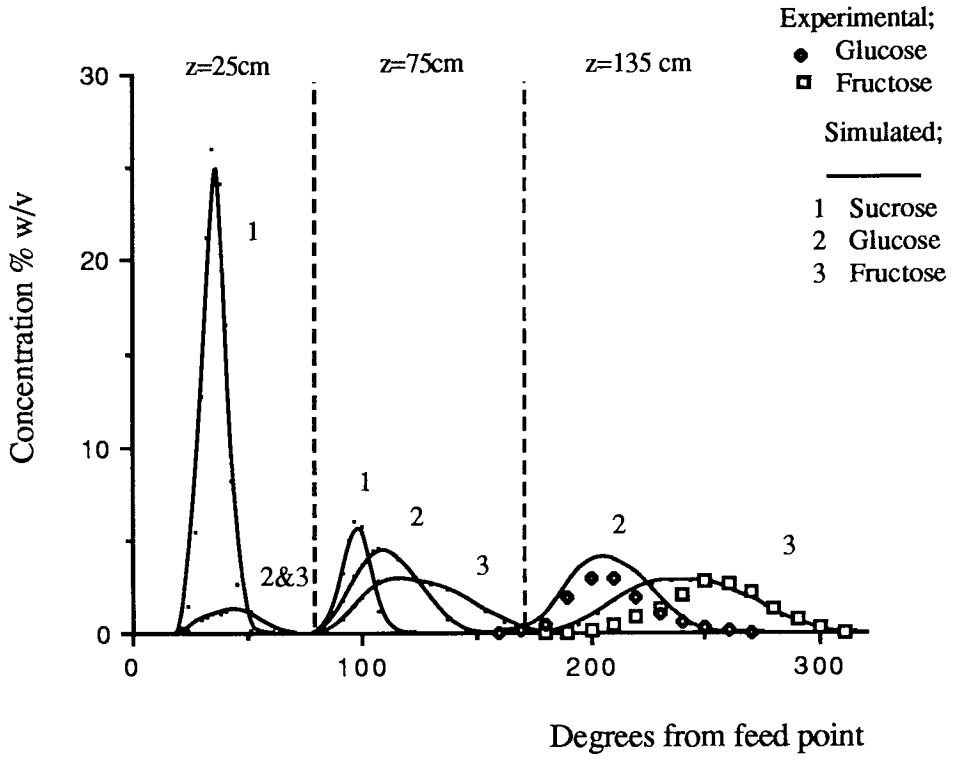

Figure 7.3 Simulated concentration profile at z=25 cm, 75 cm and 135 cm and experimental elution profiles at z= 135 cm for run 230-50-10-100-240.

7.5.2 The Effect of Enzyme Activity

The chromatograms in figure 7.4 (run 230-25-8-75-240) and figure 7.5 (run 230-25-8-100-240) compare the simulated and experimental elution profiles at increasing enzyme activity. For both runs, the simulated elution profiles compare quite well with the experimental elution profiles. The resolutions R_{G-F} of the simulated concentration profiles for run 230-25-75-240 and 230-25-8-100-240 were 0.51 and 0.55 respectively, as compared to the experimental R_{G-F} values of 0.53 and 0.57. A slight discrepancy occurs in the overall shape of the elution profiles and the exit peak positions and exit bandwidths.

Figure 7.6 shows the effect of increasing the enzyme activity for run 230-25-8-100-240 through to 500 U/cm^3. As expected, at a higher enzyme activity the elution profiles were narrower and sharper. As a result, a higher resolution and higher product concentrations

were obtained. The resolutions achieved were 0.57, 0.76 and 0.91 at 100 U/cm^3, 200 U/cm^{3}and 500 U/cm^3 enzyme activities respectively. The resolution for the simulated physical separation was 0.94 and this acted as the upper limit value under the prevailing operating conditions. At a 500 U/cm^3 enzyme activity, the resolution approached this upper limit. To reach this upper limit, the reaction has to be instantaneous, thus the whole column length is used for the separation of the products. However, this is not possible in practice since a finite time is required for the enzyme and the substrate to mix and react.

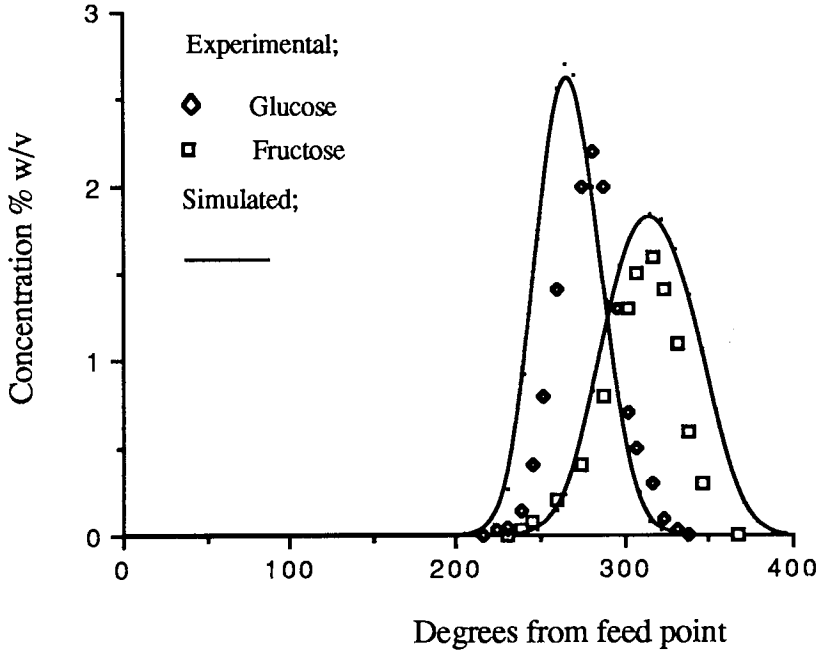

Figure 7.4 Experimental and simulated elution profiles at the base of the column \ (z=135 cm) for run 230-25-8-75-240

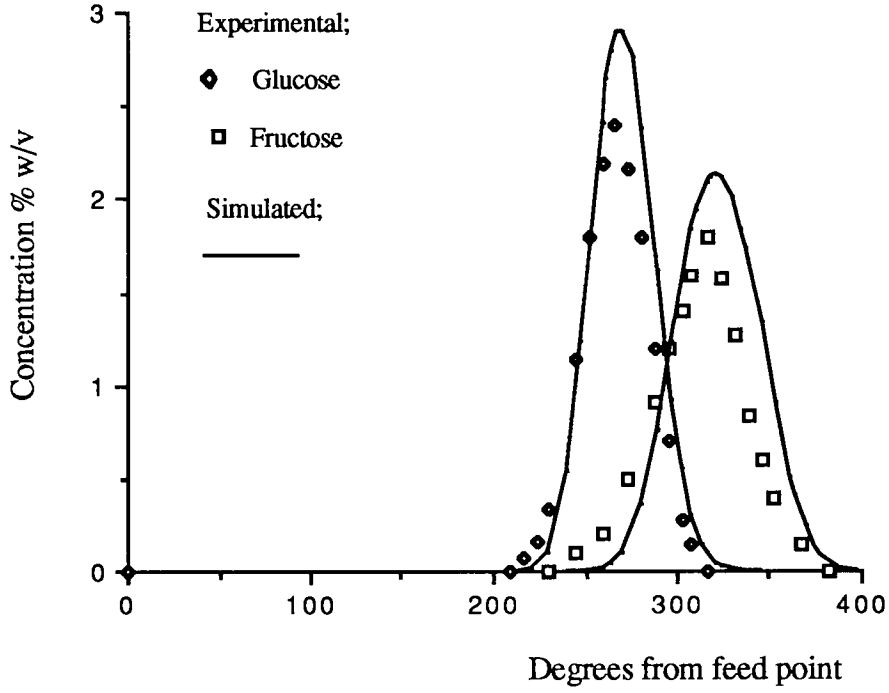

Figure 7.5 Experimental and simulated elution profiles at the base of the column (z=135 cm) for run 230-25-8-100-240

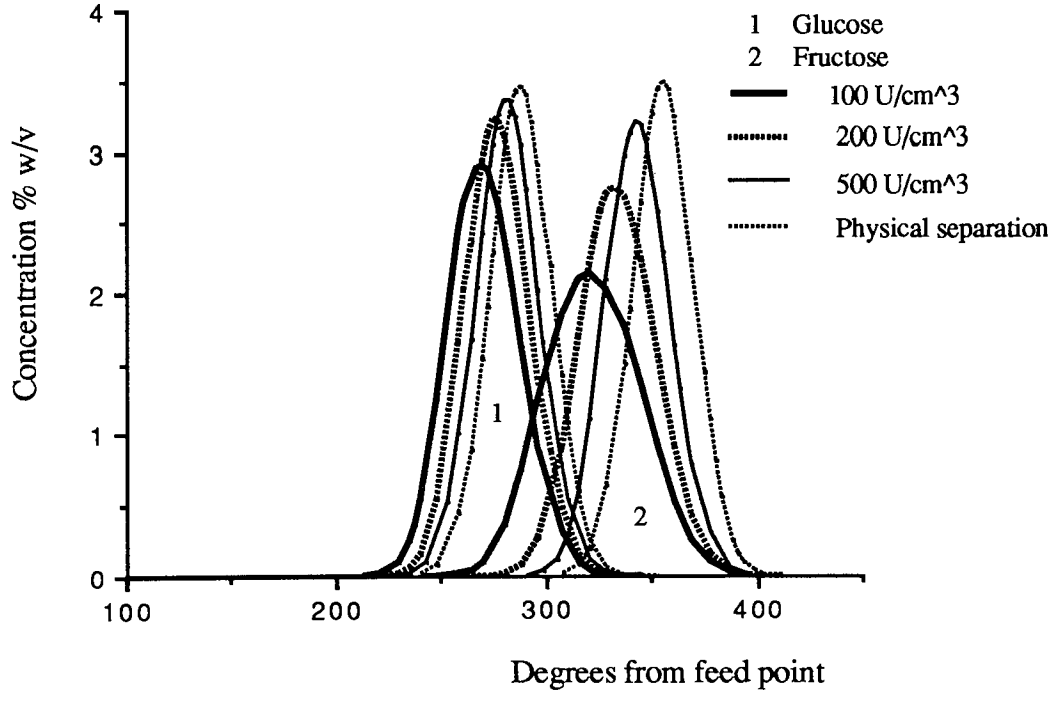

Figure 7.6 Simulated concentration profiles at z = 135 cm, for run 230-25-8-100,200,500-240 and simulated physical separation of inverted sucrose at the same conditions.

7.5.3 The Effect of the Reactor Length

From run 230-25-8-75-240 as shown by figure 7.3 the elution profile indicated there was insufficient column for the separation of the products to fully develop. Figure 7.7 shows the effect of increasing the column length for simulation run 230-25-8-75-240. Increasing the column lengths to z=150 cm and 175 cm increased the resolution to 0.58 and 0.69 respectively. The elution profiles became sharper and almost symmetrical. However, there was a slight reduction in the product concentrations. The reduction in the product concentrations was due to a dilution effect as they were eluted over a longer distance. From figure 7.7 the gain in the product separation is greater than the loss in product concentration. However a longer column will cause a greater pressure drop in the column. This factor would have to be taken into consideration in any optimization exercise.

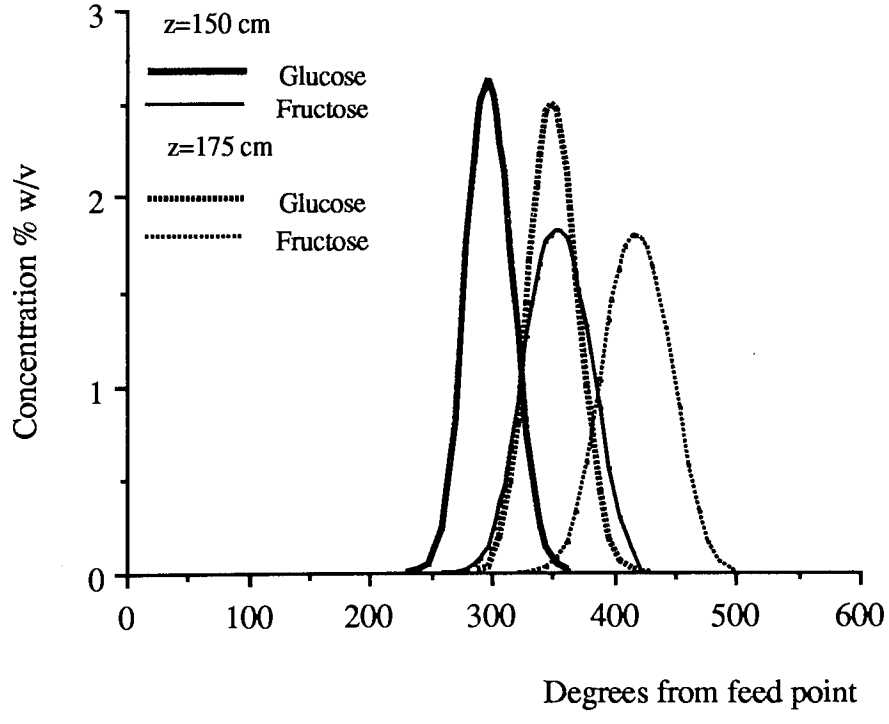

Figure 7.7 Simulated elution profile for run 230-25-240 at z=150 cm and z=175 cm

CHAPTER 8

CONCLUSIONS AND RECOMMENDATIONS

8.1 Conclusions

The main conclusions from this work are summarised below:

Sucrose Inversion Experiments

The kinetics of sucrose inversion to glucose and fructose using the enzyme invertase were quantified using inhibited Michaelis-Menten kinetics (Section 4.3.2). The kinetic constants were used in the computer simulation study.

The reaction and separation results on the inversion of sucrose to glucose and fructose have shown for the first time that it is possible to carry out continuous bioreaction and separation using a CRAC. Complete conversions for feeds of up to 50 % w/v sucrose concentration and product purity of 95% have been obtained. This indicated that substrate inhibition of the enzyme was minimised (Sections 5.4)

The separation performance of the CRAC under bioreaction and separation duties showed a decrease in performance as compared to the performance under solely a separation duty (Section 4.2.7).

The main factors affecting the performance of the CRAC under bioreaction and separation duties were identified to be the feed rate, feed concentration and eluent rate. Under the experimental conditions investigated, feed rate and feed concentration have negative effects on the resolution, while the eluent rate showed a positive effect on the resolution.

Statistical analysis also showed out that in high conversion runs mass overload produced a better performance than volume overload conditions. The main reason for this behaviour

was due to the effect of volume overload and concentration overload on the shape of the individual elution profiles of the products (Sections 5.3.3.1 and 5.3.3.2)

The most significant factor was the interaction between feed rate and eluent rate. The positive interacting effect suggested that dilution of the feed by a higher eluent rate helped to enhance the performance of the system (Section 5.3.3.5).

The bioreaction and separation studies on a CRAC showed that, at feed throughputs of up to 17.2 kg sucrose per m^3 resin per hour at 50%w/v of sucrose, complete conversion could be achieved using only 78% of the enzyme required by a conventional batch bioreactor. In terms of product concentration and enzyme usage (Section 5.5), the performance of the SCCR-S1 system was slightly better than the CRAC under bioreaction and separation duties.

A notable advantage of a CRAC over the SCCR-S1 system is the versatility in the product fraction collection. Since any number of products fraction can be collected in a run, the system can handle a multicomponent separation. Also a CRAC requires less time to attain the steady state condition. Twelve operation cycles (60 hours) is required for the SCCR-S1 system to reach equilibrium compared to two eluent residence times (about 2 hours) with a CRAC.

Saccharification of modified Starch to Maltose Experiments

The second enzymic reaction, the saccharification of modified starch to maltose employing the enzyme maltogenase has also been successfully carried out in a batch liquid chromatographic reactor and in a CRAC (Sections 6.2 and 6.3).

Factors that effect the conversion of modified starch to maltose in a conventional batch reactor batch were the types of starch, DE value of the starch, starch concentration and

maltogenase activity level. However the nature of the inhibition mechanism, either by substrate inhibition or by product inhibition has not been established (Section 4.3.3.3).

The conversion of liquefied starch to maltose in the batch chromatographic reactor and in the CRAC were comparable to the steady state conversion under batch reaction conditions. The much shorter time required for the reaction to approach the steady state conversion in the CRAC indicated that the effect of the inhibition of either the substrate or the product was minimised by carrying out the reaction in chromatographic reactors (Sections 4.3.2, 6.2 and 6.3).

The limit of the performance of the CRAC under simultaneous biochemical reaction and separation conditions was found by performing experiments under both volume overload and concentration overload conditions. To maximise the performance of the system, it was found that a choice has to be made between a high percentage of pure product recovered or a high throughput (Section 6.3.2)

Mathematical Modelling and Computer Simulation

A mathematical model to simulate the operation of a CRAC under simultaneous biochemical reaction and separation has been formulated. The model was based on a semi-ideal model incorporating inhibited Michaelis-Menten kinetics and axial dispersion. The equations were solved using the finite difference analysis method. The model was capable of predicting the effect of various parameters over a wide range of operating conditions.

8.2 Recommendation for Future Work

The following recommendation are made for future work.

(1) A systematic approach of screening reaction and separation systems should be carried out to identify the appropriate enzymes, stationary phase and substrates for wider application of simultaneous biochemical reaction and separation in chromatogrhapic reactors.

(2) A universal performance criterion should be developed as a basis of comparing biochemical chromatographic reactors and conventional bioreactors with some subsequent separation.

(3) Increase the performance of the CRAC by using a smaller diameter resin. This could be done by replacing the existing glass outer shell with a stainless steel shell to enable higher working pressures to be achieved.

(4) Investigate the possibility of using an immobilised enzyme in a CRAC to reduce the consumption of the flowing enzyme. This could be done by either immobilising the enzyme directly on to the stationary phase or on to a suitable carrier.

(5) Carry out a rigorous extension of the mathematical model to include the interaction effects of multicomponent systems and non-linear adsorption isotherms. Also attempt to include explicitly the effect of non equilibrium mass transfer between the mobile and stationary phases.

NOMENCLATURE

A_a	cross-section area of the annulus
As	asymmetry factor
c_i	concentration of solute i in mobile phase
$\overline{C}_G$	average concentration of glucose in the product stream
$\overline{C}_F$	average concentration of frutcose in the product stream
$\hat{C}_G$	peak concentration of glucose
$\hat{C}_F$	peak concentration of fructose
DE	dextrose equivalent
D_θ	angular diffusivity
D_z	axial diffusivity
F	fructose
FRP	fructose rich product
G	glucose
GRP	glucose rich product
K_{di}	distribution coefficient of component i
K_e	equilibrium constant
K_m	Michaelis-Menten constant
K_I	Inhibition constant
k_3	constant relating maximum initial reaction velocity and enzyme concentration
L	bed length
Q_f	feed rate
Q_e	eluent rate
P_G	glucose product throughput
P_F	fructose product throughput
Pe_z	axial Peclet number
q_i	concentration of solute i in stationary phase
R	particle radius
Re	Reynold's Number
R_{1-2}	resolution between component 1 and 2
T_G	glucose product throughput (kg sugar/m^3 resin/h)
T_F	fructose product throughput (kg sugar/m^3 resin/h)
s	sucrose
U_g	fluid phase velocity in equation 2.14
U_s	solid phase velocity in equation 2.14

v	interstitial velocity
V	mobile phase velocity
V_{max}	maximum initial reaction velocity
$W_{1 \text{ or } 2}$	exit bandwidth of component 1 or 2
x	dimensionless axial distance
Y_G	yield of pure glucose
Y_F	yield of pure fructose
z	axial distance

Greek letters

ε	voidage
ρ	fluid density
μ	fluid viscosity
θ	angular coordinate
$\theta_{1 \text{ or } 2}$	peak position of component 1 or 2
θ_f	feed bandwidth
ϕ	dimensionless angular coordinate
ω	rotation rate

REFERENCES

1 Knight, P., 1989, Downstream processing, *Biotechnology*, **7**(8) 783.

2 Bailey, J.E, and Ollis, D.F., 1986, Biochemical Engineering Fundamental, 2nd ed., New York, McGraw-Hill.

3 Knight, P., 1989, Chromatography: 1989 Report. *Biotechnology*, **7**(3) 243.

4 Ramalingham, A. and Finn, R. K., 1977, Vacuferm Process: New approach to fermentation alcohol. *Biotech. Bioeng.*, **19** 583-589.

5 Cysewski, G. R. and Wilke, C. R., 1978, Process design and economic studies of alternative fermentation method for the production of ethanol. *Biotech. Bioeng.*, **20** 1421-1444.

6 Altshuler, G. L., Dziewalski, D. M., Sowek, J. A. and Belfort, G., 1986, Continuous hybridoma growth and monoclonal antibody production in hollow fiber reactor-separator *Biotech. Bioeng.*, **28** 646-658.

7 Griethuysen-Dilber, E. V., Flaschel, E. and Renken, A., 1988, Process development for the hydrolysis of lactose in whey by immobilised lactase of *Aspergillus oryzae. Process Biochemistry* , **23**, 27.

8 Setford, S. J, Barker, P. E. and Ganetsos, G., 1992, The development of a continuous bioreactor-separator for the production of dextran, in Proceedings of *The 1992 ICHEME Research Event*, Published by Institution of Chemical Engineers, Rugby, U.K., 281-283.

9 Setford, S. J., 1992, Combined bioreaction and separation in centrifugal field, PhD Thesis, Aston University, Birmingham.

10 Barker, P. E., Zafar, I. and Alsop, R. M., 1987, A novel method for the production of dextran and fructose, in *International Conference on Bioreactor, Biotransformation,* Gleneagles, Scotland. Paper D1, pp. 141-157. Elsevier, Amsterdam.

11 Barker, P. E., Zafar. I. and Alsop, R. M., 1987, Production of dextran and fructose in a chromatographic reactor-separator, in *Separations for Biotechnology,* Chap. 7, pp. 127-152. Ellis Horwood, Chichester.

12 Zafar, I. and Barker, P. E., 1988, An Experimental and computational study of a biochemical polymerisation reaction in a chromatographic reactor separator. *Chem. Eng. Sci.* **43**(9), 2369-2375.

13 Akintoye, A., Ganetsos, G. and Barker, P. E.,1991, The inversion of sucrose on a semicontinuous counter-current chromatographic bioreactor-separator. *Trans. IChemE*, Vol.**69**, part C, 35-44.

14 Shieh, M. T., Ajongwen, J. N., Barker, P. E. and Ganetsos, G., 1992 Chromatographic biochemical reactor-separator for the biosynthesis of macromolecules. In Proceedings of *The 1992 ICHEME Research Event*, Published by Institution of Chemical Engineers, Rugby, U.K., 199-201.

15 Jeng, C. Y. and Langer, S. H., 1992, Reaction kinetics and processes in modern liquid chromatographic reactors. *J. Chromatogr.*, **589**, 1-30.

16 Knight, P., 1989, Bioseparation media and mode, *Biotechnology*, **8**(3) 200.

17 Lin, Y. S. and Ma, Y. H., 1989, A comparative chromatoraphic study of liquid adsorption and diffusion in microporous and macroporous adsorbents. *Ind. Chem. Res.* **28** 622-630.

18 Mashall, D. B., Burn, J. W. and Connolly, D. E., 1986, Direct measurement of liquid chromatographic sorption-desorption kinetics and the kinetic contribution to band broadening. *J. Chromatogr.*, **360**, 13-24.

19 Muller, A. J. and Carr, P. W., 1984, Examination of kinetic effects in the high performance liquid affinity chromatography of glycoproteins by stopped-flow and pulsed elution method. *J. Chromatogr.*, **294**, 235-246.

20 Muller, A. J. and Carr, P. W., 1986, Examination of the thermodynamic and kinetic characteristics of microparticulate affinity chromatography supports. *J. Chromatogr.*, **357**, 11-32.

21 Bolme, M. W. and langer, S. H., 1983, The liquid chromatographic reactor for kinetic studies. *J. Phys. Chem.* **87** 3363-3366.

22 Benedek, K., Dong, S. and Karger, B. L., 1984, Kinetics of unfolding of proteins on hydrophobic surfaces in reversed-phase liquid chromatography. *J. Chromatogr.*, **317**, 227-243.

23 Melton, H. R., Bailey, D. C. and Langer, S. H., 1981, Adaptation of liquid chromatograph as a micro reactor; Immobilised lactase kinetics. *J. Chem. Tech. Biotechnol.*, **31** 44.

24 Jeng, C. Y. and Langer, S. H., 1991, Hydroquinone oxidation kinetics in adsorptive liquid chromatographic beds. *J. Chromatogr.*, **556**, 383-394.

25 Jeng, C. Y. and Langer, S. H., 1989,.Hydroquinone Oxidation for the detection of catalytic activity in liquid chromatographic columns. *J. Chromatogr. Sci.*, **27**, 549-552.

26 Chu, A. H. and Langer, S. H., 1985, Characterisation of a chemically bonded stationary phase with kinetics in a liquid chromatographic reactor. *Anal.Chem.*, **57** 2197-2204.

27 Chu, A. H. and Langer, S. H., 1986, Measurement of reaction rate constants in the liquid chromatographic reactor: Mass transfer effect. *Anal. Chem.*, **58** 1617-1625.

28. Whetherold, R. G., Wissler, E. H. and Bischoff, K. B. 1974, An experimental and computational study of the hydrolysis of methyl formate in a chromatographic reactor. *Adv. Chem. Ser.* **133**, 181-190.

29 Cho, B.K., Carr, R., Aris, R., 1980, A continuous chromatographic reactor. *Chem. Eng. Sci.*, **35** 74-81.

30 Sardin, M.,Schweich, D. and Villermaux, J., Preparative fixed-bed chromatographic reactor in Ganetsos, G and Barker, P.E. (Eds.), 1992, Preparative and production scale chromatography, Chromatographic science series, Vol 61, Marcel Dekker, New York.

31 Schweich, D. and Villermaux, J., 1982, The preparative chromatographic reactor revisited. *Chem. Eng. J.*, **21**, 99-109.

32 Ganetsos, G and Barker, P.E. (Eds.), 1992, Preparative and production scale chromatography, Chromatographic science series, Vol 61, Marcel Dekker, New York.

33. Matsen, J. M., Harding, J. W. and Magee, E., 1965, Chemical reaction in chromatographic column. *J. Phys. Chem.*, **69** (2) 522-527.

34 Roginskii, S. Z., Yanovskii, M. I. and Gaziev, G. A., 1961, Chemical reactions under chromatographic conditions. Doklady Akademii Nauk SSSR, Vol 140, N0 5, 1125-1127.

35 Unger, D. B., and Rinker, R. G., 1976, Ammonia-synthesis reaction in chromatographic reactor. *Ind. Eng. Chem. Fundam.*, **15** (3) 225-227.

36 Langer, S. H., Yurchak, J. Y., Patton, J. E., 1969, The gas chromatographic column as a chemical reactor. *Ind. Eng. Chem.*, **61**, (4) 11-21.

37 Magee, E. M., 1963, A course of a reaction in a chromatographic column. *Ind. Eng. Chem. Fundam.* **2** (1) 32-36.

38 Dinwiddie and Morgan, W., 1961, Fixed bed type reactor. US. Patent 2, 976 132.

39 Magee, E., 1961, Catalytic conversion process. Canadian Patent, 631,882 .

40 Chu, C. and Tsang, L. C., 1971, Behaviour of a chromatographic reactor. *Ind. Eng. Process Des. Develop.*, **10**(1) 47-53.

41 Zafar, I. A., 1986, Biosynthesis and separation of dextran-fructose mixtures in a Chromatographic Reactor, PhD Thesis, Aston University, Birmingham.

42 Karger, B. L., Snyder, L. R. and Horvath, Cs., 1973, An introduction to separation science, Wiley-Interscience, New York.

43 Hupe, K. P. and Lauer, H. H., 1981, Selection of optimal conditions in preparative liquid chromatography; Part 1, Theory. *J. Chromatogr.*, **203**, 42-52.

44 Cretier, G. and Rocca, J., L., 1987, Optimisation of injection conditions in preparative liquid chromatography in Grushka, E., (Ed.) 1987, Preparative scale chromatography, *Separation Science and Technology*, **22**(8-10) 1881-1907.

45 Schweich, D. and Villermaux, J., 1978, The chromatographic reactor . A new theoretical approach. *Ind. Eng. Chem. Fundam.*, **17**(1) 1-7.

46 Henri, C., Large-scale high performance preparative liquid chromatography.in Ganetsos, G and Barker, P.E. (Eds.), 1992, Preparative and production scale chromatography, Chromatographic science series, Vol 61, Marcel Dekker, New York.

47 Barker, P. E. and Liodakis, S. E., 1978, Sequential separation of fatty ester and fatty acid derivatives using preparative scale sequential gas-liquid chromatographic equipment. *Chromatographia.* **11** 703-714.

48 Barker, P. E. & Thawait, S., 1986, Separation of fructose from carbohydrate mixtures by batch and semi-continuous chromatographic operation. *Chem. Eng. Res. Des.*, **64** 302-307.

49 Barker, P.E. and Chuah, A., 1982, A continuous chromatographic process for obtaining fructose from a glucose-dextran contaminated carbohydrate mixture. *Inst. Chem. Eng. Symp. Ser.*, **76** 313-37.

51 Barker, P.E. and Ganetsos, G., 1985, Production of high purity fructose from barley syrups using semi-continuous chromatography, *J. Chem. Tech. Biotechnol.*, 35B 217-228.

52 Broughton, D. B., 1968, Molex; case history of a process. *Chem. Eng. Prog.* **64**(8),60-65.

53 Barker, P.E. &Thirkill, C., 1988, Separation of carbohydrate mixtures using a rotating annular chromatograph, in Proceeding of Chemeca' 88, Australian Bicentennial Conference, Sydney, Australia, Published by the Institute of Engineers, Canbera, Australia.

54 Barker, P. E. and Bridges, S., 1991, Continuous annular chromatography for the separation of beet molasses. *J. Chem. Tech. Biotechnol.*, **51**, 347-359.

55 Begovich, J.M. & Sisson, W. W., 1984, A rotating annular chromatograph for continuous separations. *AIChE J.*, **30** 5 705-710.

56 Carta, G., DeCarli, J. P., Byers, C. H. & Sisson, W. G., 1989, Separation of metals by continuous annular chromatography with step elution. *Chem. Eng. Commun.*, **79** 207-227.

57 Scott, C. D., Spence, R.D. and Sisson, W.G., 1976. Pressurised annular chromatograph for continuous separations. *J Chromatogr.*,1 **126**, 381-400.

58 Goto, M., Goto, S., 1987, Continuous separation using an annular chromatograph with rotating inlet and outlet. *Chem.Eng. Japan*, **20** (6) 598-603.

59 Carr, R. W., Continuous reaction chromatography, in Ganetsos, G and Barker, P.E. (Eds.), 1992, Preparative and production scale chromatography, Chromatographic science series, Vol 61, Marcel Dekker, New York.

60 Wardwell, A. W., 1981, Continuous reaction gas chromatography. PhD. Thesis, University of Minesota.

61 Viswanathan, S. and Aris, R., 1974, Countercurrent moving bed chromatographic reactors. *Proc. 3rd ISCRE, Adv. Chem. Ser.* **133**, 191-204.

62 Viswanathan, S. and Aris, R., 1974, An analysis of the countercurrent moving bed reactor. *SIAM-AMS Proc.* **8**, 99-124.

63 Altshuller, D., 1983, Design equations and transient behaviour of the countercurrent moving bed chromatographic reactor. *Chem. Eng. Commun.* **19**, 363-375.

64 Petroulas, T., Aris, R. and Carr, R. W., 1984, Mathematical analysis of a chroatographic reactor. *Proc. 5 th IMACS International Symposium.* 183-190.

65 Petroulas, T., Aris, R. and Carr, R. W., 1985, Analysis of a countercurrent moving bed chromatographic reactor. *Chem. Eng. Sci.*, **40**, 2233-2240.

66 Fish, B. B, Carr, R. W. and Aris, R., 1988, Computer aided experimentation in countercurrent and simulated countercurrent chromatography. *Chem. Eng. Sci.*, **43**, 1867-1873.

67 Takeuchi, K. and Urugachi, 1976, Separation conditions of the reactant and the product with a chromatographic moving bed reactor. *J. Chem. Eng. Japan.* **9**, 164-166.

68 Takeuchi, K. and Urugachi, 1978, Computational studies of a chromatographic moving bed reactor for consecutive and reversible reactions. *J. Chem. Eng. Japan.* **11**, 216-220.

69 Takeuchi, K. and Urugachi, 1976, Basic design of a chromatographic moving bed reactors for product refining. *J. Chem. Eng. Japan.* **9**, 246-248.

70 Takeuchi, K. and Urugachi, 1977, Experimental studies of a chromatographic moving bed reactor. *J. Chem. Eng. Japan.* **10**, 455-460.

71 Barker, P. E. and Critcher, D., 1960, The separation of volatile liquid mixtures by a continuous gas-liquid chromatography. *Chem. Eng. Sci.,* **13** 82.

72 Fish, B. B, Carr, R. W. and Aris, R., 1988, An experimental study of the countercurrent moving bed chromatographic reactor. *Chem. Eng. Sci.*, **44**, 1773-1783.

73 Ruthven, D. M. and Ching, C. B., 1989, Review article no. 31; Counter-current and simulated counter-current adsoption separation process. *Chem. Eng. Sci.,* **44**, 1011-1038.

74 Ray, A., Tonkovich, A. L., Aris, R. and Carr, R. W, 1990, The simulated countercurrent moving bed chromatographic reactor. *Chem. Eng. Sci.,* **45**, 2431-2437.

75 Barker, P. E., Ganetsos, G. Ajongwen, J. N. and Akintoye, A., 1990, Continuous chromatographic bioreaction-separation in *Separations for Biotechnology Vol. 2* (Ed.) Pyle, D. L., Elsevier Applied Science Publishers, 549-557.

76 Shieh, M. T. and Barker, P. E., 1993 Simulated counter-current chromatographic bioreactor-separators (SCCR-S). In Proceeding of *The 1993 ICHEME Research Event*, Published by Institution of Chemical Engineers, Rugby, U.K., 144-146.

77 Shieh, M. T., 1993, Private communication.

78 Hashimoto, K., Shuji, A., Hiromitsu, N. & Ueda, Y., 1983, a new process combining adsorption and enzyme reaction for producing higher-fructose syrup. *Biotech. Bioeng.*, **25**, 2371-2393.

79 Hashimoto, K., Shuji, A. and Yoshihito, S., Development of new bioreactor of a simulated moving bed type.in Ganetsos, G and Barker, P.E. (Eds.), 1992, Preparative and production scale chromatography, Chromatographic science series, Vol 61, Marcel Dekker, New York.

80 Thirkill, C., 1986, The crossflow chromatographic separation of carbohydrate mixtures. PhD Thesis, University of Aston, Birmingham.

81 Bridges, S., 1990, Continuous annular chromatography for the Separation of Carbohydrate Mixtures, PhD Thesis, University of Aston, Birmingham.

82. Akintoye, A., 1990, Continuous chromatographic biochemical reaction-separation, PhD Thesis, University of Aston, Birmingham.

83 Heftmann, E., (Ed.). 1991, *Chromatography (Journal of Chromatography Library,* vol. 51B), Elsevier, B242-B245.

84 Determination of invertase activity using 3.5 dinitro salicylic acid. Biocon Biochemical Standard Analytical Method , 1987, No. SAM 007-10. Tenbury Wells, Worcetershire.

85 Hausser, A. G., Goldberg, B. S. & Mertens, J. L., An immobilized two-enzyme system (fungal alpha-amylase/glucoamylase) and its use in the continuous production of high conversion maltose-containing corn syrups. *Biotech. Bioeng.* **25** (1983) 525-539.

86 Vlachogiannis, G.,J., 1982, Dextran polymer fractionation by production scale chromatography and ultrafiltration, Ph.D Thesis, University of Aston, Birmingham.

87 Maeda, H, Tsao,G. T. and Chen, L. F., 1978, Preparation of immobilized soybean β-amylase on porous cellulose beads and continuous maltose production. *Biotech. Bioeng.* **XX** 383-402.

88 Welstein, H. and Sauer, C., Separation of glucose and fructose: effects of resin characterictics on separation in *Ion exchange Technology*, (Eds.) Nader, P. and Streat, M., Ellis Horwood, Chichester, 1984, 463-471

89 Bauski, I., Saini, R., Ryu, D.Y., Vieth, W.R., (1971) Kinetic modelling of sucrose by invertase, *Biotech. Bioeng.*, Vol 13, 641-650 .

90 Fullbrook, P. D., (Ed.) Industrial enzymology Nature Press, 1984.

91 Ion Exchange Resins, Bio-Rad catalogue K1985.

92 Goulding, R. W., Liquid chromatography of sugars and related polyhydric alcohols on cation exchangers. *J. Chromatogr.*, **103** (1975) 229-239

93 Pigman, W. and Horton, D., (Eds) 1972, The Carbohydrates; Chemistry and Biochemistry, Volume 1A. Academic Press New York.

94 Stoddart, J. F., 1971, Streochemistry of carbohydrates. Wiley-Interscience, London

95 Rees, D. A., 1977, Polysaccharide shapes. Chapman and Hall, London.

96 Lehniger, A. 1982, Principles of Biochemistry, Worth Publisher Inc. New York.

97 Shallenberger, R., 1977, Specific rotation of α-D- and β-D-fructofuranose. *Carbohydrate Res.*, **58** 205.

98 Angyal, S. J., 1971, Complexes of sugar with cation in Carbohydrate in solution, Advances in chemistry series 117 (Ed.) Isbel, H. S., 106-121.

99 Bowski, R. S., Ryu, D. Y. and Vieth, W. R., 1971, Kinetic modelling of sucrose by invertase, *Biotech. Bioeng.* Vol **XIII**, 641-656.

100 Dickensheets, P. A., Chen, L. F. and Tsao, G., 1977, Characteristics of yeast invertase immobilised on porous cellulose beads, *Biotech. Bioeng.* Vol **XIX**, 365-375.

101 Nakajima, M., Jimbo, N., Nishizawa, K., Nabetani, H. and Watanabe, A., 1988, Conversion of sucrose by immobilized invertase in an asymmetric membrane reactor, *Process Biochemistry*, **4** 32-35.

102 Kobayashi, T. and Moo-Young, M., 1973, The kinetic and mass transfer behaviour of immobilized invertase on ion-exchange resin beads, *Biotech. Bioeng.* Vol **XV**, 47-67.

103 Imison, B. W. and Yang, R. Y. K., 1980, Kinetics of sucrose inversion by invertase-multiple steady states in a CSTR, *Chem. Eng. Commun.* **6** 151-160.

104 Mansfield, J. and Schellenberger, A., 1987, Invertase immobilized on macroporous polystyrene: properties and kinetic characterisation, *Biotech. Bioeng.* Vol **XXIX**, 72-78.

105 Outtrup, H. & Norman, B. E., Properties and application of a thermostable maltogenic amylase produced by a strain of bacillus modified by recombinant-DNA techniques. Novo-Nordisk Technical publication A05863 (1984).

106 Takasaki, Y and Yamanobe, T., 1981, Production of maltose by pullulanase and β-amylase in Enzyme and Food processing (Eds.) Birch, G. G., Blakebrough, N. and Parker, K. J., Applied Science Publisher Ltd. London 73-88.

107 Banks, W and Greenwood, C. T.,1975, Starch and its components. Edinburgh University Press.

108 Ghose, T. K., (Ed.) 1990, Bioprocess computations in biotechnology, Ellis Horwood Ltd.

109 Dixon, M. and Webb, E., 1979, Enzymes, 3rd edition, Longmans, London.

110 Yau, W. W., 1977, Characterizing skewed chromatographic band broadening. *Anal. Chem.,* **49**(3) 395-398.

111 Foley, J. and Dorsey, J. G., 1983, Equations for calculation of chromatographic figures of merit fro ideal and skewed peaks. *Anal. Chem.,*, **55**(4) 731-737.

112 Jeansonne, M. S. and Foley, J., 1992, Improved equations for the calculation of chromatographic figures of merit for ideal and skewed chromatographic peaks. *J Chromatogr.*, **594** 1-8.

113 Davies, D.L., Design and Analysis of Industrial Experiments 2nd. Ed., Oliver and Boyd Tweeddale Court, Edinburgh, UK, (1971).

114 Winer, B. J., 1962, Statistical principles in experimental design. McGraw-Hill , New York.

115 Wheeler, D. J., 1987, Understanding industrial experimentation, SPC Press. Tennessee.

116 Myers, R. H., 1975, Response surface methodology. Allyn Bacon,Boston.

117 Shiraishi, F., Kawakami, K., Yuasa, A., Kojima, T. and Kusunoki, K., 1986, Kinetic expression for maltose production from soluble starch by simultaneous use of β-amylase and debranching enzyme. *Biotech. Bioeng.* Vol **XXX**, 374-380.

118 De Carli, II. J. P., Carta, G. and Byers, C. H., 1990, Displacement separations by continuous annular chromatography. *AIChE J.,* **36**(8) 1220-1228.

119 Howard, A.J., Carte, G., Byers. 1987, Separation of sugars by continuous annular chromatography. Oak Ridge National Laboratory, Report ONRL/TM-10318.

120 Bratzler, R. L. and begovich, J. M., 1980, Mathematical model for multicomponent separations on the the Continuous Annular Chromatography, Oak Ridge National Laboratory. Report ONRL/TM-6706

121 Bridges, S. and Barker, P. E., 1992, Modelling continuous chromatographic separations, *Chem. Eng. Sci.*, **47**(5) 1299-1306.

122 Bellot, J. C. and Condoret, J. S., 1991, Liquid chromatography modelling: A review. *Process Biochemistry*, **26** 363-376.

123 Wankat, P. C., 1977, The relationship between one dimensional and two dimensional separation processes. *AIChE J.*, **23**(6) 859-863.

124 Lapidus, L. and Pinder, G. F., 1982, *Numerical solution of partial Differential equations in Science and Engineering,* Wiley, New York.

125 Chung, F.S. and Wen,C. Y., 1968, Longitudinal dispersion of liquid flowing through fixed and fluidised beds. *AIChE J,* **14** 857.

126 Lin, B., Zidu, M. A. and Guichon, G., 1989, Influence of calculation errors in the numerical simulation of chromatographic elution band profiles using an ideal or semi-ideal model. *J. Chromatogr.,* **484** 83-102.

127 Carta, G., Maharajan, A. J. Cohen, M. L. and Byers, H. C., 1992, Chromatography of reversibly reacting mixtures: mutarotation effects in sugar separation. *Chem. Eng. Sci.*, **47**(7) 1645-1657.

128 Ramirez, W., F., 1989, Computational Methods for process simulation. Butterworth series in Chemical engineering, London.

129 Daugulis, A. J., 1988, Integrated reaction and product recovery in bioreactor systems. *Biotech. Prog.*, Vol. **4** No. 3, 113-122

130 Saha, B. and Zeikus, G. J., 1987, Biotechnology of maltose syrup production. *Process Biochemistry,* June 79-82.

131 Sarmidi, M R. and Barker, P. E., Saccharification of modified starch to maltose in a continuous rotating annular chromatograph. Accepted for publication in *J. Chem. tech. Biotechnol.*

132 Sarmidi, M R. and Barker, P. E., Simultaneous biochemical reaction and separation in a continuous rotating annular chromatograph. Accepted for publication in *Chem. Eng Sci.*

133 Cretier, G., Macherel, L. and Rocca, J.L., Preparative liquid chromatography; Influence of column efficiency on optimum injection conditions under isocratic elution. *J. Chromatogr.,* **590** 175-188.

Appendix A1

Determination of Voidage and Distribution Coefficients on a CRAC

Voidage ε is defined as;

$$\varepsilon = \frac{\text{Volume of void in the resin bed}}{\text{Volume of the resin bed}} \qquad \text{A1.1}$$

With a CRAC the voidage was calculated using an equation derived from plate theory of chromatography [57]. The equation used was;

$$\theta_D = \frac{\omega L}{V}(\varepsilon + (1 - \varepsilon) K_{dD}) \qquad \text{A1.2}$$

Since blue dextran is totally excluded from the pores of the resin, its distribution coefficient K_{dD} is zero. Under the experimental condition given in section 4.2.6, the exit position of blue dextran was 137^{o}.

$$\varepsilon = \frac{\theta_D V}{\omega L} = \frac{\frac{137 \times 2\pi}{360} \times 1.56}{0.0698 \times 135} = 0.395 = 0.4$$

The distribution coefficient of the saccharides was caculated using Equation A1.2.
By rearranging equation A1.2 an expression for K_{di} was obtained.

$$K_{di} = \frac{\frac{\theta V}{\omega L} - \varepsilon}{1 - \varepsilon} \qquad \text{A1.3}$$

Appendix A2

Determination of Michaelis-Menten Kinetics Constants

The modified Michaelis-Menten equation [90,108] was used to quantify the substrate inhibition effect. The substrate inhibition effect is visualised by the binding of one substrate molecule to the catalytic site on the enzyme molecule, with a simultaneous binding of a second substrate molecule to a separate site on the same enzyme molecule, forming a non-productive complex. This is due to the increase in probability of double binding of substrate molecules as a result of a high concentration. The modified Michaelis-Menten kinetic model can be represented by equation A2.1 :

$$\begin{array}{ccccc} S + E & \rightleftharpoons & ES & \longrightarrow & P + E \\ & & \uparrow\downarrow & & \\ & & SES & & \end{array} \qquad \text{A2.1}$$

where S, E , P and SES represent substrate, enzyme, enzyme double complex and product. The kinetic equation is written as follows:

$$\upsilon = \frac{V_{max}\, S}{K_m + S + \frac{S^2}{K_i}} \qquad \text{A2.2}$$

where υ = initial reaction velocity

V_{max} = maximum reaction velocity

K_m = Michaelis Menten constant

S = sustrate concentration

K_i = substrate inhibition constant.

The kinetic constants K_m and V_{max} were obtained from figure A2.1. Figure A2.1 was drawn using a direct linear plot method [109] based on data from the linear section of the

graph in figure A2.1. The values of K_m and V_{max} are 0.024 g/ cm^3 and 0.012 $g/cm^3/min$.

The substrate inhibition constant K_i was calculated from equation A2.1. Equation A2.1 was diferentiated at the maximum initial reaction velocity and the following expression was obtained [108]:

$$\frac{d\upsilon}{dS} = V_{max} \left(\frac{-1\left(\frac{-K_m}{S^2} + \frac{1}{K_i}\right)}{\left(1 + \frac{K_m}{S} + \frac{S}{K_i}\right)^2} \right) = 0 \qquad \text{A2.2}$$

$$\therefore \quad S_{max} = \sqrt{K_m}\, K_i \qquad \text{A2.3}$$

From equation A2.3, K_i was calculated to be 0.6 g/ cm^3 (K_m and S_{max} were already known).

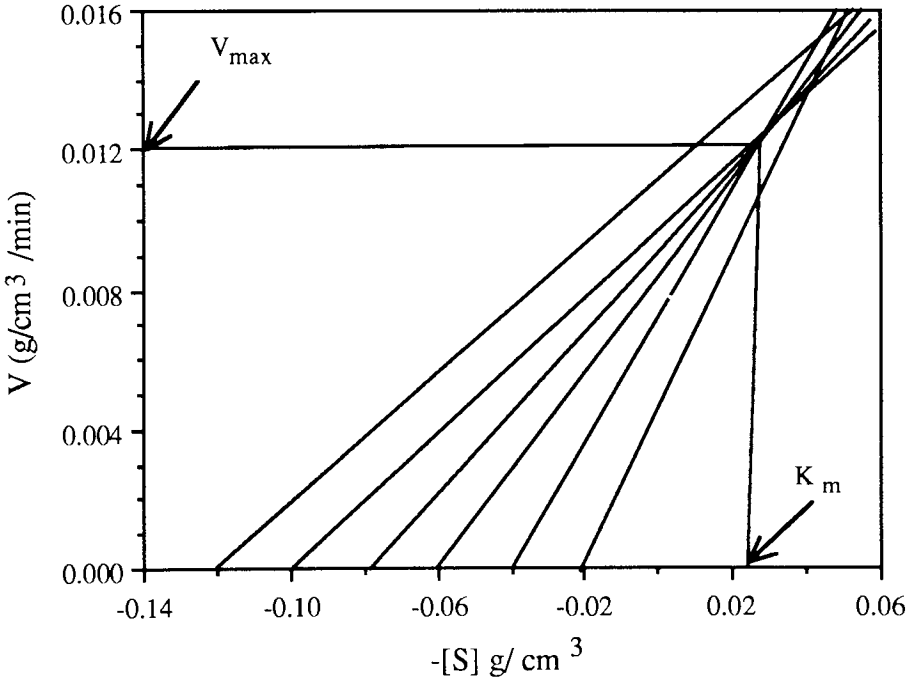

Figure A2.1 Direct linear plot

APPENDIX A3

The Elution Profiles of the Preliminary Experiments

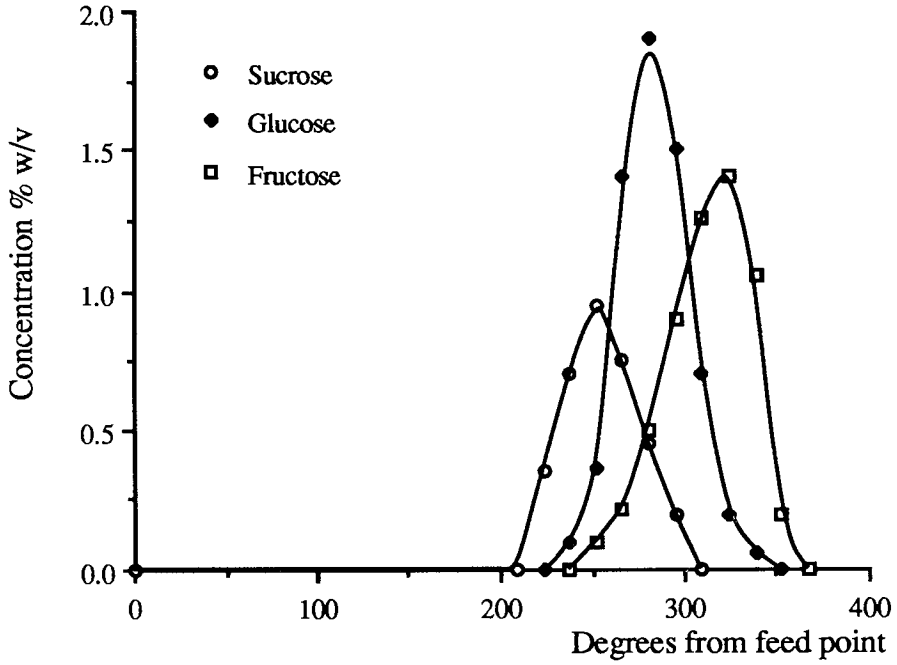

Figure A3.1 Elution profile for run 230-25-8-60-240

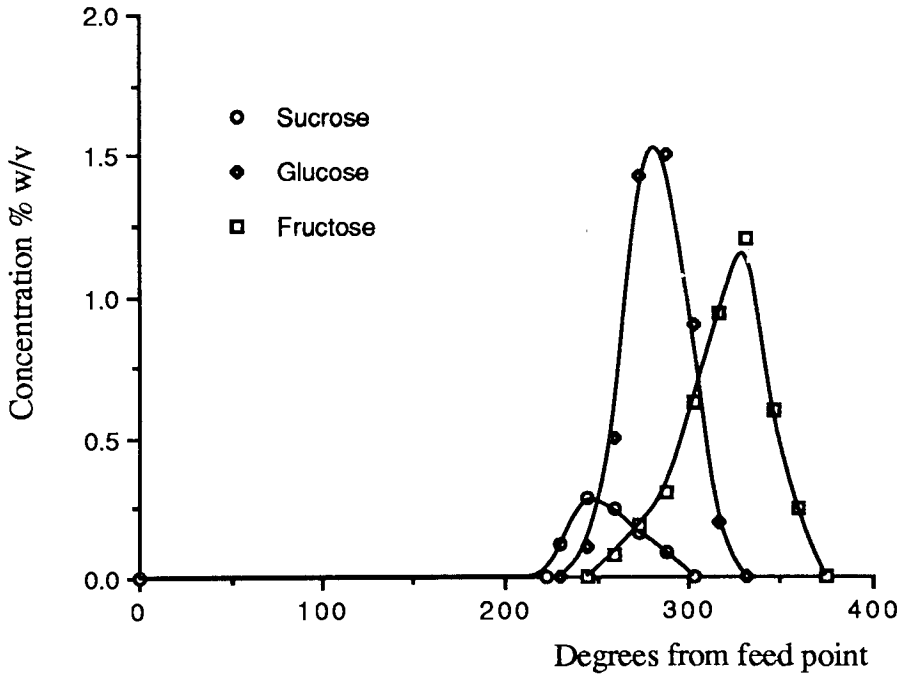

Figure A3.2 Elution profile for run 230-12.5-8-60-240

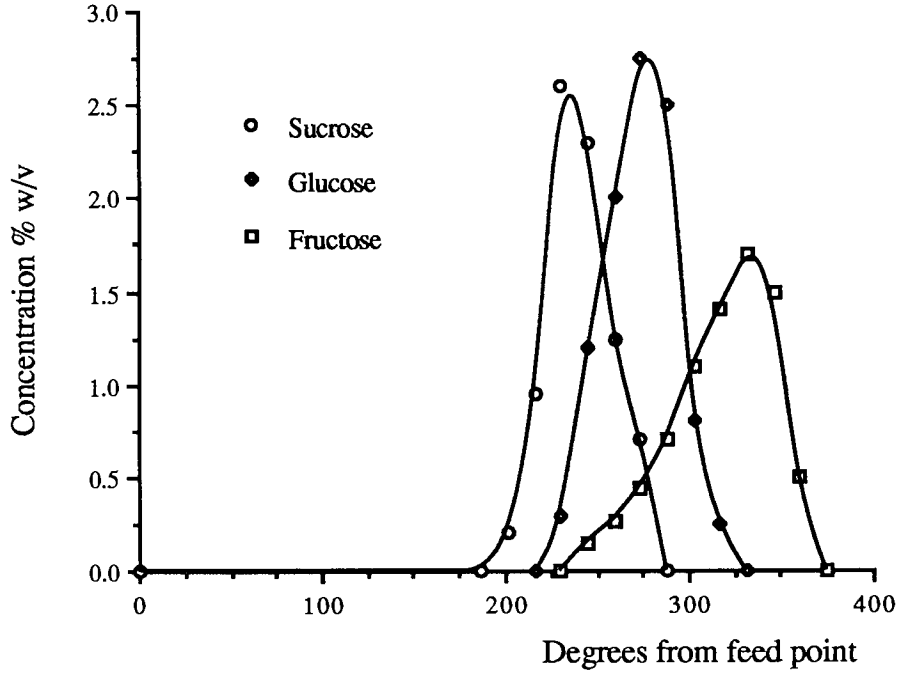

Figure A3.3 Elution profile for run 150-50-8-60-240

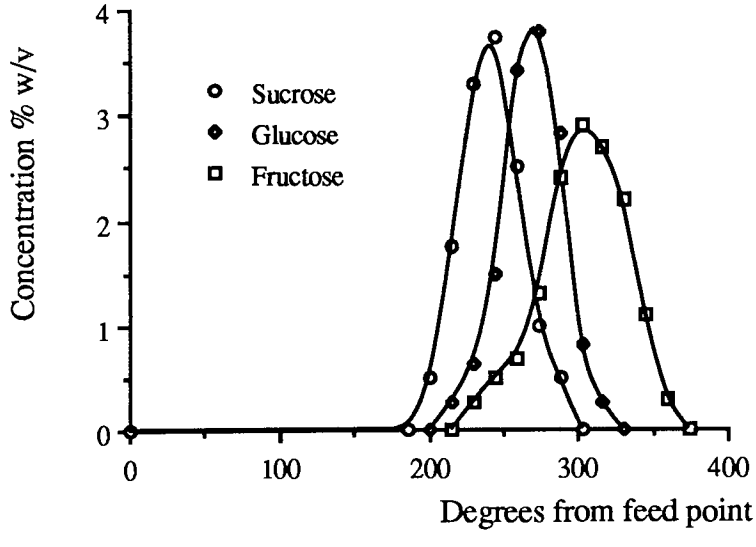

Figure A3.4 Elution profile for run 230-50-8-60-240

APPENDIX 4

The Analysis of the Experimental Data Reported in Section 5.3.2

In this method, the treatment combinations and the responses are arranged in a standard order, as in Table A4.1. The first value of the top half of column (1) is the sum of the first two responses (0.76+0.5); the second value is the sum of the second pair (0.65+0.3) and so on until the last pair. The lower half is derived from the response column by taking the differences of the same pairs. Column (2) was derived from the result in column (1) by summing and differencing sucessive pairs. The other columns (2), (3) and (4) were derived in a similar manner. The actual effects of the factors are obtained by dividing the entries in column (4) by 8. While the mean square values or the variances were obtained by squaring the entries in column (4) and dividing the results by 16. The analysis of the variances were also checked by using a statistic software package called Statview^{R} on a Macintosh^{R} personal computer.

Table A4.1 Analysis of glucose-fructose resolution data

Treatment combinations	R_{G-F}	(1)	(2)	(3)	(4)	Effect	Mean square	F Value
$A_1B_1C_1D_1$	0.76	1.26	2.21	4.63	10.13			
$A_2B_1C_1D_1$	0.5	0.95	2.42	5.5	-0.89	-0.111	0.049	12.25
$A_1B_2C_1D_1$	0.65	1.28	2.48	-0.85	-0.57	-0.071	0.02	5.0
$A_2B_2C_1D_1$	0.3	1.14	2.7	-0.04	-0.03	-0.0038	0.00006	0.015
$A_1B_1C_2D_1$	0.71	1.46	-0.61	-0.45	0.11	-0.014	0.00075	0.188
$A_2B_1C_2D_1$	0.57	1.34	-0.24	-0.12	0.33	0.041	0.0068	1.7
$A_1B_2C_2D_1$	0.62	1.35	0.0	-0.05	0.29	0.036	0.0052	1.3
$A_2B_2C_2D_1$	0.52	1.35	-0.04	0.02	0.39	0.0487	0.0095	2.38
$A_1B_1C_1D_2$	0.7	-0.26	-0.31	0.21	0.78	0.108	0.0473	11.83
$A_2B_1C_1D_2$	0.76	-0.35	-0.14	-0.1	0.81	0.1	0.041	10.25
$A_1B_2C_1D_2$	0.7	-0.14	-0.12	0.37	0.33	0.041	0.0068	1.7
$A_2B_2C_1D_2$	0.64	-0.1	0.0	-0.04	0.07	0.0087	0.0003	0.075
$A_1B_1C_2D_2$	0.72	0.06	-0.09	0.17	-0.31	-0.039	0.006	1.5
$A_2B_1C_2D_2$	0.63	-0.06	0.04	0.12	-0.41	-0.051	0.0105	2.63
$A_1B_2C_2D_2$	0.65	-0.09	-0.12	0.13	-0.05	-0.006	0.00015	0.038
$A_2B_2C_2D_2$	0.7	0.05	0.14	0.26	0.13	0.0162	0.00105	0.26
Total	10.13						0.206	

Table A4.2 Analysis of glucose peak concentration data

Treatment combinations	$\hat{C}_G$ % w/v	(1)	(2)	(3)	(4)	Effect	Mean square	F Value
$A_1B_1C_1D_1$	1.32	3.52	10.47	22.24	42.43			
$A_2B_1C_1D_1$	2.2	6.95	11.77	20.19	8.13	1.01	4.13	103.5
$A_1B_2C_1D_1$	3.4	10.21	2.66	2.66	10.57	1.32	6.98	174.9
$A_2B_2C_1D_1$	3.55	7.95	9.98	5.47	-0.93	-0.11	0.054	1.35
$A_1B_1C_2D_1$	1.42	4.21	1.03	7.56	-1.07	0.13	0.072	1.80
$A_2B_1C_2D_1$	2.4	6.0	1.63	3.01	-0.91	-0.11	0.052	1.30
$A_1B_2C_2D_1$	3.65	4.38	3.49	-1.06	0.13	0.016	0.001	0.025
$A_2B_2C_2D_1$	4.3	5.6	1.98	0.13	-1.29	0.16	0.104	2.61
$A_1B_1C_1D_2$	1.46	0.88	3.43	1.3	-2.05	-0.26	0.263	6.59
$A_2B_1C_1D_2$	2.75	0.15	4.13	-0.23	2.81	0.35	0.494	12.38
$A_1B_2C_1D_2$	1.9	0.98	1.79	0.60	-4.55	-0.57	1.29	32.33
$A_2B_2C_1D_2$	4.1	0.65	1.22	-1.51	1.19	0.15	0.089	2.23
$A_1B_1C_2D_2$	1.5	1.29	-0.73	0.7	-1.53	-0.2	0.146	3.66
$A_2B_1C_2D_2$	2.88	2.2	-0.33	-0.57	-2.11	-0.26	0.278	6.96
$A_1B_2C_2D_2$	2.5	1.38	0.91	0.4	-1.27	-0.16	0.101	2.53
$A_2B_2C_2D_2$	3.1	0.6	-0.78	-1.69	-2.09	-0.26	0.273	6.84
Total	42.43						14.33	

Table A4.3 Analysis of fructose peak concentration data

Treatment combinations	$\hat{C}_F$ % w/v	(1)	(2)	(3)	(4)	Effect	Mean square	F Value
$A_1B_1C_1D_1$	1.22	2.82	8.88	18.6	35.86			
$A_2B_1C_1D_1$	1.6	6.06	9.72	17.26	5.9	0.737	2.176	103.6
$A_1B_2C_1D_1$	2.96	2.92	8.66	1.8	9.58	1.19	5.736	273.1
$A_2B_2C_1D_1$	3.1	6.8	8.6	4.1	0.46	0.057	0.013	0.62
$A_1B_1C_2D_1$	1.32	3.7	0.52	7.12	0.78	0.097	0.038	1.81
$A_2B_1C_2D_1$	1.6	4.96	2.4	2.46	0.06	0.0075	0.00023	0.01
$A_1B_2C_2D_1$	2.9	3.7	1.7	0.48	0.58	0.072	0.021	1.0
$A_2B_2C_2D_1$	3.9	4.9	3.24	-0.02	-0.02	-0.0025	0.00003	0.001
$A_1B_1C_1D_2$	1.37	0.38	3.24	0.84	-1.34	-0.167	0.112	5.33
$A_2B_1C_1D_2$	2.33	0.14	3.88	-0.06	2.3	0.287	0.331	15.76
$A_1B_2C_1D_2$	1.76	0.28	1.26	0.76	-4.66	-0.58	1.357	64.62
$A_2B_2C_1D_2$	3.2	1.0	1.2	-0.7	-0.5	-0.06	0.016	0.76
$A_1B_1C_2D_2$	1.3	0.96	-0.24	0.64	-0.9	-0.112	0.051	2.43
$A_2B_1C_2D_2$	2.4	1.44	0.72	-0.06	-1.46	-0.18	0.133	6.33
$A_1B_2C_2D_2$	2.15	1.1	0.48	0.96	-0.7	-0.087	0.031	1.48
$A_2B_2C_2D_2$	2.75	0.6	-0.5	-0.98	-1.94	-0.24	0.235	11.19
Total	35.86						10.25	

Table A4.4 Analysis % of glucose recovery data

Treatment combinations	Y_G	(1)	(2)	(3)	(4)	Effect	Mean square	F Value
$A_1B_1C_1D_1$	24.5	25.09	54.79	112.76	271.8			
$A_2B_1C_1D_1$	0.59	29.7	57.97	169.04	-75.94	-9.5	360.43	9.17
$A_1B_2C_1D_1$	27.6	19.07	82.57	-79.98	-41.06	-5.13	105.37	2.68
$A_2B_2C_1D_1$	2.1	38.9	86.47	4.04	-66.06	-8.26	272.9	6.94
$A_1B_1C_2D_1$	16.67	73.0	-49.41	24.44	7.08	0.89	3.133	0.08
$A_2B_1C_2D_1$	2.4	9.57	-30.57	-65.5	-31.06	-3.88	60.29	1.53
$A_1B_2C_2D_1$	27.6	44.27	26.97	3.62	76.58	9.57	366.53	9.62
$A_2B_2C_2D_1$	11.3	42.2	-22.93	-69.7	12.72	1.59	10.11	0.26
$A_1B_1C_1D_2$	19.3	-23.91	4.61	3.18	56.28	7.03	197.96	5.04
$A_2B_1C_1D_2$	53.6	-25.5	19.83	3.9	84.02	10.5	441.21	11.22
$A_1B_2C_1D_2$	8.4	-14.27	-63.43	18.84	-89.94	-11.24	505.58	12.87
$A_2B_2C_1D_2$	1.17	-16.3	-2.07	-49.9	66.08	8.26	272.91	6.94
$A_1B_1C_2D_2$	20.8	34.2	-1.59	15.22	0.72	0.09	0.032	0.0004
$A_2B_1C_2D_2$	23.47	-7.23	-2.03	61.36	-68.74	-8.59	295.32	7.51
$A_1B_2C_2D_2$	33.9	2.67	-41.43	-0.44	46.14	5.78	133.05	3.39
$A_2B_2C_2D_2$	8.3	-25.6	-28.27	13.16	13.6	1.7	11.56	0.29
Total	281.7						3099.48	

Table A4.5 Analysis of % of fructose recovery data

Treatment combinations	Y_F	(1)	(2)	(3)	(4)	Effect	Mean square	F Value
$A_1B_1C_1D_1$	37.6	42.9	74.37	183.77	405.26			
$A_2B_1C_1D_1$	5.3	31.47	109.4	221.49	-96.9	-12.11	586.85	16.14
$A_1B_2C_1D_1$	26.8	53.06	95.39	-72.19	-46.66	-5.83	136.07	3.74
$A_2B_2C_1D_1$	4.67	56.54	126.1	-24.71	-3.58	-0.44	0.80	0.02
$A_1B_1C_2D_1$	25.8	46.4	-54.43	-7.95	65.74	8.21	271.76	7.43
$A_2B_1C_2D_1$	27.3	48.99	-17.76	-38.71	6.47	0.81	2.54	0.07
$A_1B_2C_2D_1$	37.9	83.7	2.79	-10.61	-28.98	-3.62	52.49	1.44
$A_2B_2C_2D_1$	18.6	42.4	-27.5	7.09	-13.5	-1.69	11.39	0.31
$A_1B_1C_1D_2$	21.2	-32.3	-11.43	35.03	37.72	4.72	88.92	2.44
$A_2B_1C_1D_2$	25.2	-22.13	3.48	30.71	47.48	5.94	140.9	3.88
$A_1B_2C_1D_2$	25.1	1.54	2.59	36.67	-30.76	-3.85	59.14	1.62
$A_2B_2C_1D_2$	23.9	-19.3	-41.3	-30.2	17.76	2.22	19.71	0.54
$A_1B_1C_2D_2$	51.8	4.0	10.17	14.91	-4.32	-0.54	1.17	0.032
$A_2B_1C_2D_2$	31.9	-1.21	-20.84	-43.89	-66.87	-8.36	279.47	7.69
$A_1B_2C_2D_2$	25.0	-19.9	-5.21	-31.0	-58.8	-7.35	216.09	5.94
$A_2B_2C_2D_2$	17.4	-7.6	12.3	17.51	48.52	6.07	147.14	4.04
Total	405.4						2012.87	

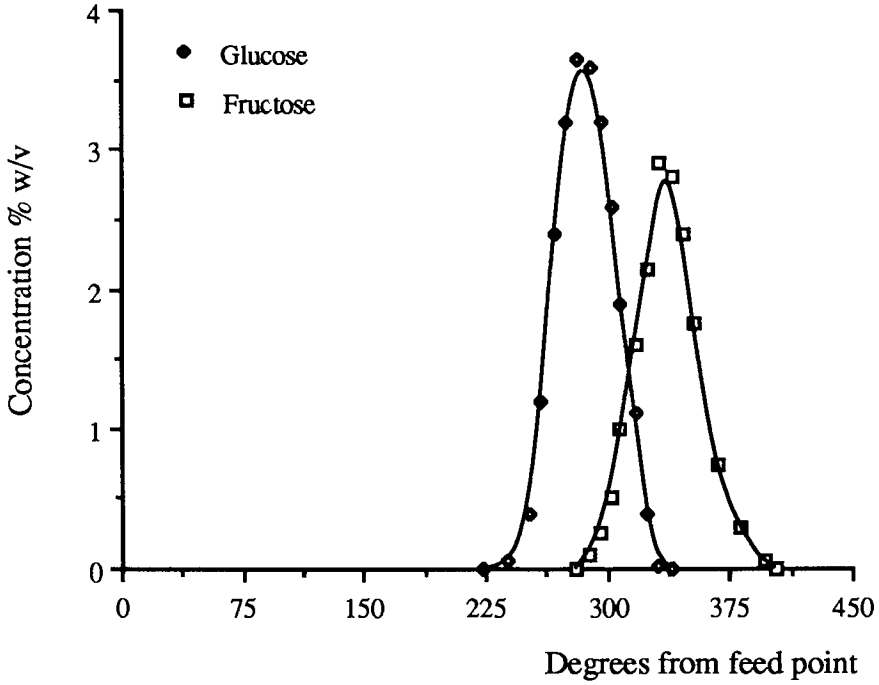

Figure A4.1 Elution profile for treatment combination $A_1B_2C_2D_1$ (Run 150-230-8-100-240)

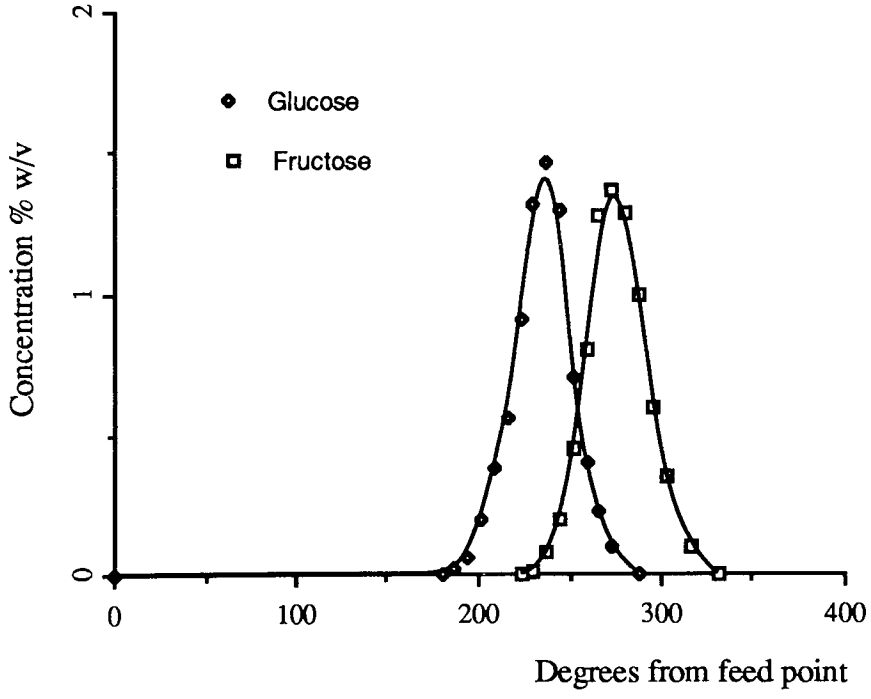

Figure A4.2. Elution profile for treatment combination $A_1B_1C_1D_2$ (Run 150-25-10-75-240)

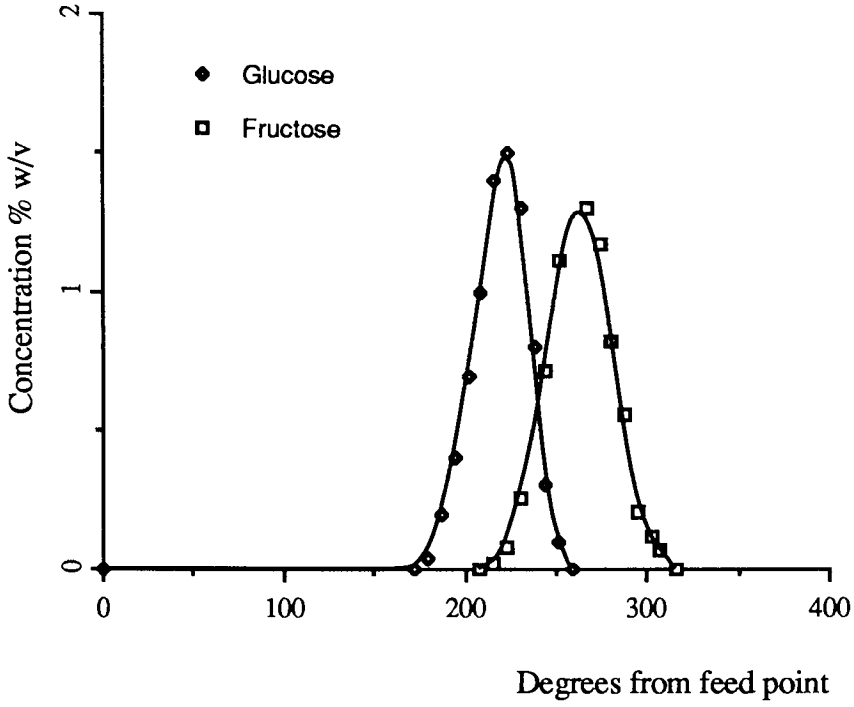

Figure A4.3 Elution profile for treatment combination $A_1B_1C_2D_2$ (Run 150-25-10-100-240)

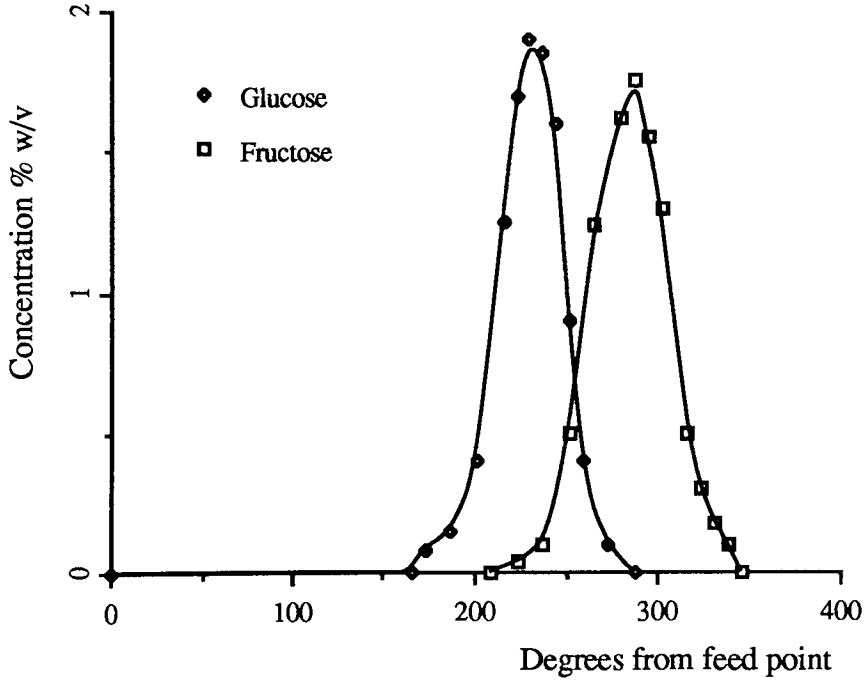

Figure A4.4 Elution profile for treatment combination $A_1B_2C_1D_1$ (Run 150-25-10-100-240)

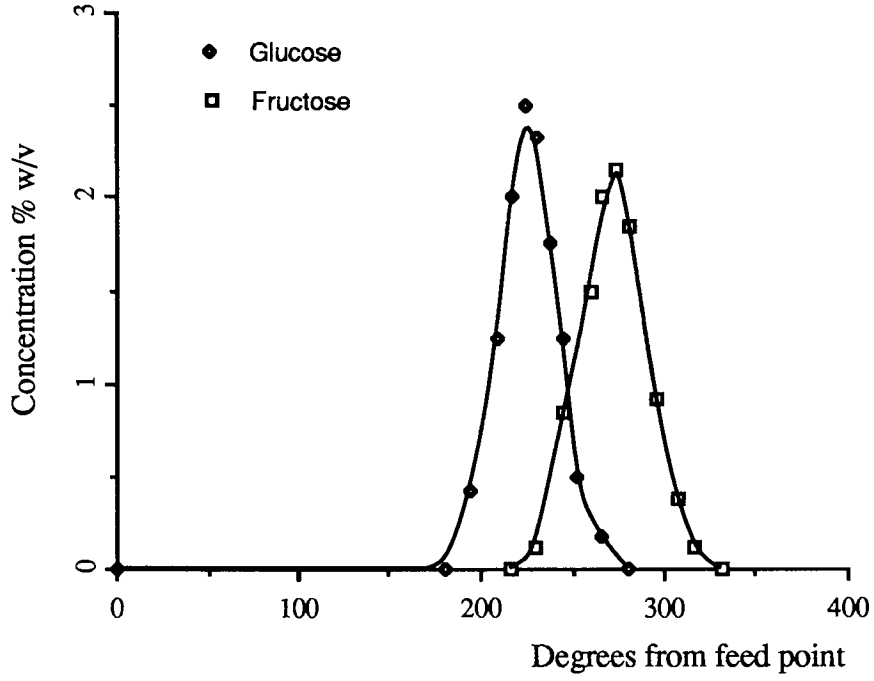

Figure A4.5 Elution profile for treatment combination $A_1B_2C_2D_2$ (Run 150-50-10-100-240

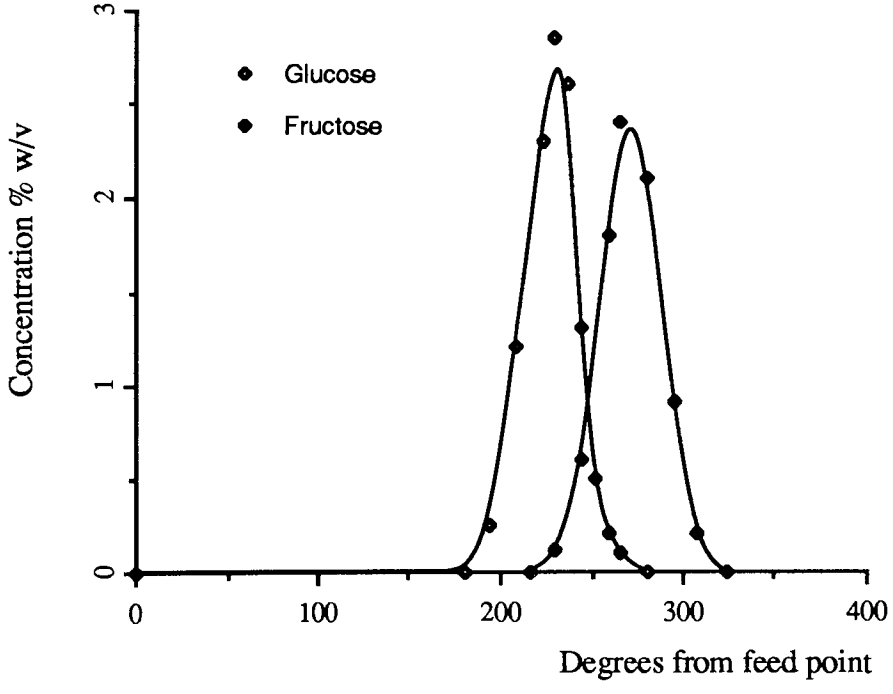

Figure A4.6 Elution profile for treatment combination $A_2B_1C_2D_2$ (Run 230-25-10-100-240)

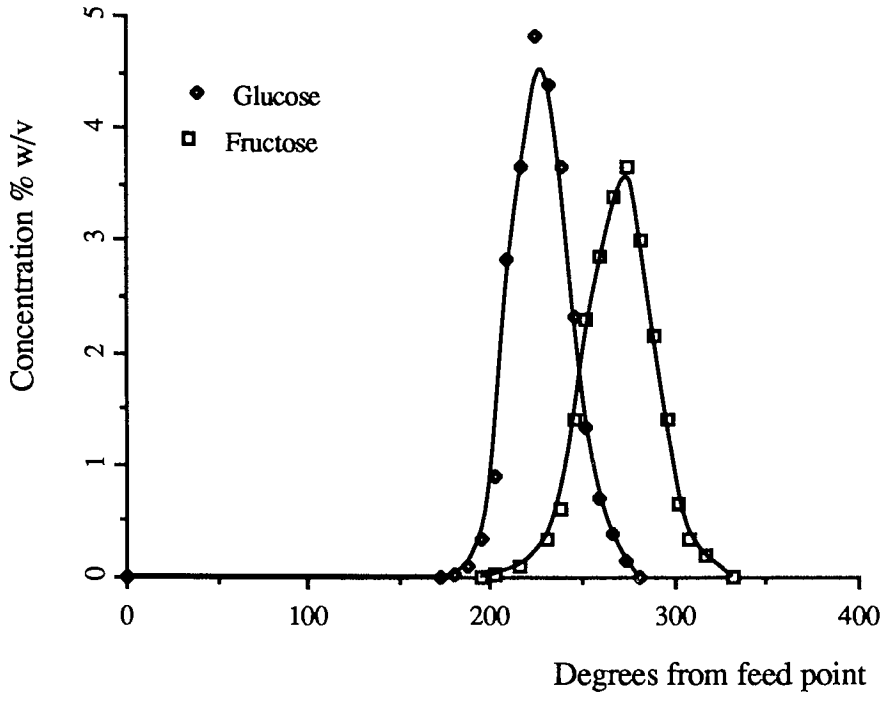

Figure A4.7 Elution profile for treatment combination $A_2B_2C_1D_2$ (Run 230-50-10-75-240)

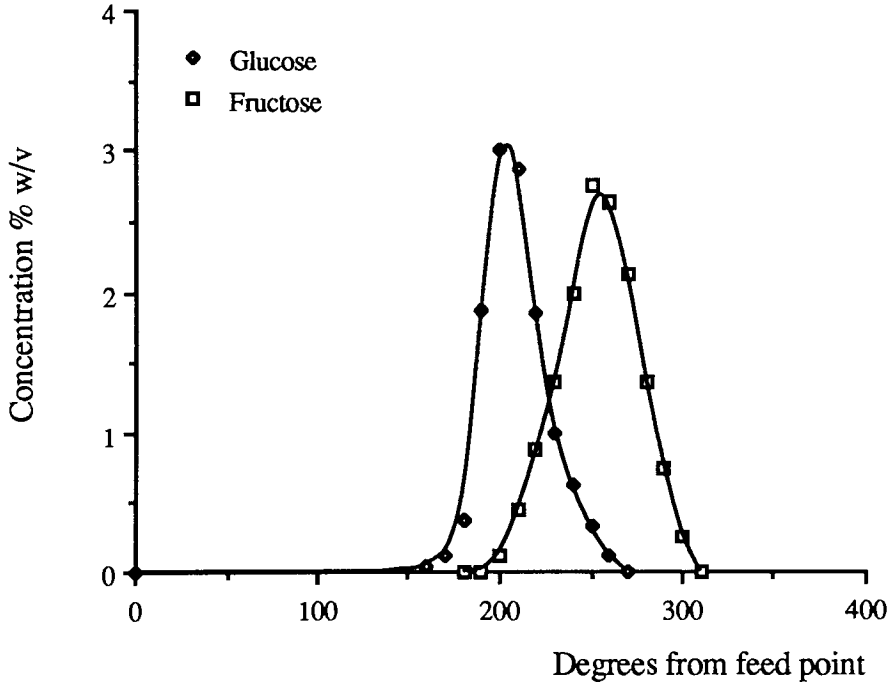

Figure A4.8 Elution profile for treatment combination $A_2B_2C_2D_2$ (Run 230-50-10-100-240)

APPENDIX A5

Enzyme Usage Calculation for Run 250-50-7.5-75-240

1unit of enzyme is the amount of enzyme that will convert 1 mmole of sucrose in one minute at pH 5.5 and temperature of 55°C.

1 unit ---------- 3.44×10^{-4} g of sucrose in 1 minute.

2907 unit ---------- 1 g of sucrose in 1 minute

Enzyme activity in the eluent = 75 U/cm^3

Total enzyme activity used in the eluent = 125x75 = 9375 U/cm^3

Concentration of sucrose fed into the system = 50 %w/v

Volumetric rate of sucrose fed into the system = 4.2 cm^3/min

Mass of sucrose fed into the system = 0.5x4.2=2.1 g/min

Therefore 9375 Units of enzyme convert 2.1 g/min of sucrose

Theoretical amount of enzyme required to convert 2.1 g/min

=2907x2.1=6104.7 Units

$$\text{Therefore the enzyme usage} = \frac{\text{actual enzyme used}}{\text{theoretical enzyme used}}$$

$$= \frac{9375}{6104.7} = 1.53$$

Assuming two feed points, the enzyme usage = 0.76

APPENDIX A6

```
C       SARMIDI, M. R 1992,CEAC UNIVERSITY OF ASTON
C       THE PROGRAM CALCULATES THE ELUTION PROFILE OF SUCROSE,
C       GLUCOSE, FRUCTOSE AT VARIOUS VARIOUS COLUMN HEIGHT
C       ANGULAR DISPLACEMENT

        DIMENSION C(1000,2000),CG(1000,2000),CF(1000,2000)
        OPEN (4,FILE='F10.DAT',STATUS='NEW')
        WRITE(6,*)'INPUT TL, VMAX,VKM,E,QF,VF,DEGR,PE'
        READ(5,*)TL,VMAX,VKM,E,QF,VF,DEGR,PE

        CDS=0.14
        CDG=0.42
        CDF=0.68
C
         AF=(1.0+(CDF*(1.0-E)/E))
        AS=(1.0+(CDS*(1.0-E)/E))
        AG=(1.0+(CDG*(1.0-E)/E))
        THETA=0.0
        DELTI=0.0015
        THETAF=QF*2.0*3.1415/(QF+VF)
        PHIF=THETAF/(2.0*3.1415)

        WFN=PHIF/DELTI
        WRITE(6,*)WFN
        WRITE(6,*)' INPUT,CON,WFN=N'
        READ(5,*)CON,N

        OMEGA=(DEGR*2.0*3.1415)/(360.0*60)
        AN=107.1
        SV=VF/(E*AN*60.0)
C       P=(135.0*VMAX)/SV
        TR=(OMEGA*135.0)/(2.0*3.1415*SV)
        BS=AS*TR
        BG=AG*TR
        BF=AF*TR
        CN=0.000075
        DELZ=(DELTI*CON)/BS
        RA=DELZ/DELTI
        M=1
        RO=(BS*DELZ)/DELTI
        WRITE(6,*)'DELZ','DELTI','CON'
        WRITE(6,*)DELZ,DELTI,CON
C       WRITE(4,*)'DELZ','DELTI','CON'
C       WRITE(4,*)DELZ,DELTI,CON
        Z=0.0
        DF=1.0/(PE*DELZ)
        TI=0.0
C       SET THE INITIAL CONDITIONS

        DO 3 J=1,2000
        C(1,J)=0.0
        CG(1,J)=0.0
        CF(1,J)=0.0
3       CONTINUE
```

```
      DO 4 I=2,N+1
      C(I,1)=0.250
      CG(I,1)=0.0
      CF(I,1)=0.0
4     CONTINUE

      DO 6 I=N+2,800
      C(I,1)=0.0
      CG(I,1)=0.0
      CF(I,1)=0.0


6     CONTINUE

      L=1
      DO 5 J=1,2000
      THETA=0.0
      L=L+1
      Z=Z+DELZ
      K=1
      DO 10 I=2,780

      K=K+1
      VMAX1=VMAX*0.75*(1.0-(C(I,J)/0.25))
      P=(135.0*VMAX1)/SV
      R=((DELZ*P*C(I,J))/(C(I,J)+VKM
     1  +((C(I,J)*C(I,J))/0.453)))

      C(I,J+1)=C(I,J)-(RA*BS*(C(I,J)-C(I-1,J)))
     1  +DF*(C(I+1,J)-(2*C(I,J))+C(I-1,J))
     1  -R

      IF (C(I,J+1).LT.0.0) THEN
      C(I,J+1)=0.0
      END IF

      IF (C(I+1,J).LT.0.0) THEN
      C(I+1,J)=0.0
      END IF

      IF (C(I-1,J).LT.0.0) THEN
      C(I-1,J)=0.0
      END IF

      IF (C(I,J).LT.0.0) THEN
      C(I,J)=0.0
      END IF

      IF (CG(I,J+1).LT.0.0) THEN
      CG(I,J+1)=0.0
      END IF

      CG(I,J+1)=CG(I,J)-(RA*BG*(CG(I,J)-CG(I-1,J)))
     1  +DF*(CG(I+1,J)-(2*CG(I,J))+CG(I-1,J))
     2  +0.5*R

      IF (CG(I,J).LT.0.0) THEN
      CG(I,J)=0.0
      END IF
```

```
            THETA=THETA+DELTI

            IF (CF(I,J+1).LT.0.0) THEN
            CF(I,J+1)=0.0
            END IF

            CF(I,J+1)=CF(I,J)-(RA*BF*(CF(I,J)-CF(I-1,J)))
          1 +DF*(CF(I+1,J)-(2*CF(I,J))+CF(I-1,J))
          2 +0.5*R

            IF(CG(I-1,J).LT.0.0) THEN
            CG(I-1,J)=0.0
            END IF

            IF(CG(I,J+1).LT.0.0) THEN
            CG(I,J+1)=0.0
            END IF

            IF (CF(I,J+1).LT.0.0) THEN
            CF(I,J+1)=0.0
            END IF

            IF (CF(I,J).LT.0.0) THEN
            CF(I,J)=0.0
            END IF

            IF (CF(I-1,J).LT.0.0) THEN
            CF(I-1,J)=0.0
            END IF

           TI=THETA*360
           ZL=Z*135.0
           IF (ZL.LT.TL) GO TO 30
           IF (K.LE.5) GO TO 77
           IF (C(I,J+1).GT.CN.OR.CG(I,J+1).GT.
         1 CN.OR.CF(I,J+1).GT.CN) THEN
           WRITE(4,*)TI,C(I,J+1),CG(I,J+1),CF(I,J+1)
200        FORMAT(F6.4,5X,F6.5,5X,F6.5,5X,F6.5)
           END IF
           K=1
77         CC=1
30         M=M+1
10         CONTINUE

           IF (ZL.GE.TL) THEN
           GO TO 500
           END IF

5          CONTINUE

500        STOP
           END
```

PUBLICATIONS

1 Sarmidi, M R. and Barker, P. E., Simultaneous biochemical reaction and separation in a continuous rotating annular chromatograph. Accepted for publication in *Chem Eng Sci.*

2 Sarmidi, M R. and Barker, P. E., Saccharification of modified starch to maltose in a continuous rotating annular chromatograph. Accepted for publication in *J Chem Tech Biotechnol* .